Development of a High-Throughput Glucose Uptake Assay in Muscle Cells and Its Application to Screen Functional Food Substances Promising for Regulation of the Blood Glucose Levels

Yamamoto, Norio

(Degree)
博士（農学）

(Date of Degree)
2011-09-09

(Date of Publication)
2014-08-21

(Resource Type)
doctoral thesis

(Report Number)
乙3168

(URL)
https://hdl.handle.net/20.500.14094/D2003168

Doctoral Dissertation

Development of a High-Throughput Glucose Uptake Assay in Muscle Cells and Its Application to Screen Functional Food Substances Promising for Regulation of the Blood Glucose Levels

筋肉糖取込を評価する多検体対応測定方法の開発と血糖調節作用を有する食品素材の探索への応用に関する研究

July 2011

YAMAMOTO Norio

This doctoral dissertation is based on the following peer-reviewed papers.

I. **Norio Yamamoto**, Takuya Sato, Kengo Kawasaki, Shinji Murosaki and Yoshihiro Yamamoto., A nonradioisotope, enzymatic assay for 2-deoxyglucose uptake in L6 skeletal muscle cells cultured in a 96-well microplate., *Analytical Biochemistry*, **351** (1), 139–145 (2006).

II. **Norio Yamamoto**, Kengo Kawasaki, Takuya Sato, Yoshitaka Hirose, Koutarou Muroyama., A nonradioisotopic, enzymatic microplate assay for in vivo evaluation of 2-deoxyglucose uptake in muscle tissue., *Analytical Biochemistry*, **375** (2), 397–399 (2008).

III. **Norio Yamamoto**, Kengo Kawasaki, Kyuichi Kawabata, Hitoshi Ashida., An enzymatic fluorimetric assay to quantitate 2-deoxyglucose and 2-deoxyglucose-6-phosphate for in vitro and in vivo use., *Analytical Biochemistry*, **404** (2), 238–240 (2010).

IV. **Norio Yamamoto**, Manabu Ueda, Kyuichi Kawabata, Takuya Sato, Kengo Kawasaki, Takashi Hashimoto and Hitoshi Ashida., *Artemisia princeps* extract promotes glucose uptake in cultured L6 muscle cells via glucose transporter 4 translocation., *Bioscience, Biotechnology, and Biochemistry*, **74** (10), 2036–2042 (2010).

V. **Norio Yamamoto**, Yuki Kanemoto, Manabu Ueda, Kengo Kawasaki, Itsuko Fukuda and Hitoshi Ashida., Anti-obesity and anti-diabetic effects of ethanol extract of *Artemisia princeps* in C57BL/6 mice fed a high-fat diet., *Food & Function*, **2**, 45–52 (2011)

VI. **Norio Yamamoto**, Kyuichi Kawabata, Keisuke Sawada, Manabu Ueda, Kengo Kawasaki, Itsuko Fukuda, Akira Murakami and Hitoshi Ashida., Cardamonin stimulated glucose uptake in L6 myotubes through translocation of glucose transporter-4., *Phytotherapy Research*, (in press), DOI: 10.1002/ptr.3416

Contents

Abbreviations

ACO	acyl-CoA oxidase
AICAR	aminoimidazole carboxamide ribonucleotide
α-MEM	α-minimal essential medium (minimum essential medium alpha modification)
AMP	adenosine 5'-monophosphate
AMPK	5'-adenosine monophosphate-activated protein kinase
ANOVA	analysis of variance
AUC	area under the curve
aPKC	atypical protein kinase C
APE	ethanol extract of *Artemisia princeps*
ATP	adenosine-5'-triphosphate
BMI	body mass index
BSA	bovine serum albumin
CHD	coronary heart disease
CPT	carnitine palmitoyltransferase
CVD	cardiovascular diseases
2DG	2-deoxy-D-glucose
DG6P	2-deoxyglucose-6-phosphate
DMEM	Dulbecco's modified Eagle medium
DMSO	dimethyl sulfoxide
DTT	dithiothreitol
EDTA	ethylene diamine tetra acetic acid
ELISA	enzyme-linked immunosorbent assay
ERK1/2	extracellular-signal-regulated kinases 1/2
EtOAc	ethyl acetate
FAS	fatty acid synthetase
FBS	fetal bovine serum
FFA	free fatty acid
G6PDH	glucose-6-phosphate dehydrogenase
Glc	glucose
GLUT	glucose transporter
GOD	glucose oxidase
HDL-C	high density lipoprotein-cholesterol
HEPES	4-(2-hydroxyethyl)-1-piperazineethanesulfonic acid
HF	high-fat

HK	hexokinase
^{1}H-NMR	proton nuclear magnetic resonance
HOMA-IR	homeostasis model assessment-insulin Resistance
HPLC	high-performance liquid chromatography
HTS	high-throughput screening
IgG	immunoglobulin G
IL-6	Interleukin-6
INT	2-(4-iodophenyl)-3-(4-nitrophenyl)-5-phenyl tetrazolium chloride
IOTF	The International Obesity Task Force
IRβ	insulin receptor β subunit
IRS	insulin receptor substrate
KRH	Krebs–Ringer-Hepes
KRPH	Krebs-Ringer-Phosphate-Hepes
LDLR	low density lipoprotein receptor
LKB1	liver kinase B1
MEM	minimum essential medium
3MG	3-*O*-methylglucose
mPMS	1-methoxy-5-methylphenazinium methyl sulfate
mTOR	mammalian target of rapamycin
mTORC2	mammalian target of rapamycin complex 2
MTT	3-(4,5-dimethylthiazol-2-yl)-2,5-diphenyltetrazolium bromide
MFS	Major Facilitator Superfamily
NAD	nicotinamide adenine dinucleotide (oxidized form)
NADH	nicotinamide adenine dinucleotide (reduced form)
NADP	nicotinamide adenine dinucleotide phosphate (oxidized form)
NADPH	nicotinamide adenine dinucleotide phosphate (reduced form)
NEFA	non-esterifies fatty acids
NIDDM	non-insulin-dependent diabetes mellitus
OGTT	oral glucose tolerance test
6PDGA	6-phospho-2-deoxyglucuronic acid
PDK1/2	phosphoinositide-dependent protein kinase 1/2
6PGA	6-phosphoglucuronic acid
PI3K	phosphatidylinositol-3 kinase
PIP2	phosphatidylinositol-(4,5)- bisphosphate
PIP3	phosphatidylinositol-(3,4,5)-trisphosphate
PKB	protein kinase B

PKC	protein kinase C
PPARγ	peroxisome proliferator-activated receptor γ
PVDF	polyvinylidene fluoride
RI	radioisotope
SD	standard deviation
SDS	sodium dodecyl sulfate
SE	standard error of the mean
T2DM	type 2 diabetes mellitus
TBST	Tris buffered saline with Tween 20
TEA	triethanolamine
TLC	thin layer chromatography
Tris	2-amino-2-hydroxymethyl-propane-1,3-diol
UV	ultra violet
VLDL	very-low-density lipoprotein
WST-1	4-[3-(4-iodophenyl)-2-(4-nitrophenyl)-2H-5-tetrazolio]-1,3-benzene disulfonate sodium salt
WST-8	4-[3-(2-methoxy-4-nitrophenyl)-2-(4-nitrophenyl)-2H-5-tetrazolio]-1,3-benzene disulfonate sodium salt

Chapter 1

General introduction

Metabolic syndrome

For most of the 20th century, cardiovascular disease (CVD) was identified as major cause of morbidity and mortality in the developed world. During this period there was considerable effort to understand the underlying biology of the disease and to identify the contributing risk factors. As risk factors were identified, it became apparent that more than one were often present in the same individual. Toward the end of the century, the clustering of CVD risk factors was first described, most notably the simultaneous presence of obesity, type 2 diabetes (T2DM, also known as non-insulin-dependent diabetes mellitus, NIDDM), hyperlipidemia, and hypertension. Although insulin resistance (i.e., resistance to insulin-stimulated glucose uptake) as a feature of T2DM was first described many years earlier [1], hyperlipidemia was also found to be a key feature of T2DM [6,7], as well as hyperlipidemia [9-11], obesity [12-15], and hypertension [14-16]. This risk factor clustering, and its association with insulin resistance, led investigators to propose the existence of a unique pathophysiological condition, called the "metabolic" or "insulin resistance" syndrome. The underlying cause of the metabolic syndrome continues to challenge the experts but both insulin resistance and central obesity are considered significant factors [17,18]. Genetics, physical inactivity, aging, a proinflammatory state and hormonal changes may also have a causal effect, but the role of these may vary depending on ethnic group [3,19,20].

Insulin resistance

Insulin resistance occurs when cells in the body (liver, skeletal muscle and adipose/fat tissue) become less sensitive and eventually resistant to insulin, hormone which is produced by beta cells in the pancreas to facilitate glucose absorption. Glucose can no longer be absorbed in by the cells but remains in the blood, triggering the need for more and more insulin (hyperinsulinaemia) to be produced in an attempt to process the glucose. The production of ever-increasing amounts of insulin weakens and may eventually wear out the beta cells. Once the pancreas is no longer able to produce enough insulin then a person becomes hyperglycemic (too much glucose in the blood) and will be diagnosed with T2DM. Even before this happens, damage is occurring to the body, including a build-up of triglycerides which further impairs insulin sensitivity. Insulin resistance manifests as a broad clinical spectrum evolving progressively from hyperinsulinemia to glucose intolerance and eventually to frank diabetes. Therefore, the diagnosis of insulin resistance in the various definitions of

metabolic syndrome has required the presence of one or more features from this spectrum. Genetic susceptibility, along with environmental factors such as lifestyle, diet, stress, and smoking, can trigger the development of insulin resistance [3,8,21]. The metabolic consequences, hyperinsulinemia, hyperglycemia, and lipid and lipoprotein dysregulation, act in synergy to potentiate and sustain the pathologic state of insulin resistance. With the evaluation of insulin resistance, endothelial dysfunction, inflammation, and atherosclerosis worsen progressively [22,23].

Obesity

Obesity is associated with insulin resistance and the metabolic syndrome. Obesity contributes to hypertension, high serum cholesterol, low HDL-C and hyperglycemia, and is independently associated with higher CVD risk [17,24,25]. The risk of serious health consequences in the form of T2DM, coronary heart disease (CHD) and range of other conditions, including some forms cancer, has been shown to rise with an increase in body mass index (BMI) [26], but it is an excess of body fat in the abdomen, measured simply by waist circumference, that is more indicative of metabolic syndrome profile than BMI [27-29]. The International Obesity Task Force (IOTF) reported that 1.7 billion of the world's population is already at a heightened risk of weight-related, non-communicable disease such as T2DM. The mechanism *via* which obesity causes insulin resistance in skeletal muscle is related to accumulation of fat in the myocytes. Muscle biopsy studies [30,31] have demonstrated increased triglyceride content in skeletal muscle of obese normal-glucose-tolerance subjects compared to lean individuals and an inverse relationship between muscle insulin sensitivity and the intramuscular triglyceride content.

Muscle

The word muscle is derived from the Latin for mouse (*L. musculus*), an early anatomist thought that the belly (fleshy part) of muscle and the long thin tendon, looked like the head, body and tail of mouse. The three types of muscle tissue are skeletal, cardiac, and smooth. Skeletal muscle serves the following overlapping purpose: movement, posture, stability, communication, heat production, and cold tolerance. Very importantly, skeletal muscle is a major mass peripheral tissue. For example, this lean tissue, accounts for ~40% of the total body mass (36% for females, and 42% for males) and >30% of energy expenditure. Hence, skeletal muscle has a paramount role in energy balance, and is the primary tissue of insulin stimulated glucose uptake, disposal, and storage (four-fold the glycogen content of liver), regulates cholesterol efflux and strongly influence metabolism *via* modulation of circulating and stored lipid flux. For example, lipid catabolism supplies up to 70% of the energy requirements for resting muscle. Initial aerobic exercise utilized stored muscle glycogen,

however, as exercise continues, glucose and stored muscle triglycerides increasingly depends on fatty acids and, lipid mobilization from other tissue. This underscores the importance of fatty acid and glucose utilization as an energy source in muscle. Consequently skeletal muscle has a significant role in insulin sensitivity, the blood lipid profile, and obesity. Skeletal muscle is involved in significant homeostatic interrelationships between the muscular system, and other body system, for example, the cardiovascular, endocrine, lymphatic system, etc. Therefore, skeletal muscle must be considered an important therapeutic target tissue in the battle against CVD.

Skeletal muscle metabolism

Skeletal muscle utilizes both glucose and free fatty acid (FFA) as fuel sources for energy production. During the postabsorptive state, the plasma insulin concentration is low. Since the plasma insulin concentration is the principal factor that restrains lipolysis in adipocytes and stimulates glucose uptake in skeletal muscle, during the fasting state, muscle glucose uptake is low and plasma FFA concentration elevated [32]. Thus, under fasting conditions, FFA serves as principal fuel source for energy production in skeletal muscle, while the brain exclusively utilized glucose. Following glucose ingestion, the increase in plasma glucose concentration stimulates insulin secretion from beta cell and resultant hyperinsulinemia suppress lipolysis, leading to decline in plasma FFA concentration and subsequent decrease in the rate of lipid oxidation. Simultaneously, insulin stimulated glucose uptake in skeletal muscle, and the increased glucose flux into skeletal muscle, together with the activation of key enzymes in glucose metabolism by insulin, leads a marked increase in muscle glucose oxidation. Thus, under postprandial conditions, for example, mixed meal, muscle energy metabolism switches from predominant oxidation of fat during the fasting state, to predominant oxidation of glucose [33]. The ability of skeletal muscle to switch from fat oxidation during the fasting state to glucose oxidation during the postprandial state has been referred to as metabolic flexibility [34]. After glucose is transported into myocyte *via* the glucose transporter-4 (GLUT4), it is immediately phosphorylated by hexokinase, and phosphorylated glucose either is converted to, and stored as glycogen, or enters the glycolytic pathway for oxidation. Approximately 90 % of glucose entering the glycolysis is oxidized and remaining 10% is released as lactate. At low plasma insulin concentration, for example, fasting state, and glucose oxidation contribute equally to glucose disposal. However, with increasing plasma insulin concentration, glycogen synthase is activated by insulin and glycogen synthesis predominate (~70% of glucose disposal) [35].

Differences between diabetics and control subjects in the amount and fate of glucose taken up by different tissures in the body during the euglycemic insulin clamp are shown in **Fig. 1-1** [2]. The hight of eache bar represents the total amount of glucose uptake up by the entire body during the insulin clanp in control and T2DM subjects. Net splanchnic glucose uptake, quantitated by the hepatic vein catheterization technique, is similar in both groups and average s 0.5 mg/kg min. Adipose tissue

glucose uptake, which was not measured directly, represents approximately 2–3% of total-body glucose disposal. Brain glucose uptake is estimated to be 1.0–1.2 mg/kg/min in the postabsorptive state, and is unaltered by hyperinsulinemia. Muscle glucose uptake (extrapolated from leg catheterization data) in control subjects represents about 75% of the total glucose uptake. In T2DM subjects, essentially all the impairment in insulinmediated glucose uptake can be accounted for by impaired muscle glucose disposal. Finally, it is important to understand that the metabolic fate of the glucose which is taken up by peripheral tissues, primarily muscle, is not normal in type 2 diabetic patients.

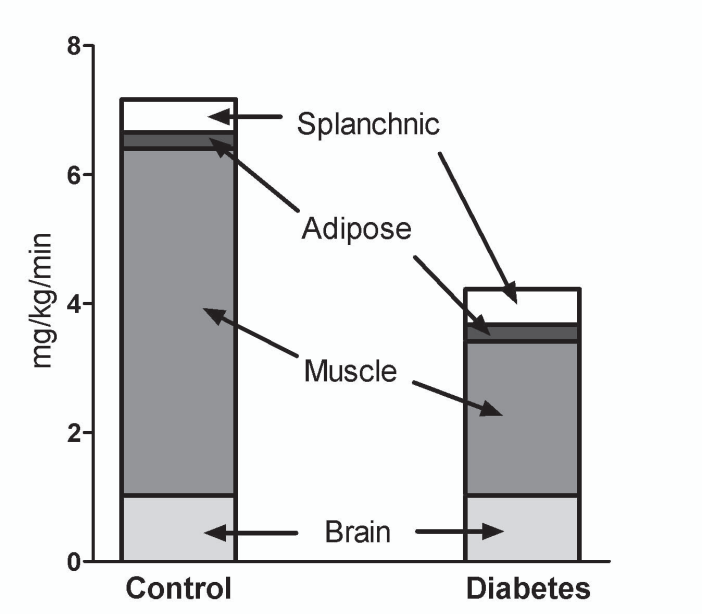

Fig. 1-1. Summary of glucose metabolism during euglycemic insulin (+ 100 U/ml) clamp studies performed in normal-weight T2DM and control subjects. (Source: DeFronzo et al. [2].)

Table 1-1. Tissue specific expression of the GLUT family members.
(Source: Joost *et al.* and Medina *et al.* [41,43].)

Isoform	Other names	Gene names	Expression	Function	Ref.
GLUT1		SLC2A1	All tissues (abundant in brain and erythrocytes)	Basal uptake	[54,55]
GLUT2		SLC2A2	Liver; Pancreatic β-cell; Kidney proximal tubule; Retina; Small intestine (basolateral membranes)	Glucose sensing	[56]
GLUT3		SLC2A3	Brain; Nerve cells; Placenta (low levels), Kidney (low levels); Liver (low levels); Heart (low levels)	Supplements GLUT1 in tissues in tissues with high energy demand	[57]
GLUT4		SLC2A4	Muscle; Heart; Adipose tissue	Insulin responsive	[56,58-60]
GLUT5		SLC2A5	Small intestine (apical membranes); Brain; Muscle (low levels); Adipose tissue (low levels)	Fructose transport	[61,62]
GLUT6	GLUT9	SLC2A6	Spleen; Leukocytes; Brain		[63]
GLUT7		SLC2A7	Microsomal glucose transporter; Liver		[64]
GLUT8	GLUTX1	SLC2A8	Testis; Blastocyst; Brain		[65-67]
GLUT9	GLUTX	SLC2A9	Liver; Kidney		[68]
GLUT10		SLC2A10	Liver; Pancreas		[69]
GLUT11	GLUT10	SLC2A11	Heart; Muscle		[70]
GLUT12	GLUT8	SLC2A12	Heart; Prostate		[71]
GLUT13		SLC2A13	Brain	Proton-coupled myoinositol transporter (HMIT)	[72]
GLUT14		SLC2A14	Testis		[73]

Glucose transport

Because glucose is the main energy source for cells there has been extensive and research on its actions as a cellular metabolite and on the mechanisms controlling its accumulation into tissue. In higher organisms, the preservation of energetic integrity requires adaptation to external resources and extensive interorgan communication. In this context, glucose has acquired a role as a signaling

molecule to control glucose and energy homeostasis. Glucose can regulate gene transcription, enzyme activity, hormone secretion, and the activity of glucoregulatory neurons [36]. In pancreatic β-cells, glucose is the principal regulator of These neurons are involved in the control of feeding, energy expenditure, and glucose homeostasis insulin secretion, and, in the brain, groups of glucose-sensitive neurons are activated or inhibited by rises in glucose concentrations [37]. A number of diseases are associated with glucose transport and metabolic disorders, including myocardial ischemia [38]), Type 2 diabetes [39], and cancer [40]. Facilitative glucose transport systems responsible for mediating the uptake of this nutrient are located on the membrane of all virtually all animal cells. In general, glucose is transported across membranes by two different mechanisms: a Na^+-coupled active carrier system, and a family of structurally related Na^+-independent glucose transporter glycoproteins. These latter , which is known as glucose transporter (GLUT) or SLC2A family, facilitate the movement of glucose across the plasma membrane down its chemical gradient either into or out of cells. They are specific for D-glucose and are not coupled to any energy-requiring components, such as ATP hydrolysis or a H^+ gradient. The facilitative glucose transporters are distinct from the Na^+-dependent transporters, which actively accumulate this carbohydrate. These various glucoregulatory functions are usually secondary to glucose uptake, a step that, in most tissues (with the notable exception of hepatocytes and pancreatic β-cells), is controlled by the level of GLUT expression at the cell surface. The existence of multiple GLUT isoforms, with different kinetic properties and regulated cell surface expression, provides the basis for the fine tuning of glucose uptake, metabolism, and signal generation in order to preserve cellular and whole body metabolic integrity. All mammalian cells contain one or more members of the GLUT family (**Table 1-1**) [5,41]. These proteins display a high degree of stereoselectivity, providing for the bidirectional transport of substrate, with passive diffusion down its concentration gradient. The GLUTs regulate the movement of glucose between extracellular and intracellular compartments, thereby maintaining a constant supply of this essential element. The GLUT protein family belongs to the Major Facilitator Superfamily (MFS) of membrane transporters [42]. GLUTs are proteins of ~500 amino acids and are predicted to possess 12 transmembrane-spanning alpha helices and a single N-linked oligosaccharide. The GLUT family members can be grouped into three different classes based on their sequence similarities [43]. Fourteen GLUT proteins are expressed in the human and they include transporters for substrates other than glucose, including fructose, myoinositol, and urate. The primary physiological substrates for at least half of the 14 GLUT proteins are either uncertain or unknown. The class I molecules GLUTs 1–4 have been most extensively characterized and are known to have distinct regulatory and/or kinetic properties that reflect their specific roles in cellular and whole body glucose homeostasis [36].

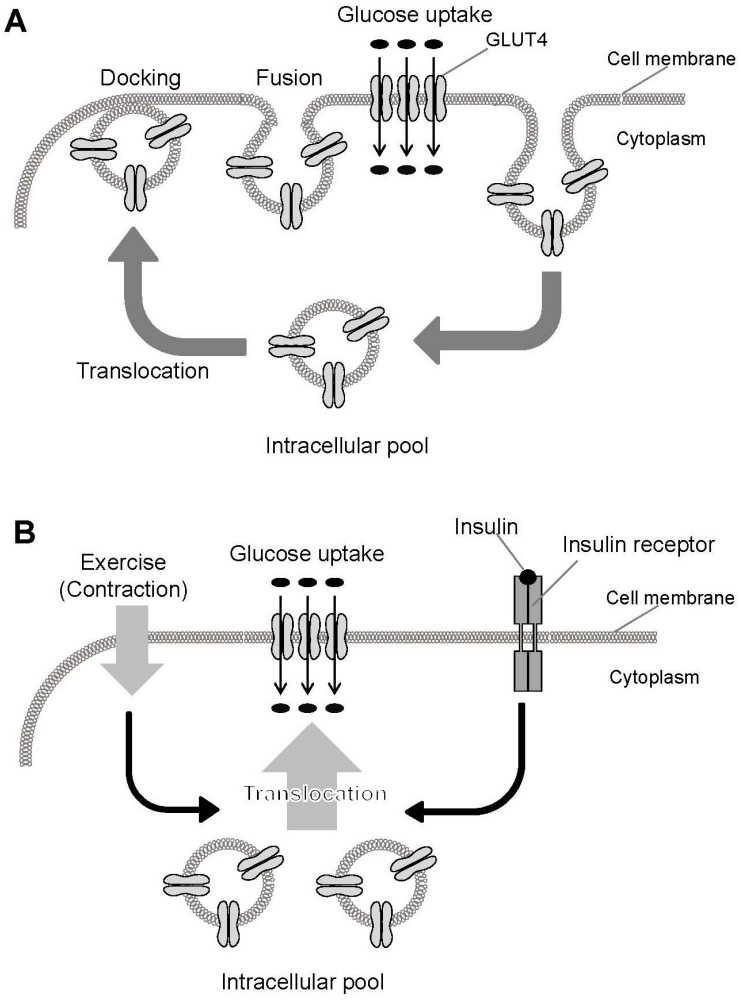

Fig. 1-2. Glucose uptake and GLUT4 translocation. Glucose enters the cell by a carrier-mediated, facilitated diffusion mechanism, which, in most tissues, exhibits no energy or counter-ion requirements. In adipose tissues and skeletal muscle, glucose entry is acutely regulated by insulin and other hormones [3]. Indeed, in those tissues, GLUT4 is the chief isoform which is, in basal conditions, retained in a specific intracellular storage compartment [5]. The GLUT4-containing vesicles are translocated to the plasma membrane in response to insulin, thus allowing for the massive entry of glucose into the cells [3,8]. Adipocytes also contain a small proportion of the ubiquituously expressed glucose transporter, GLUT1, which is at a similar level at the plasma membranes and inside the cell [5]. Because of this basal distribution, insulin effect on GLUT1 translocation is minor.

Glucose transport is generally assumed to represent the rate-limiting step for lipogenesis in adipose tissue *in vivo* and in adipocytes *in vitro*, at least under conditions of low to moderate concentration of glucose in the plasma and incubation medium, respectively. Its stimulation by insulin is of exquisite sensitivity and responsiveness. Insulin resistance is defined as reduced ability of cells or tissues to respond to physiological levels of insulin and is characteristic of T2DM. Skeletal muscle is the primary tissue responsible for the postprandial uptake of glucose from blood. Two major transporters expressed in adipose tissue and skeletal muscle are the muscle and fat-specific glucose

transporter GLUT4 and ubiquitous transporter GLUT1. The insulin-stimulated acute activation of glucose transport mainly occurs by one of two mechanisms: translocation of GLUT4 and GLUT1 from intracellular vesicles to the plasma membrane and augmentation of intrinsic catalytic activities of transporters. The molecular mechanism underling the glucose transport and its regulation are similar for adipose and muscle cells. Consequently, adipocytes are more widely used for transport studies than myocytes due to their more convenient accessibility and more pronounced insulin responsiveness. However, studies for clarification of the mechanism by which compound with insulin-like and/or insulin-sensitizing activity stimulate glucose uptake in skeletal muscle for the treatment of T2DM have to be performed with assay systems into myotubes, cultured L6 muscle cells possess many express both GLUT4 and GLUT1 and are capable of increasing glucose transport *via* insulin stimulation. Under most conditions, glucose transport across the plasma membrane is the rate-limiting step for its metabolism in skeletal muscle [44]. Glucose transport into muscle occurs by facilitated diffusion process mediated by specific transporter proteins [45-47]. Skeletal muscle expresses two isoforms of the glucose transporter, GLUT1 and GLUT4. GLUT1 is preferentially targeted to sarcolemma [48], and is thought to mediate basal glucose transport. In the basal state, skeletal muscle GLUT4 is targeted primarily to an intracellular compartment [49,50]. After stimulation by insulin or contractile activity, GLUT4 is translocated to plasma membrane, resulting in an increase in glucose transport activity [49,51-53].

Insulin-stimulated glucose uptake

The insulin receptor is a tyrosine kinase receptor which upon activation phosphorylates insulin receptor substrate proteins (IRS1-4) [74]. Tyrosine phosphorylation of IRS activates phosphatidylinositol-3-kinase (PI3K) which induces the phosphorylation of phosphatidylinositol-(4,5)-bisphosphate (PIP2) on the 3rd position generating phosphatidylinositol-(3,4,5)-trisphosphate (PIP3) [75]. Experiments using selective PI3K inhibitors, PI3K dominant negative mutants or microinjections of blocking antibodies show that PI3K is important in insulin-stimulated glucose uptake in rat and mouse adipocytes [76,77]. PIP3 activates a phosphoinositide-dependent kinase, PDK1, which can activate Akt by translocating this kinase to the plasma membrane and by phosphorylating Thr-308 and/or Ser-473 residues of Akt [78]. It is postulated that PDK1 can activate atypical protein kinase C (PKC)-λ/ζ, which are critical for GLUT4 translocation to the plasma membrane and stimulation of glucose uptake in rat adipocytes [79-81]. Insulin induces translocation of GLUT4 to the cell plasma membrane, stimulates exocytosis of GLUT4 containing vesicles and inhibits internalization of GLUT4 in insulin-sensitive tissues by this promoting increase in glucose uptake [82,83]. GLUT4 shuttles between the cell interior and the cell surface via both general endosomes and specialized compartments. In unstimulated adipocytes and muscle cells, GLUT4 is distributed approximately equally between the endosomes and specific compartments [84,85]. GLUT1 is abundantly expressed

in all type of cells and it is shown to be responsible primarily for basal glucose uptake. However, a number of reports demonstrate that GLUT1 is also activated or translocated to the plasma membrane of the cell. For example, in cardiac myocytes, the mitochondrial inhibitor rotenone recruited GLUT1 and GLUT4 to the plasma membrane from the endosomal pool, whereas insulin induced a dramatic reduction of GLUT4 protein from the storage pool and stimulated GLUT1 translocation to the plasma membrane from the endosomal pool [86]. Isoprenaline stimulates GLUT1 translocation to the plasma membrane in rat perfused heart [87]. In brown adipose tissue prolonged cold exposure or adrenergic stimulation increases GLUT4 protein amount [88-90]. Surgical sympathetic denervation prevents the increase in GLUT4 mRNA induced by cold exposure of rats [88] suggesting that norepinephrine release affects GLUT4 amount. In primary rat cultured brown adipocytes, insulin and norepinephrine additively stimulate glucose uptake [91]. In this system norepinephrine induces glucose uptake by increasing GLUT1 activity without promoting GLUT4 translocation [91].

AMPK

There has been much interest recently in AMP-activated protein kinase (AMPK), which has been suggested to act as a sensor of energy homeostasis [92-94]. When ATP levels in the cell are decreased, the AMP levels rise. Increased amounts of AMP are a signal that the energy status in the cell is low leading to activation of AMPK [95]. Mammalian AMPK consists of an α catalytic subunit and β, γ regulatory subunits. Each of the subunits comprises different isoforms: α1, α2, β1, β2 and γ1–γ3. AMPK is expressed in skeletal and cardiac muscle, liver, brain and adipose tissue [92,94,96]. Activation of AMPK by AMP can occur by three different mechanisms: allosteric activation, phosphorylation on the Thr-172 residue and inhibition of dephosphorylation [92]. This way of activation points out that the system is extremely sensitive to small changes in cellular AMP levels and ensures rapid responses to fluctuations in cellular energy states. Thus, AMPK is activated under conditions when ATP levels in the cell are depleted, for example: heat shock [97], glucose deprivation [98], hypoxia [99,100]; in skeletal muscle during exercise, depending on duration and intensity of exercise [95,101], in adipose tissue and liver under exercise (as a result of exercise-induced release of molecules, for example, IL-6 from muscle) [102]. A number of investigations have shown an importance of low levels of circulating adiponectin and leptin in a variety of abnormalities associated with the metabolic syndrome and insulin resistance [103-107]. It was shown that adiponectin and leptin stimulate AMPK activity [108-110]. Adiponectin and leptin increase energy expenditure by stimulation of fatty acid oxidation, in other words these hormones stimulate fat burning when its storage is excessive and AMPK is probably a key molecule in adiponectins and leptins intracellular signaling cascade. Activation of AMPK in adipose tissue increases fatty acid oxidation by suppression of ACC (acetyl-CoA-carboxylase) activity, a decrease in malonyl-CoA content and correspondingly activation of the carnitine-palmitoyltransferase activity, resulting in increase of fatty acids oxidation

[108,111] because it can be activated by metformin [112] and thiazolidinediones [113] which inhibit Complex I of the respiratory chain and by this, probably, activate AMPK. Thiazolidinediones also increase the AMP/ATP ratio in the L6 skeletal muscle cell line to stimulate AMPK activity, whereas metformin induces phosphorylation of AMPK without causing changes in ATP levels in cells [114]. Treatment of cells with AICAR (cell-permeable AMPK activator 5-aminoimidazole-4-carboxamide ribonucleoside) increases glucose uptake in skeletal and cardiac muscle [115], and also induces insulin release from β-cells [116], indicating possible role of AMPK in glucose homeostasis. The role of AMPK in adipose tissue is poorly understood because of a numbers of contradictory results. Adrenergically stimulated lipolysis after AMPK activation can be stimulated [117] or for inhibition [118,119]. Stimulation of AMPK with AICAR does not increase glucose transport and decreases insulin-stimulated glucose uptake in 3T3-L1 adipocytes [120]. AICAR is shown to increase glucose uptake independently on AMPK in adipocytes [121]. More studies are needed to clarify the possible role of AMPK and it modulators of activity in treatment of T2DM.

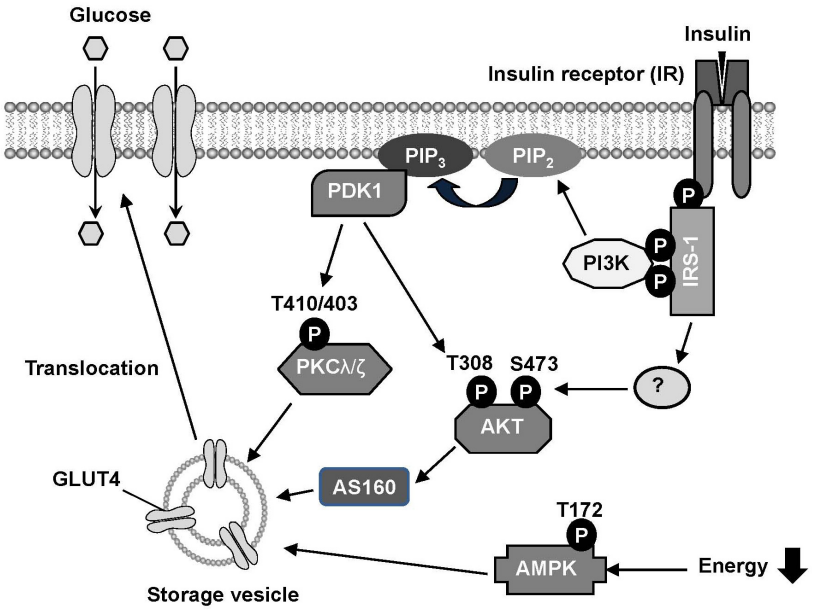

Fig. 1-3. Glucose uptake *via* insulin-stimulated GLUT4 translocation and fusion in muscle and adipose tissues. Steps: (i) extracellular insulin binds to the α-subunit of the insulin receptor (IR), triggering autophosphorylation and activation of the β-subunit kinase activity; (ii) this induces recruitment of IRS-1, and (iii) IRS-1 recruits PI3K. (iv) PI3K phosphorylates PIP2 to yield PIP3. (v) PIP3 recruits PDK1 to the PM, where it (vi) phosphorylates and activates AKT. (vii) AKT phosphorylates AS160, and (viii) AS160 targets multiple Rabs present on GLUT4-containing vesicles (ix), although the precise mechanisms beyond this remain unclear. (x) vesicle fusion occurs *via* the SNARE proteins, resulting in GLUT4 integration into the plasma membrane to facilitate (xi) glucose uptake. It is postulated that PDK1 can activate atypical protein kinase C (PKC)-λ/ζ, which are critical for GLUT4 translocation to the plasma membrane and stimulation of glucose uptake in rat adipocytes. Independent of insulin, exercise and muscle contraction have also been shown to increase glucose uptake into skeletal muscle. Increased amounts of AMP are a signal that the energy status in the cell is low leading to activation of AMPK. Activation of AMPK in skeletal muscle cells also stimulates glucose uptake *via* GLUT4 translocation.

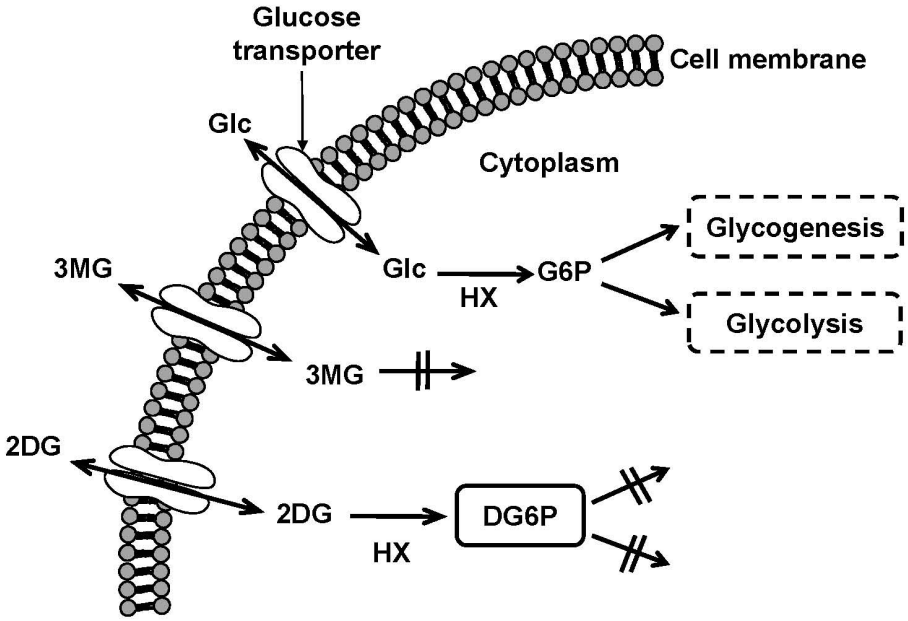

Fig. 1-4. Schematic transport of glucose (Glc), 3-*O*-methyl-D-glucose (3MG) and 2-deoxy–D-glucose (2DG). Glucose transported through the glucose transporters (GLUTs) is further metabolized by subsequent steps in the pathways of glucose metabolism, and glucose and glucose-6-phosphate do not accumulate in cell. 3MG enters cell through GLUTs and is unable to undergo further metabolism. However, 3MG is permeable to cell membrane. 2DG enters cell through GLUTs and is phosphorylated by hexokinase (HX). Due to low levels of intracellular phosphatase, 2-deoxyglucose-6-phosphate (DG6P) accumulates in cell. DG6P is unable to undergo further metabolism.

Glucose uptake assay based on the glucose analogue

Skeletal muscle is the major insulin-sensitive tissue and normally takes up most of the glucose that enters the blood after a meal [122,123]. Exercise markedly increases the rate of glucose disposal by directly activating muscle glucose uptake [124,125] and by potentiating the action of insulin [126,127]. Resistance of skeletal muscle to insulin is major component of pathophysiology of NIDDM in majority of patients with this disease [128]. Therefore, because of central role of muscle in the regulation of glucose homeostasis, the mechanism involved in the control of skeletal muscle glucose uptake are subject of intense research interest. The glucose analogues 3-*O*-methyl-D-glucose (3MG) and 2-deoxy-D-glucose (2DG) have been used to study skeletal muscle glucose transport. 3MG is transported into the cell but is not further metabolized; thus its rate of intracellular accumulation is an index of transport per se and is not influenced by subsequent steps in the pathways of glucose metabolism [129]. A limitation of the use of 3MG is that efflux becomes a significant problem when the intracellular concentration reaches ~25% of extracellular concentration in rat skeletal muscle [44], resulting in an underestimation of glucose transport activity. This is a major problem in the study of

certain muscle types under conditions where transport rates are high, i.e., maximal or near-maximal activation by insulin and/or contractile activity. The problem of efflux can be avoided by using 2DG, which is phosphorylated by hexokinase after its transport into cell. Phosphorylation serves to trap 2DG in the cell, inasmuch as glucose-6-phosphatase activity is very low in skeletal muscle [130]. This makes it possible to measure sugar transport for a sufficiently long period to render relatively unimportant the contribution of the underestimation of the rate of sugar transport during the equilibration period. Thus the accumulation of intracellular 2-deoxyglucose 6 phosphate (DG6P) can be used to measure glucose transport activity when transport rate are high.

High-throughput screening

The mechanism-based approach which corresponds to the target-based approach screens for compounds with a specific mode of action. The highly effective nature of high-throughput screening (HTS) for identification of highly target specific compounds is attributed to its precise focus on single mechanism. Of late High-Throughput Screening (HTS) a high-tech approach for drug discovery is more and more gaining popularity among industrial researchers as well as students doing their post-graduate and/or doctorate research projects. It is basically a process of screening and assaying huge number of biological modulators and effectors against selected and specific targets. The principles and methods of HTS find their application for screening of combinatorial chemistry, genomics, protein, and peptide libraries. HTS is a novel method for drug discovery but it is not the only method. HTS not only helps in drug discovery but also in development of present drug moieties to optimize their activity. In past years many advances in science and technology and economic pressures have kept every researcher to develop speedy and precise drug development and screening technologies to combat the ever increasing diseases and many pathogens acquiring resistance to present available drugs. This also applies to screening the ever increasing compound libraries waiting to be screened due to increase in the parallel and combinatorial chemical synthesis.

Objectives

T2DM presents a vast and growing world health problem. This disease is characterized by impaired cellular responses to the insulin hormone. Skeletal muscle is principal site for insulin-stimulated glucose uptake. In patients with T2DM, insulin-mediated glucose utilization in skeletal muscle is markedly impaired. Nutrition overload often leads to the development insulin resistance in obesity and T2DM. Like every living cell, skeletal muscle has several sensory systems that detects nutrient and energy signals and adjust the flux through metabolic pathways accordingly. A vast number of environmental impositions (nutrient overload, contractile activity) can be overcome by

means of adaptive response from skeletal muscle. In the context of developing functional foods or nutraceutical strategies for both prevention and treatment of obesity/diabetes, our research is directed at screening specific nutrients and phytochemical ingredients (e.g. polyphenols) with quantitatively important impact on thermogenesis, fat oxidation and insulin sensitivity, and in studying the underlying mechanisms of action of potentially useful candidate bioactive food ingredients.

In this thesis, we have developed a method for evaluating glucose uptake in cultured cells especially muscle cells without using radioisotope, and explore the possibility that naturally occurring chemicals (phytochemicals) found in vegetables and spices have the power to restore insulin sensitivity, and thus normal glucose metabolism, in individuals with T2DM.

Chapter 2

A high-throughput, enzymatic assay for 2-deoxyglucose uptake in L6 skeletal muscle cells cultured in a 96-well microplate

2-1. Introduction

Facilitative glucose transport systems are ubiquitous in animal cells and are responsible for transporting glucose across the cell surface membrane. Uptake of glucose in cultured cells is commonly determined by using nonmetabolizable radioactive hexoses, such as 3-*O*-methylglucose (3MG) or 2-deoxyglucose (2DG), labeled with a high specific activity of tritium [131]. [^{3}H]3MG necessitates a very short incubation time due to fast equilibration of the analog across the cell membrane and requires either rapid separation of the water phase from the incubation mixture, usually by centrifugation through a suitable lipid phase [131], or the prevention of 3MG efflux by washing with a mercuric chloride solution [132]. Uptake assays based on [^{3}H or ^{14}C]2DG are more convenient because 2DG is phosphorylated to a stable and impermeable derivative, 2-deoxyglucose-6-phosphate (DG6P), by hexokinase or glucokinase [133]. However, routine use of these radiolabeled analogs is costly and requires a specialized institution where isotopes can be handled.

Insulin resistance is defined as the reduced ability of cells or tissues to respond to physiological levels of insulin and is characteristic of non-insulin-dependent diabetes mellitus (NIDDM) [134]. Skeletal muscle is the primary tissue responsible for the postprandial uptake of glucose from the blood. The two major transporters expressed in skeletal muscle are the muscle/fat-specific glucose transporter GLUT4 and the ubiquitous transporter GLUT1 [135]. When differentiated into myotubes, murine L6 muscle cells possess many of the properties of mature skeletal muscle tissue [136]. They express both GLUT4 and GLUT1 and are capable of increasing glucose transport *via* insulin stimulation. The insulin-stimulated acute activation of glucose transport mainly occurs by one of two mechanisms: translocation of GLUT4 and GLUT1 from intracellular vesicles to the plasma membrane and augmentation of the intrinsic catalytic activities of the transporters [137,138]. Therefore, it is important to clarify the mechanism by which insulin-mimetic and/or insulin sensitizing agents stimulate glucose uptake in skeletal muscle for the treatment of NIDDM.

In this study, we have developed a nonradioisotopic, enzymatic assay based on the methods of Manchester *et al*. [139] and Sasson *et al*. [131] for measuring DG6P in tissues and cultured cells. Their methods enable the detection of DG6P accumulating in cells by measurement of the fluorescence of NADPH produced from $NADP^{+}$, which is coupled to the oxidation of 2DG to DG6P by glucose-6-phosphate dehydrogenase (G6PDH). This approach, however, requires the cultivation of many cells on large plates and the preparation of cell extracts because the fluorescence of NADPH is rather weak. Thus, here we adopted a diaphorase–resazurin system that produces a potent fluorescent

substance in the presence of NADPH. Uptake of 2DG into the cells could be measured by the addition of a single assay solution to the cell culture, followed by a simple incubation. To confirm the reliability of this method, the effects of insulin and other chemicals on 2DG uptake by L6 myotubes were evaluated.

2-2. Materials and methods

2-2-1. Materials

2DG (Grade III), hexokinase (HX, from *Saccharomyces cerevisiae*), G6PDH (from *Leuconostoc mesenteroides*), cytochalasin B, LY294002, and insulin (from bovine pancreas) were purchased from Sigma-Aldrich (St. Louis, MO). Resazurin sodium salt and triethanolamine hydrochloride (TEA) were obtained from Wako Pure Chemical (Osaka, Japan). Adenosine 5'-triphosphate disodium salt (ATP), β-nicotinamide adenine dinucleotide phosphate ($NADP^+$), and diaphorase (from *Clostridium kluyvery*; Type II-L) were purchased from Oriental Yeast (Tokyo, Japan). General chemicals and buffer components were purchased from Wako Pure Chemical. The pioglitazone hydrochloride used in this study was isolated from a pharmaceutical pill, ACTOS (Takeda Pharmaceuticals, Osaka, Japan). The ethanol extract from ground tablets (30 mg/tablet of pioglitazone hydrochloride) was applied to a Bond-Elut-C18 solid-phase-extraction cartridge (Varian, Lake Forest, CA), which had been preconditioned with ethanol and water and eluted with ethanol. The eluant was subjected to evaporation and its purity was checked by UV detection (254 nm) of a reverse-phase TLC plate (RP-18 F_{254S}; Merck, Darmstadt, Germany) developed with Methanol/H_2O (80:20, v/v).

2-2-2. Determination of 2DG by resazurin–diaphorase system

To determine the low concentrations of 2DG and/or DG6P present in a 96-well microplate, a diaphorase-NADPH amplifying system was combined with previous methods [131,139] for measuring DG6P in tissues and cultured cells. In brief, 50 μL of 2DG solution at various concentrations was dispensed into each well of a 96-well plate and incubated for 90 min at 37°C after the addition of 150 μL of an assay cocktail of 50 mM TEA (pH 8.1), 50 mM KCl, 0.5 mM $MgCl_2$, 0.02% BSA, 670 μM ATP, 0.12 μM $NADP^+$, 25 μM resazurin sodium salt, 5.5 units/mL hexokinase, 16 units/mL G6PDH, and 1 unit/mL diaphorase. The assay cocktail was prepared before each assay from stock solutions of enzyme, coenzyme, and substrate that were maintained in the freezer or refrigerator. At the end of the incubation, fluorescence at 590 nm with excitation at 530 nm was measured by a MTP-32 microplate reader (Corona Electric, Hitachinaka, Japan) to detect the resorufin derived from reduced resazurin. To assay DG6P alone, ATP and HX were left out of the assay cocktail described above.

2-2-3. Determination of 2DG using tetrazolium salts

To detect NADPH generated from oxidation of DG6P by G6PDH, highly water-soluble

tetrazolium salts, WST-1 (4-[3-(4-iodophenyl)-2-(4-nitrophenyl)-2*H*-5- tetrazolio]-1,3-benzene disulfonate sodium salt) and WST-8 (4-[3-(2-methoxy-4- nitrophenyl)-2-(4-nitrophenyl)-2*H*-5-tetrazolio]-1,3-benzene disulfonate sodium salt) were applied to the assay of 2DG determination, and 1-methoxy-5-methylphenazinium methyl sulfate (mPMS) and diaphorase were used as a hydrogen carrier. WST-1, WST-8 (Cell Counting Kit-8) and mPMS were obtained from Dojindo Laboratories (Kumamoto, Japan). Compositions of reaction solutions are shown in the following table. 2DG solution (20 μL) was dispensed in a 96 well assay plate and incubated for 60 min at 37°C after the addition of 150 μL of assay solution and absorbance at 415 nm was measured in case of WST-1, and absorbance at 415 nm was measured in case of WST-8. Compositions of each assay solution were shown in **Table 2-1**.

Table 2-1. Composition of assay solutions.

Amplification systems	WST-1 + diaphorase	WST-1 + 1-methoxy PMS	WST-8 + 1-methoxy PMS	Resazurin (high) + diaphorase	Resazurin (low) + diaphorase
TEA buffer (pH 8.1)	50 mM	50 mM	50 mM	50 mM	50 mM
KCl	50 mM	50 mM	50 mM	50 mM	50 mM
Magnesium acetate	2 mM	2 mM	2 mM	2 mM	2 mM
Bovine serum albumin (BSA)	0.02%	0.02%	0.02%	0.02%	0.02%
NADP	0.1 mM	0.1 mM	0.1 mM	0.1 mM	0.1 mM
ATP	0.5 mM	0.5 mM	0.5 mM	0.5 mM	0.5 mM
WST-1	100 μM	100 μM	---	---	---
WST-8*	---	---	100 μM	---	---
Resazurin sodium salt	---	---	---	10 μM	2 μM
Diaphorase	0.2 units/mL	---	---	0.2 units/mL	0.2 units/mL
1-methoxy PMS	---	20 μM	20 μM*	---	---
Hexokinase	2 units/mL	2 units/mL	2 units/mL	2 units/mL	2 units/mL
G6PDH from*L. mesenteroides*	20 units/mL	20 units/mL	20 units/mL	20 units/mL	20 units/mL

*Cell Counting Kit-8 (Dojindo Laboratory) containing 5 mM of WST-8 and 0.2 mM of 1-methoxy PMS was diluted and used. Since there was 4 μM (final conc.) of 1-methoxy PMS carrying in from the kit, 16 μM (final conc.) of 1-methoxy PMS was added further.

2-2-4. Cell cultures

L6 skeletal muscle cells were purchased from Dainippon Pharmaceuticals (Osaka, Japan) and were propagated at 37°C in 5% CO_2 in α-minimal essential medium (α-MEM; M-0894; Sigma) supplemented with 100 units/mL of penicillin G, 100 μg/mL of streptomycin sulfate, and 10% heat-treated fetal bovine serum (FBS). The cells were seeded (4×10^3 cells/well) in a collagen-coated

96-well microplate (growth area = 0.32 cm^2/well; IWAKI brand, Asahi Techno Glass, Osaka, Japan) and cultured in α-MEM with 10% FBS for 2 days until semiconfluent. Next, the cells were cultured in α-MEM with 2% FBS for 5 days to differentiate to myotubes, which were then used in the glucose uptake assay.

Murine 3T3-L1 preadipocytes (Dainippon Pharmaceutical Co. Ltd, Osaka, Japan) were grown and passaged in DMEM (with high glucose; Sigma) supplemented with 10% fetal bovine serum (FBS), 100 units/mL of penicillin G, 100 μg of streptomycin sulfate. For adipocyte differentiation, cells were seeded in a 24 well polylysine-coated culture plate. Two days postconfluence, differentiation was induced with 10 μg/mL insulin, 0.25 μM dexamethazone and 0.5 mM 3-isobutyl-1-methylxantine in DMEM containing 10% FBS. After 2 days, the medium was changed DMEM containing 10% FBS, 10 μg/mL insulin, and cells were cultured for additional 2 days. Then, the medium was changed to DMEM containing 10% FBS, and thereafter, the cells were maintained for 9 days with replacement of the medium every 2–3 days. The differentiated cells were used for 2DG uptake assay 9 days after differentiation induction. Before 2DG uptake assay, the cells were maintained in FBS-free DMEM for 4 h.

Primary neuronal cells were isolated from hippocampus of Wistar rat embryos at day 21 of gestation. Neurons were dissociated from fetal hippocampi in Hank's balanced salt solution containing 0.5% glucose, 2% sucrose, 1 mM sodium pyruvate and 15 mmol/L 2-(4-[2-hydroxyethyl]-1-piperazinyl) ethanesulfonic acid, and then centrifuged for 1 min at 15 000 g. Cells were plated onto poly-d-lysine-coated dishes at a density of 5×10^5 cells/mL in B27- neurobasal medium (B27-NBM). Cultured neurons were incubated with B27-NBM on a poly-lysine-coated 24-well culture plate [140]

2-2-5. Glucose uptake assay

The differentiated L6 myotubes were incubated with 170 μL/well of α-MEM with 2% FBS in the presence of insulin and/or a test compound for the indicated time. After incubation, the cells were washed twice with Krebs–Ringer–phosphate–Hepes (KRPH) buffer (pH 7.4, 20 mM Hepes, 5 mM KH_2PO_4, 1 mM $MgSO_4$, 1 mM $CaCl_2$, 136 mM NaCl, 4.7mM KCl) containing 0.1% BSA. The washed myotubes were then incubated with KRPH buffer containing 1 mM 2DG and 0.1% BSA for the indicated time (termed the 2DG-uptake period) at 37°C in 5% CO_2. After incubation, the cells were washed twice with KRPH buffer containing 0.1% BSA and then 25 μL of 0.1 N NaOH was added. To degrade NAD(P)H, $NAD(P)^+$ and any enzymes in the cells, the culture plate was subjected to one freeze-thaw cycle and incubated at 85°C for 40 min on a temperature-controlled bath. The components in the wells were then neutralized by the addition of 25 μL of 0.1N HCl and then 25 μL of 150 mM TEA buffer (pH 8.1) was added. Uptake of 2DG into the cells was measured by the enzymatic fluorescence assay described above. A standard curve was generated by placing 2DG standard solutions in wells of the culture plate that had been prepared without cells.

Mature 3T3-L1 adipocytes on a 24 well culture plate were washed with KRPH buffer containing 0.1% BSA and were stimulated for 30 min with KRPH buffer containing 100 nM insulin.

After the stimulation, cells were washed with KRPH buffer containing 0.1% BSA and were added KRPH buffer containing 1mM 2DG and 0.1% BSA to start 2DG uptake. After 5 min, to stop 2DG uptake, cells were washed with KRPH buffer containing 0.1% BSA and added 300 µL of 0.1 N NaOH. The culture plate was heated on a temperature-controlled bath (85°C) for about 40 min until the plate was dried. The components of the wells were neutralized by the addition of 300 µL of 0.1 N HCl and then 300 µL of 150 mM TEA buffer (pH 8.1) was added. For determination of uptake of 2DG into the cells, 25 µL of cell extract was transferred to 96 well assay plate. Concentration of DG6P was measured by the enzymatic fluorescence assay after incubation with 200 µL of assay solution (described above; The concentration of resazurin was set to 10 µM) for 45 min. A standard curve was generated by placing 2DG standard solutions in blank wells of the assay plate.

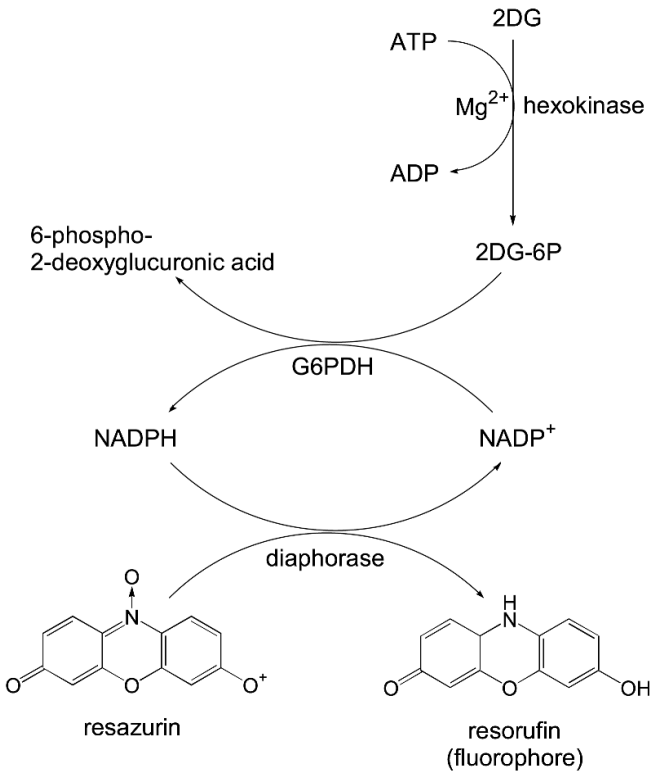

Fig. 2-1. Principle of the assay for measuring 2DG and DG6P. The complete reaction mixture comprised 50 mM TEA (pH 8.1), 50 mM KCl, 0.5mM $MgCl_2$, 0.02% BSA, 670 µM ATP, 0.12 µM $NADP^+$, 25 µM resazurin, 5.5 units/mL hexokinase, 16 units/mL G6PDH, and 1 unit/mL diaphorase. The concentration of $NADP^+$ in the assay cocktail could be kept low because $NADP^+$ is recycled in this system. For measuring DG6P alone, ATP and hexokinase could be left out of the assay cocktail described above. Theoretically, the amount of resorufin derived should be equal to the amount of 2DG and/or DG6P if the reaction goes to completion.

At day 14 after plating the hippocampal cells, neurons were washed twice with Locke's buffer (154 mM NaCl, 5.6 mM KCl, 2.3 mM CaCl, 3.6 mM NaHCO, 3.5 mM HEPES) without serum

or glucose. Neurons were incubated in Locke's buffer for 1 h at 37°C in 5% CO_2 for insulin starvation with and without glucose glucose, followed by exposure to insulin (1 mM) for 4 h. After terminating the exposure to insulin, the cells were treated with 40 mM KCl for 3 min, and then incubated with Lokes buffere containing 1 mM 2DG for 20 min. The incorporation of 2DG was terminated by three washes with ice-cold PBS and then uptaken 2DG was determined by an enzymatic assay described above. A standard curve was generated by placing 2DG standard solutions in wells of a culture plate lacking cells but prepared similarly.

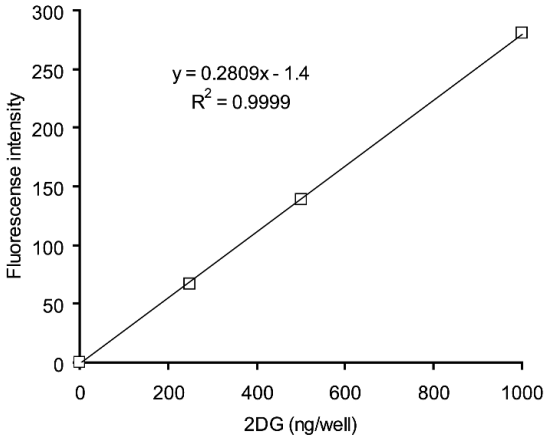

Fig. 2-2. Determination of 2DG in a 96-well plate by an enzymatic fluorescence assay. 2DG solution (50 μL) was dispensed into a 96-well microplate and mixed with 150 μL of assay cocktail as described under Materials and Methods. After incubation of the plate for 90 min at 37°C, the fluorescence (excitation, 590 nm; emission, 530 nm) was measured.

2-3. Results

2-3-1. Determination of 2DG in a 96-well microplate format by an enzymatic fluorescence assay

To facilitate the determination of low concentrations of 2DG and/or DG6P in a 96-well microplate format, we developed a nonradioisotope enzymatic assay based on previously described methods [131,139]. In contrast to these previous methods, which were based on NADPH detection, we detected the fluorescence of resorufin, which is generated from resazurin in the presence of NADPH and diaphorase (**Fig. 2-1**). Whereas the method of Sasson *et al*. [131], which detected NADPH fluorescence, required stoichiometric quantities of $NADP^+$ (120 μM), a low concentration of $NADP^+$ (0.12 μM) could be used in our assay cocktail because $NADP^+$ was recycled by the diaphorase–resazurin system. In our assay system, free 2DG was phosphorylated to DG6P by

hexokinase contained in the assay cocktail, but if needed an assay cocktail lacking ATP and hexokinase could theoretically be used to react with only DG6P. Fifty microliters of 2DG solutions of known concentration was dispensed into a 96-well plate and mixed with 150 μL of the assay cocktail. After incubation of the plate for 90 min at 37°C, fluorescence intensity was measured to detect resorufin derived from reduced resazurin (**Fig. 2-2**). The fluorescence intensity was found to correlate linearly with the increasing concentrations of 2DG and the enzymatic assay was able to detect 2DG on a nanomole scale.

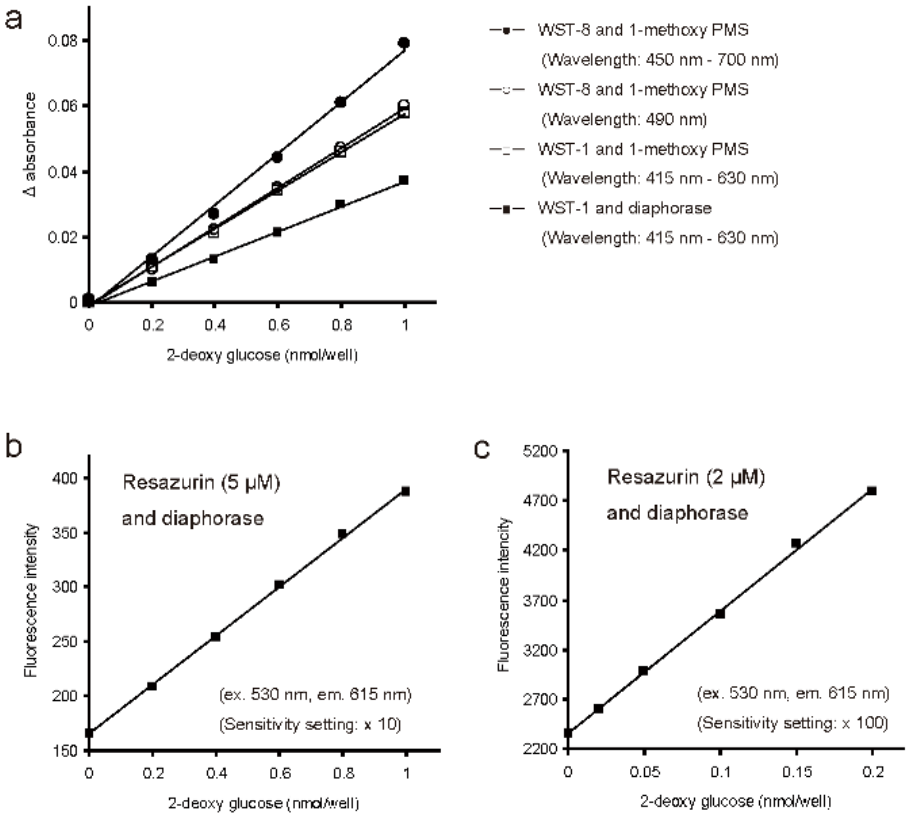

Fig. 2-3. Sensitivity comparison of amplifications to measure 2DG by resazurin and tetrazolium salts. (a) Tetrazolium salts-amplified determination of 2DG. (b) Resazurin-diaphorase-amplified determination of 2DG. (c) Resazurin-diaphorase-amplified determination of further low concentration of 2DG.; Highly water soluble tetrazolium salts, WST-1 and WST-8, were applied to an enzymatic 2DG determination, and diaphorase or 1-methoxy PMS was used as an electron carrier. How to prepare and compositions of the assay solution were described in *Materials and methods* and shown in Table 2-1. An assay solution containing WST-8 was prepared by utilizing a Cell Counting Kit-8 (Dojindo Laboratory) containing 5 mM WST-8 and 0.2 mM 1-methoxy PMS. Various concentrations of 2DG solutions (20 μL) were dispensed in a clear polystyrene 96-well assay plate and 150 μL of assay solution was added, followed by incubation at 37°C for 60 min. In case of tetrazolium salts, absorbance was recorded by a plate reader, and in case of resazaurin, fluorescence was recorded.

2-3-2. Comparison of amplification by resazurin and tetrazolium salts

Given that the amplification obtained by using resazurin and diaphorase detected the amount

of NAD(P)H, other amplification systems which detect NAD(P)H were tested. Highly water-soluble tetrazolium salts, WST-1 and WST-8 were used in the assay of 2DG, and mPMS, which is less photosensitive than phenazine methosulfate, and diaphorase were used as hydrogen carriers. All the systems which used WST-1/diaphorase, WST-1/mPMS and WST-8/mPMS allowed the measurement of 2DG (**Fig. 2-3**). The use of tetrazolium salts would be particularly useful in laboratories lacking a fluorescent plate reader. However, the system of resazurin-diaphorase is much more sensitive.

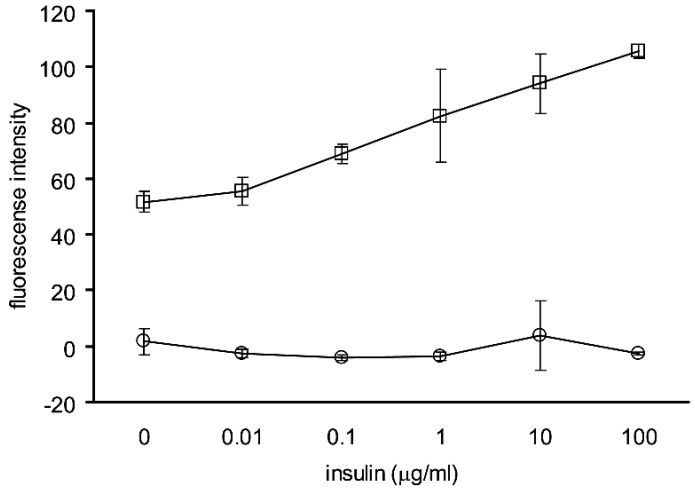

Fig. 2-4. Effect of insulin on 2DG uptake into cultured L6 skeletal muscle cells. Differentiated L6 myotubes in a 96-well plate were stimulated with insulin for 4 h and then incubated with 1mM 2DG in KRPH buffer (–□–) or α-MEM containing ca. 5 mM glucose (–○–) for 2 h. After the glucose uptake period, the myotubes were lysed with alkali solution and heated and neutralized, and then 2DG and 2DG6P in the cell lysate were measured by the enzymatic fluorescence assay. Each data point is the mean ± SD from triplicate determinations.

2-3-3. Detection of insulin-stimulated 2DG uptake in L6 myotubes in a 96-well microplate format

To confirm that our assay system could evaluate the uptake of 2DG in response to insulin stimulation in cultured skeletal muscle cells, differentiated L6 myotubes were stimulated with insulin (~100 μg/mL in α-MEM) for 4h, and then incubated for 2 h with either KRPH buffer plus 1 mM 2DG or α-MEM without 2DG. After incubation, the myotubes were lysed and heat-treated with alkali, and 2DG uptake in the cells was measured by our enzymatic fluorescence assay system (**Fig. 2-4**). The accumulation of 2DG in the incubated myotubes could be measured, and the uptake of 2DG was increased dose-dependently by stimulation with insulin. Although glucose and glucose-6-phosphate were detected by this enzymatic assay, the fluorescence intensity of the control myotubes not treated with 2DG did not increase despite the presence of a high concentration (ca. 5 mM) of glucose in the

medium. The reason for this lack of fluorescence increase is that, although glucose and 2DG are transported similarly into cells and phosphorylated by hexokinase, the DG6P form accumulates because, unlike glucose, it cannot be converted to an analog of fructose-6-phosphate or another rapidly metabolized form [133].

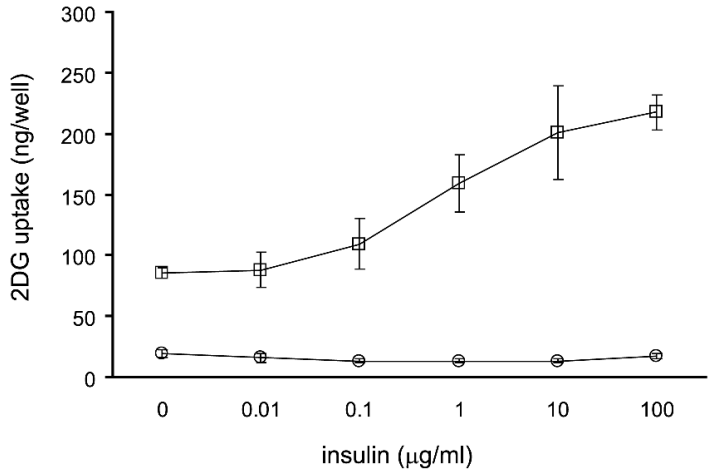

Fig. 2-5. Effect of cytochalasin B on insulin-stimulated 2DG-uptake into L6 myotubes. Differentiated L6 cells were preincubated with insulin (~100 μg/mL), followed by incubation with 1 mM 2DG for 30 min with 10 μM cytochalasin B (–○–) or without cytochalasin B (–□–). After the 2DG-uptake period, the uptake of 2DG in the cells was measured as described under Materials and Methods. Each data point is the mean ± SD from triplicate determinations.

2-3-3. Evaluation of regulators of 2DG uptake in cultured myotubes

As regulators of glucose uptake have been reported, we were able to further test our assay system by evaluating the effects of cytochalasin B, an inhibitor of the hexose carrier [141], and LY294002, an inhibitor of GLUT translocation that acts through blocking phosphatidylinositol 3-kinase (PI3K) [142]. L6 myotubes were differentiated in 96-well microplates, stimulated with insulin for 4h, and then incubated for 30 min with KRPH buffer containing 1 mM 2DG and 10 μM cytochalasin B. After incubation, the uptake of 2DG was determined by our enzymatic assay. As shown in **Fig. 2-5**, cytochalasin B completely inhibited the uptake of 2DG in myotubes, despite stimulation with insulin. As a second test, L6 myotubes differentiated in a 96-well microplate were treated with 25 μM LY294002 for 30 min and then stimulated with 100 nM insulin plus 25 μM LY294002 for 4 h. After stimulation, the myotubes were incubated with 1 mM 2DG in KRPH buffer and 2DG uptake in the myotubes was determined by our enzymatic assay. As shown in **Fig. 2-6**, LY294002 inhibited the insulin-stimulated uptake of 2DG in myotubes. Moreover, we evaluated the effect of pioglitazone, a derivative of thiazolidinediones that acts as insulin-sensitizing diabetes agents [143,144], on the uptake of 2DG in cultured skeletal muscle cells. L6 myotubes differentiated in a

96-well microplate were stimulated with pioglitazone for 4 h, and then incubated with 2DG for 30 min before the uptake of 2DG was determined. As shown in **Fig. 2-7**, pioglitazone dose-dependently increased uptake of 2DG into the myotubes in the absence of insulin.

2-3-4. Application of the enzymatic 2DG uptake assay to adipocytes and nerunal cells

To confirm that our assay system could evaluate the uptake of 2DG in response to insulin stimulation in cultured adipose cells, differentiated 3T3-L1 adipocytes in a 24 well plate were stimulated with insulin (100 nM in DMEM) for 4h, and then incubated for 2 h with either KRH buffer plus 1 mM 2DG. After the stimulation, 2DG uptake assay was carried out. As shown in **Fig. 2-8A**, up-regulation of 2DG uptake by insulin was detected. We also confirmed the application for measurement of 2DG uptake in primary nerunal cells. The uptaken 2DG in the insulin-stimulated neurons was increased statistically significantly to be compared with that of control (**Fig. 2-8B**). Though the total 2DG uptaken in nerunal cells was rather low, our assay could evaluate the 2DG uptake in the cells.

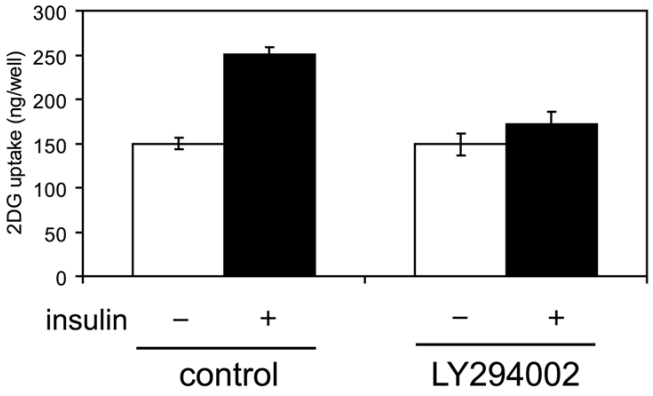

Fig. 2-6. Effect of LY294002 on insulin-stimulated 2DG-uptake into L6 myotubes. Differentiated L6 cells were preincubated with 25 μM LY294002 for 30 min and then either untreated or treated with 100 nM insulin in the presence of 25 μM LY294002 for 4 h, before being incubated with 1 mM 2DG for 20 min. Control cells were not treated with LY294002 but were treated with or without insulin. After the 2DG-uptake period, 2DG uptake into the cells was measured as described under Materials and Methods. Each data point is the mean ± SD from triplicate determinations.

2-4. Discussion

Glucose uptake in cultured cells is routinely determined by using nonmetabolizable radioactive hexoses, such as 3MG or 2DG, labeled with a high specific activity of tritium [131]. Assaying the uptake of [^{3}H]2DG is more convenient than assaying the uptake of [^{3}H]3MG because 2DG is converted to a stable and impermeable derivative DG6P through phosphorylation by hexokinase or glucokinase [133]. Because both methods rely on the use of substantial amounts of radioactive material, the concentration of the unlabeled analog is usually kept low (100–500 μM) in the uptake mixture to maintain a high specific activity [131]. Measuring the uptake of these analogs at concentrations comparable to normal or pathological blood glucose levels (>5 mM) is not practical because of the excessive amount of radioactive analog that would be required to maintain a specific activity high enough to obtain reliable data. Furthermore, the high concentration of analog needed is very expensive and a specialized institution registered for using radioactive isotopes is required. Although new radiolabeled glucose analogues for use as tracers of glucose uptake have been synthesized, none of these molecules has been found to show the same biological behavior as 2DG [145]. Therefore, 2DG is often considered to be the gold standard in reference tracers of glucose transport and phosphorylation.

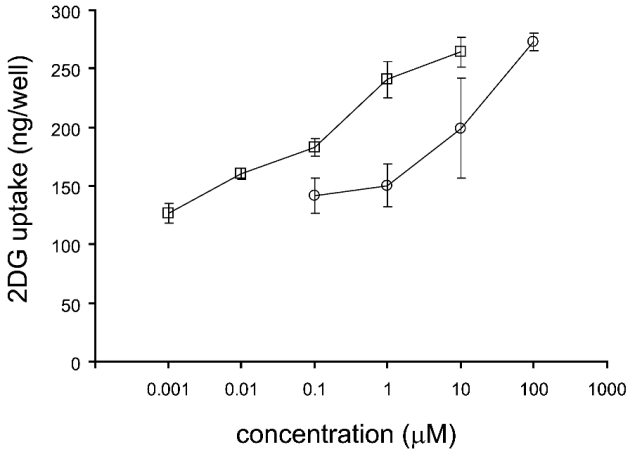

Fig. 2-7. Effects of pioglitazone on 2DG-uptake into L6 myotubes. Differentiated L6 cells were stimulated with insulin (–□–) or with pioglitazone in the absence of insulin (–○–) for 4 h and then 2DG uptake into the cells was determined as described under Materials and methods. The 2DG uptake period was set for 30 min. Each data point is the mean ± SD (N = 4).

Previously, Manchester *et al*. [139] and Sasson *et al*. [131] developed an enzymatic assay for evaluating 2DG uptake into tissues and cultured cells that avoids the need for radioisotopes. Their methods were based on the assay of DG6P, which is monitored by the detection of NADPH produced during the oxidation of DG6P to 6-phospho-2-deoxyglucronic acid. These assays permit the use of high 2DG concentrations and have the advantage of reflecting hexose transport rates at substrate levels of physiological significance [131]. In addition, the determination of DG6P can be performed in 96-well microplates and analyzed in a suitable plate-reader to expedite the procedure. Many cells are required for these assays, however, and cell extracts must be prepared because the fluorescence intensity of NADPH is rather low. Moreover, if a test compound has UV absorbency and adheres to the cell membrane, the measurement of 2DG uptake into cells may be affected because the wavelength used to detect NADPH fluorescence is in the UV range (340 nm).

The NADPH concentration can be monitored by direct measurement of its incipient fluorescence but, because it is rapidly turned over [reoxidized to $NADP^+$], absolute levels of NADPH do not reflect the level of enzymatic and metabolic activity occurring within the cell. Furthermore, background interference from other biochemical entities in a cell or from chemical compounds added during the test study can also obscure any reliable estimation. As a consequence, there is considerable interest in using reagents that are themselves selectively reduced by NADPH to produce either a colored or a fluorescent signal. Because few dye precursors react directly with NADPH, a catalyst is usually used. The catalyst is either an enzyme, such as diaphorase [146], or an electron carrier, such as mPMS [147]. For example, the NADPH-based reduction of colorless or yellow tetrazolium salts, such as 3-(4,5-dimethy-2-lthiazolyl)-2,5- diphenyl-2*H*-tetrazolium bromide (MTT) or 2-(4-iodophenyl)-3-(4-nitrophenyl)-5-phenyl-2*H*- tetrazolium chloride (INT), does not occur by a direct interaction but rather is catalyzed by the enzyme diaphorase to form an intensely colored formazan dye, which is generally insoluble and nonfluorescent. The weakly fluorescent dye resazurin, which is reduced by NADPH in the presence of either diaphorase or mPMS, has also been used to produce the strongly fluorescent dye resorufin [148]. We confirmed our ability to measure 2DG using NADPH-based reduction of highly water soluble tetrazolium salts such as WST-1 and WST-8. This reaction does not occur as a direct interaction but rather is catalyzed by the enzyme diaphorase or mPMS as electron carrier (**Fig. 2-3**). It was thought possible to also measure 2DG uptake by these methods in *in vitro* assays which would allow assays to be performed in labs which lack a means of measuring fluorescence. However, the method using resazurin was markedly superior in terms of sensitivity.

Based on the above information, we considered that the resazurin–diaphorase-amplifying system would be suitable to facilitate measurement of NADPH in the 2DG uptake assay, because the resorufin fluorophore produced is water soluble and has high fluorescence intensity; in addition, there will be little background interference from other biochemical entities in the cell or from chemical compounds added during the assay because the emission wavelength of resorufin is longer and its fluorescence wavelength is much longer than those of NADPH. Furthermore, analysis of resorufin can be measured on standard, clear tissue-culture plates because the material comprising the culture plate,

such as polystyrene, does not interfere with the fluorescence signal of resorufin.

The principle of our new method can be summarized as follows. In the first reaction, hexokinase catalyzes the conversion of 2DG to DG6P. In the second reaction, G6PDH catalyzes the conversion of DG6P to 2-deoxy-6-phosphogluconate, coupled with the conversion of $NADP^+$ to NADPH. In the third reaction, diaphorase catalyzes the conversion of resazurin to resorufin, coupled with the conversion of NADPH to $NADP^+$ (**Fig. 2-1**). In this chain reaction, $NADP^+$ and NADPH are recycled between the second and the third reaction; thus, a low concentration of $NADP^+$ (0.12 μM) can be used in the assay cocktail in contrast to the stoichiometric quantities of $NADP^+$ (120 μM) required in the method of Sasson *et al*. [131], which detected the fluorescence of NADPH. Theoretically, this chain reaction should continue until 2DG and DG6P are consumed, and the resorufin fluorophore generated should be equivalent to the amount of 2DG and DG6P. In addition, measurement of DG6P alone can be achieved by preparing an assay cocktail without ATP and hexokinase.

The G6PDH enzyme used in this method must have substrate specificity for DG6P and $NADP^+$. G6PDH enzymes can be distinguished on the basis of their nucleotide specificity [149]. One group exemplified by enzymes from brewer's yeast, *Candida utilis*, and *Escherichia coli* reacts with $NADP^+$. A second group, which appears to include animal G6PDH enzymes in general, reacts with $NADP^+$ but also reacts weakly with NAD^+ and some of its analogues. The third group of G6PDH can react approximately equally well with $NADP^+$ and NAD^+. This group includes enzymes from *Leuconostoc mesenteroides*, *Pseudomonas aeruginosa*, *Hydrogenononas H16*, and *Thiobacillus ferrooxidans* [149]. We evaluated some commercially available enzymes for their utility in 2DG and/or DG6P determination (data not shown). Among the enzymes tested, the G6PDH from *L. mesenteroides* had specificity for 2DG [149] and was found to be the most suitable. However, because its specificity for DG6P was lower than its specificity for G6P, a large amount of enzyme was needed. Because our assay system for 2DG and/or DG6P determination can be applied to high-throughput screening for enzymes with high specificity to DG6P, we expect to identify a new cost-effective enzyme in the future.

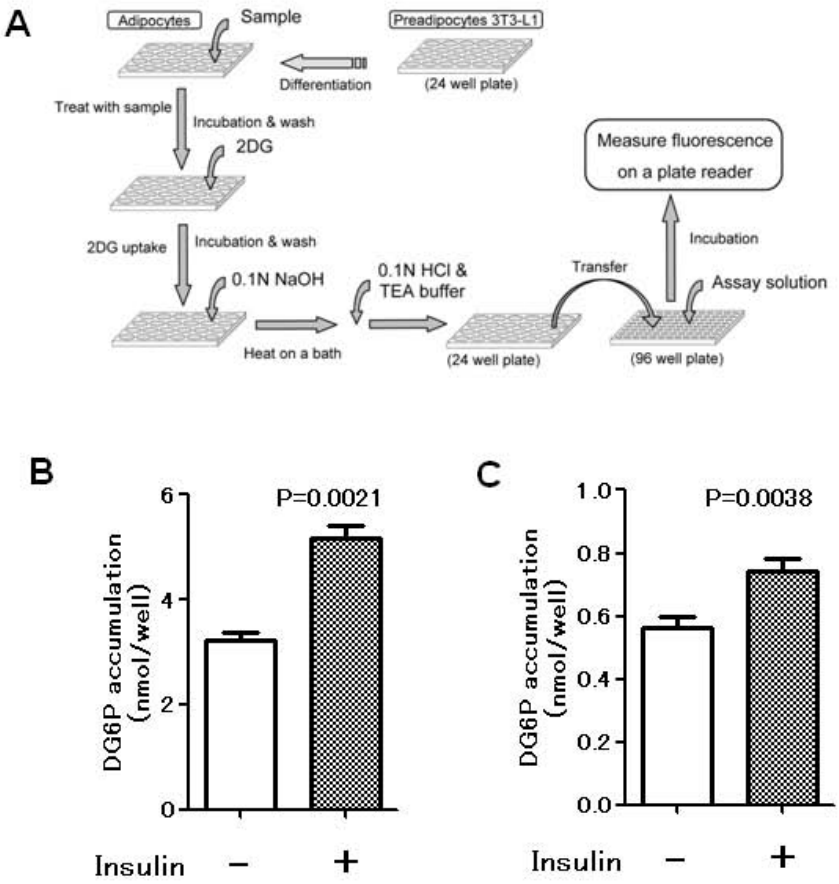

Fig. 2-8. 2DG uptake assay performed in cultured 3T3-L1 adipose cells and plimary neuronal cells. (**B**) 2DG uptake assay performed in cultured 3T3-L1 adipose cells. Mature cells (n=3) in a 24-well culture plate were stimulated with 100 nM of insulin for 30 min, and were treated with non-radiolabeled 2DG. Uptaked 2DG in cells was measured in a 96-well transparent assay plate. (**C**) 2DG uptake assay performed in cultured neuronal cells. Rat brain hippocampus neuronal cells (n=12) in a 24-well culture plate were stimulated with insulin for 4 h. After the stimulation, the cells were treated with 40 mM KCl ,and then after 3 min 2DG uptake assay was carried out. Data are shown mean ± SD and *p*-values are from unpaired Student's *t*-test.

In this study, using our new method, we evaluated the effects of insulin, cytochalasin B (hexose uptake inhibitor) [141], LY294002 (inhibitor of translocation of GLUT thorough PI3K inhibition) [142], and pioglitazone hydrochloride (insulin-sensitizing agent) [143,144] on the uptake of 2DG into L6 skeletal muscle cells cultured in a 96-well tissue culture plate. L6 myotubes stimulated by insulin showed an increase in 2DG uptake (**Fig. 2-4**), whereas 2DG uptake was completely inhibited by cytochalasin B (**Fig. 2-5**). These results suggest that 2DG uptake is increased by insulin and should reflect the amount of 2DG that was transported by GLUTs is and phosphorylated because cytochalasin B is known to inhibit glucose transport by binding to GLUTs. Uptake of 2DG into L6 myotubes was partially inhibited by LY294002 (**Fig. 2-6**), suggesting that the increase in 2DG uptake

in muscle caused by insulin is dependent on PI3K, a mediator of insulin action, and that the remaining uptake in 2DG was caused by ubiquitous GLUT1, as LY294002 is known to be an inhibitor of the PI3K that mediates GLUT4 translocation [150]. In the next test, the known insulin-sensitizing agent pioglitazone dose-dependently increased 2DG uptake into L6 myotubes in the absence of insulin (**Fig. 2-7**). This result suggests that the increased 2DG uptake induced by pioglitazone was dependent on its high affinity for the nuclear peroxisome proliferator-activated receptor γ (PPARγ), which promotes GLUT4 translocation to the cell membrane [151,152]. Thus, our method was clearly able to evaluate the effects of glucose uptake regulators in tissue culture.

Importantly, skeletal muscle is a major mass peripheral tissue, accounting for ~40% of the total body mass and >30% of energy expenditure. Hence, skeletal muscle has a paramount role in energy balance and is the primary tissue for insulin-stimulated glucose uptake, disposal, and storage (showing fourfold the glycogen content of liver). Therefore, skeletal muscle must be considered an important therapeutic target tissue in the battle against NIDDM and CVD [153]. Thus, methods for evaluating regulators of glucose uptake in muscle cells or tissue, such as our method, will be useful in strategies to develop new drugs or to evaluate food factors. Finally, although skeletal muscle cells express both GLUT4 and GLUT1 and are capable of increasing glucose transport *via* stimulation with insulin [136], it will be necessary to investigate whether uptake is caused by translocation of GLUT4.

Adipose tissue is also considered to be an important tissue in metabolic regulation and insulin resistance, and it may play an important role in the mechanism of action of glucose-uptake regulators [154]. We found that our method for measuring 2DG uptake into cells was also applicable to mature adipocytes (differentiated 3T3-L1 cells) (**Fig. 2-8B**). Because differentiated adipocytes are nonadherent, in this assay 3T3-L1 cells were differentiated in a 24-well plate, to which the test compound and 2DG were added. After the 2DG-uptake period, the cells were collected into a micro-test-tube and were lysed and heat-treated. The cell lysate was then transferred into a 96-well assay plate, and the amount of 2DG that had been taken up into the cells was measured by our enzymatic assay.

We also showed the up-regulation of 2DG uptake in rat hippocampus neuronal cells stimulated by insulin. As shown in **Fig.2-8C**, the uptaken 2DG in the insulin-stimulated neurons was increased statistically significantly to be compared with that of control. In nerve cells, insulin bind to receptors and promotes membrane transport system itself appears to be the limiting factor. It is known that two isomers, GLUT1 and GLUT3 are expressed in neuronal cells. Expression of both isoforms increased as neurons differentiated in culture, corresponding to an increase in glucose uptake [155]. It was thought that expression or translocation of these GLUTs were related with the result. Recently, using our method, Miichi et al. studied the effects of insulin on neuronal 2DG uptake in hippocampal neurons exposed to insulin (1 mM) for 30 min after insulin starvation [156]. However, they did not observed insulin-dependent increase of neuronal 2DG uptake. Whatever the case, they confirmed that our method was useful for evaluation of glucose uptake in neuronal cells.

In conclusion, we have developed a method for evaluating 2DG uptake in cells cultured in a

96-well microplate by a simple incubation with a single total-assay reaction mixture, coupled with fluorescence detection. This method is clearly able to evaluate the effects of glucose uptake regulators, such as insulin, cytochalasin B, and LY294002. Therefore, our simple method may be useful for *in vitro* high-throughput screening and for evaluating glucose-uptake regulators.

Chapter 3

A non-radioisotopic, enzymatic microplate assay for *in vivo* evaluation of 2-deoxyglucose uptake

3-1. Introduction

Skeletal muscle insulin resistance is a silent feature of type 2 diabetes (T2DM). In humans and other mammals, skeletal muscle normally accounts for approximately ~70% of whole body insulin stimulated glucose transport [128,157,158]. Therefore, in order to develop novel anti-diabetic therapeutic agents, it is important to identify small molecules that serve as insulin mimetics or insulin sensitizers in skeletal muscle. Such compounds would serve to augment glucose uptake and anabolic metabolism, thereby normalizing excessive blood glucose levels. Glucose uptake in cultured cells and in tissues is regularly determined using non-metabolizable radioactive hexoses, such as 3-*O*-methylglucose (3MG) or 2-deoxy-D-glucose (2DG), labeled with tritium or ^{14}C at high specific activities. The uptake assay of [^{3}H or ^{14}C] 2DG is more convenient due to the fact that it becomes phosphorylated to the stable and impermeable derivative 2-deoxyglucose-6-phosphate (DG6P) by hexokinase (HX) or glucokinase [133]. However, routine use of these radiolabeled analogues requires a specialized institution where isotopes can be handled.

We have previously reported a non-radioisotopic, 96-well-microplate assay that can be used to evaluate glucose uptake activity in cultured cells [159] (***see Chapter 2***). This method is based on the assay of glucose-6-phosphate dehydrogenase (G6PDH), with resazurin-diaphorase amplifying detection of NADPH produced during the oxidation of DG6P to 6-phospho-2-deoxyglucuronic acid. The reaction involves addition of a single assay solution and incubation, followed by detection of the potent fluorophore, resorufin. The assay solution contains HK, Mg^{2+}, ATP, G6PDH, NADP, diaphorase and resazurin. Although transported 2DG is converted to DG6P and accumulates in cells, 2DG could be used as a standard in the previous in vitro assay, because glucose in the culture medium was washed out. Uptake of 2DG by cells was therefore evaluated in the absence of glucose with the assay solution containing Mg^{2+}, ATP and HK, resulting in the conversion of 2DG to DG6P. The principles of the assay are based on classical enzymatic methodology and the assay allows direct and quantitative measurement of levels of DG6P, 2DG, glucose and G6P and is useful for in vitro high-throughput screening and for evaluating regulators of glucose transport [159]. Using this methodology, we confirmed that our assay system could also determine 2DG uptake in cultured adipose 3T3-L1 cells. However, to evaluate 2DG uptake in an in vivo study using the enzymatic method, separate detection of glucose, 2DG, G6P and DG6P was needed because the tissue levels of glucose are much higher than those of 2DG and DG6P.

In this chapter, we describe application of this classical enzymatic method to an in vivo

mouse study. Prior to the animal experiment, we developed methods to allow measurement of glucose, 2DG, G6P and DG6P separately. This was achieved using four different reaction solutions, the composition of which changed depending on the compound being assayed. Using this assay system, we demonstrate the detection of 2DG in blood and the detection of DG6P accumulation in muscle tissue [160]. These methods are based on the assays for DG6P and G6P, which monitor resazurin-diaphorase-amplified detection of NADPH produced during G6PDH catalyzed oxidation of DG6P and G6P. To quantitate glucose, 2DG, G6P and DG6P separately, we proposed using four independent, single reaction mixtures containing G6PDH from *Leuconostoc mesenteroides* and *Candida utilis* (tolura yeast).

Several years later, *C. utilis* G6PDH was no longer sold by Sigma-Aldrich and a substitute distributor did not exist. So, we had to improve our assay system without using *C. utilis* G6PDH. A short time later, we improved our assay method by incorporating minor modifications for the use of *L. mesenteroides* G6PDH. In this chapter, we also describe the improved assay system.

3-2. Materials and methods

3-2-1. Materials

2DG (Grade III), DG6P sodium salt, HK from *S. cerevisiae*, G6PDH from *C. utilis*, recombinant *L. mesenteroides* G6PDH and bovine pancreas insulin were purchased from Sigma–Aldrich (St. Louis, MO). ATP, β-NAD, -NADP and diaphorase from *C. kluyvery* (Type II-L) were purchased from Oriental Yeast (Tokyo, Japan). Resazurin sodium salt, triethanolamine hydrochloride (TEA), glucose oxidase (GOD, from *Aspergillus niger*) and other general chemicals were purchased from Wako Pure Chemical (Osaka, Japan).

3-2-2. Determination of glucose, 2DG, G6P and DG6P

We measured glucose, 2DG, G6P and DG6P using the previously published assay for determining 2DG uptake in cultured cells [159], with slight modification. We prepared four assay solutions (cocktails A, B, C and D) as described in **Table 3-1**. The reaction schemes are illustrated in **Fig. 3-1**. To determine total glucose, 2DG, G6P and DG6P, assay cocktail A was used. This cocktail was almost the same as the assay solution in our previous work and contained 50 mM TEA (pH 8.1), 50 mM KCl, 2 mM magnesium acetate, 0.02% BSA, 0.1 mM NADP, 0.5 mM ATP, 25 μM, 2–10 μM resazurin sodium salt, 0.2 units/mL diaphorase, 2 units/mL HK and 20 units/mL recombinant *L. mesenteroides* G6PDH. Cocktail B contained 0.1 units/mL *C. utilis* G6PDH in place of *L. mesenteroides* G6PDH in cocktail A and was used for determination of glucose plus G6P. Cocktail C was prepared by omitting magnesium acetate, ATP and HK from the preparation of cocktail A, and was used for determination of G6P plus DG6P. Cocktail D was used for determination of G6P alone and contained 0.1 units/mL *C. utilis* G6PDH in place of *L. mesenteroides* G6PDH in cocktail C. Each

assay cocktail was prepared before each assay from stock solutions of enzymes, coenzymes and substrate that were maintained in a freezer or a refrigerator. Test samples (2–10 μL in 384 well format, 5–25 μL in 96 well plate assay) were mixed with each cocktail (100 μL in 384 well format, 200 μL in 96 well format), and were then incubated. Incubation time was set to 30 min for cocktails A and C, and 45–60 min for cocktails B and D. After each incubation, fluorescence at 615 nm (excitation at 530 nm) was measured on a MTP-800 microplate reader (Corona Electric, Hitachinaka, Japan) to detect the resorufin derived from reduced resazurin. Calculations are based on standards and blanks carried through the assay. [DG6P] is calculated from the difference between [G6P + DG6P] and [G6P], and [2DG + DG6P] is calculated from the difference between [glucose + 2DG + G6P + DG6P] and [glucose + G6P]. [glucose] and [2DG] can also calculated. If the sample solution contains vanishingly small amount of G6P and DG6P, assay cocktails A and B may be also used for determination of glucose and 2DG.

Table 3-1. The final concentrations of reagents in assay solutions.

Assay Cocktail	A	B	C	D
Target compound for detection	glucose 2DG G6P DG6P	Glucose G6P	G6P DG6P	G6P
TEA buffer (pH 8.1)	50 mM	50 mM	50 mM	50 mM
KCl	50 mM	50 mM	50 mM	50 mM
Magnesium acetate	2 mM	2 mM	---	---
Bovine serum albumin (BSA)	0.02%	0.02%	0.02%	0.02%
NADP	0.1 mM	0.1 mM	0.1 mM	0.1 mM
ATP	0.5 mM	0.5 mM	---	---
Diaphorase	0.2 units/mL	0.2 units/mL	0.2 units/mL	0.2 units/mL
Resazurin sodium salt	2–10 μM	2–10 μM	2–10 μM	2–10 μM
Hexokinase	2 units/mL	2 units/mL	---	---
C. utilis G6PDH	---	0.1 units/mL	---	0.1 units/mL
L. mesenteroides G6PDH	20 units/mL	---	20 units/mL	---

Each assay solution was prepared before each assay from stock solutions of enzyme, coenzyme, and substrate that were maintained in a freezer or a refrigerator.[e.g. 200 mM TEA and 200 mM KCl solution (pH 8.1),(R*); 200 mM magnesium acetate, (R); 0.4% BSA in a freezer, (F*); 10 mM NADP, (F); 50 mM ATP, (F); 2 mM resazurin Sodium Salt in 50 mM TEA buffer, (R); 200 units/mL diaphorase in 50 mM TEA buffer, (F).Other enzymes were used as commercial enzyme solutions and were stocked as in each technical sheet. *R and F mean freezer and refrigerator to maintain a stock solution.]

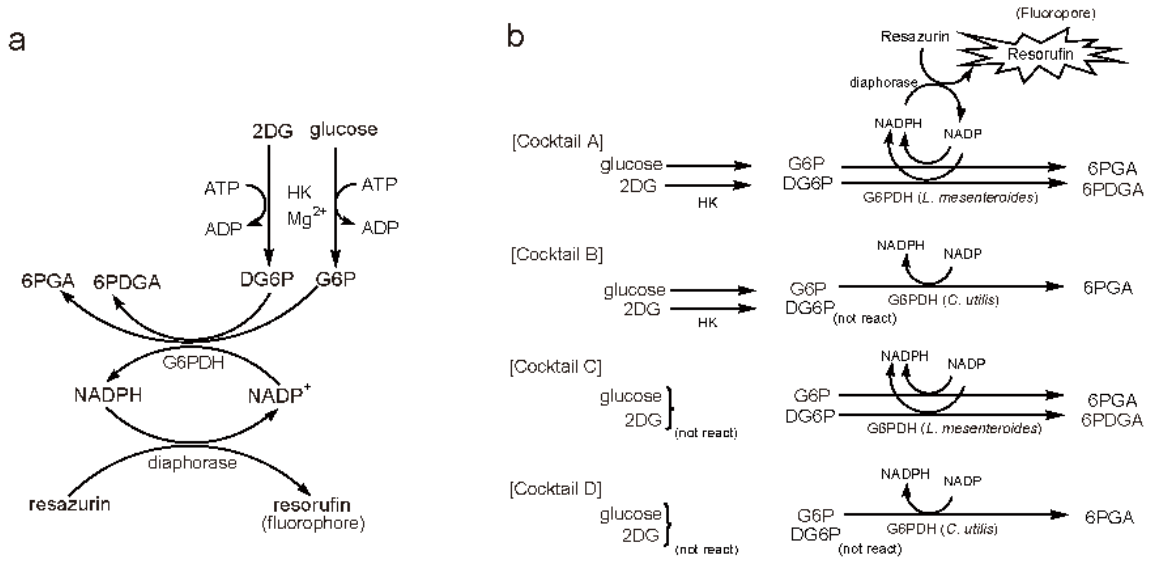

Fig. 3-1. Principle of the assay system for measuring glucose, 2DG, G6P and DG6P. (**a**) Schematic representation of the chain reaction. (i) HK catalyzes the conversion of "glucose to G6P" and "2DG to DG6P" (ii) G6PDH catalyzes the conversion of "G6P to 6PGA" and "DG6P to 6PDGA", coupled with the conversion of "$NADP^+$ to NADPH". (iii) Diaphorase catalyzes the conversion of "resazurin to resorufin", coupled with the conversion of "NADPH to $NADP^+$". Theoretically, the amount of resolufin derived should be equal to the total amount of glucose, 2DG, G6P and DG6P when the assay cocktail A is used. (**b**) Schematic representation of the detections for target molecules by each assay solutions. HK in cocktail A and B catalyzes both conversion of "glucose to G6P" and "2DG to DG6P". *L. mesentriodes* G6PDH in cocktail A and C catalyzes both conversion of "G6P to 6PGA" and "DG6P to 6PDGA", and *C. utilis* G6PDH in cocktail B and D catalyzes only the conversion of "G6P to 6PGA". The assay cocktail A detects total of glucose, 2DG, G6P and DG6P. The assay cocktail B detects total of glucose and G6P. The assay cocktail C detects total of G6P and 2DG6P, and the assay cocktail D detects only G6P. Compositions of each assay cocktail were described in **Table 3-1**. 2DG, 2-deoxyglucose; G6P, glucose-6-phosphate; DG6P, 2-deoxyglucose-6-phosphate; 6PGA, 6-phosphoglucuronic acid; 6PDGA, 6-phospho-2-deoxyglucuronic acid; HK, hexokinase; G6PDH, glucose-6-phosphate dehydrogenase.

3-2-3. Glucose oxidase method

We used a commercial assay kit, Glucose-CII-Test-Wako (Wako Pure Chemical), according to Miwa *et al.* [161], to determine glucose and 2DG by the glucose oxidase (GOD) method. GOD-enriched reaction solution was prepared by adding GOD (from *Aspergillus niger*, Wako Pure Chemical) to a prepared reagent in the kit (plus 100 units/mL in a assay solution of the kit) (**Table 3-2**). Standard solution (10 μL) of glucose or 2DG were placed into a 96 well assay plate and 200 μL of assay solution ("a prepared reagent in the kit" or "a GOD-enriched reagent") was added and then incubated at 37°C. Absorbance at 492 nm was measured by a MTP-800 microplate reader (Corona electric, Hitachinaka, Japan).

3-2-4. Animals

Protocols for animal use were reviewed and approved by the Animal Care Committee of House Wellness Foods Corporation and were in accordance with the guidelines of The Science Council of Japan. Male CD1 (also called ICR) mice were obtained from the Atsugi firm of Charles River Japan (Yokohama, Japan) and were housed in a 12 h light/dark cycle and were fed standard rodent chow, CE-2 (Clea Japan, Tokyo, Japan).

Table 3-2. Composition of assay solution for GOD assay.

	Normal assay solution (a)	GOD-enriched assay solution (b)
phosphate buffer (pH7.1)	60 mM	60 mM
phenol	5.3 mM	5.3 mM
mutarose	0.13 units/mL	0.13 units/mL
GOD	9 units/mL	100 units/mL
horse radish peroxidase	0.65 units/mL	0.65 units/mL
4-aminoantipyline	0.50 mM	0.50 mM
ascorbic acid oxidase	2.7 units/mL	2.7 units/mL

A commercial available kit, Glucose-CII-Test-Wako (Wako Pure Chemical) was used for a normal assay solution (a), and a GOD-enriched assay solution was prepared by adding GOD to the kit (b).

3-2-5. Animal study

Mice (9 weeks old) were food restricted for 6 h (09:00 – 15:00) before the study. 2DG (2 mmol/kg body weight) and insulin (1.5 units/kg body weight) dissolved in saline were intravenously injected into the tail vein of subjects simultaneously (*N*=3). Control mice were injected with 2DG only (*N*=3). Blood samples (ca. 20 μL) were collected at 5 min intervals after the injection and the obtained plasma samples stored in a deep freezer (–85°C). Another set of mice (9 weeks old) were divided into three groups and two groups were intravenously injected with 2DG plus insulin or 2DG alone. The remaining group was untreated. Femoral muscle tissues were removed 30 min after the injection and were 'snap-frozen' in liquid nitrogen and stored in a deep freezer (–85°C).

3-2-6. Determination of glucose and 2DG in blood

The blood samples were diluted 500 fold with H_2O and the diluted plasma (5 μL) was placed in a 384-well assay plate (LUMITRAC 200, Greiner Bio-one). Concentration of [Glucose + 2DG] was determined using 100 μL of assay cocktail A in which the concentration of resazurin was set to 5 μM, and [glucose] was determined using assay cocktail B in which resazurin was set to 5 μM. Concentration of [2DG] was calculated as the difference between [glucose + 2DG] and [glucose] assay values.

3-2-7. Determination of DG6P in muscle

Frozen femoral muscle (50–100 mg) was homogenized on ice in a 9-fold volume of ice-cold deionized water in a 2 mL polypropylene micro-test-tube using a TH-Homogenizer fitted with a 7 mm diameter saw tooth generator probe (Omni International, Warrenton, VA). An aliquot (100 μL) of the homogenate was transferred to a 1.5 mL polypropylene micro-test-tube and 200 μL of 0.1 N NaOH was added, followed by heat treatment at 85°C for 45 min to destroy endogenous NAD(P)H, NAD(P) and enzymes. After heating, the micro-test-tube was cooled and 200 μL of 0.1 N HCl was added to neutralize the alkali and the sample centrifuged at 10,000 × *g* for 5 min. The supernatant (10 μL) was transferred to a 384-well assay plate and incubated with 100 μL assay cocktail C or D, in which the concentration of resazurin was set to 2 μM, for 60 min at 30°C. At the end of the incubation, fluorescence was measured on a plate reader. A standard curve was generated using standards of DG6P and G6P in the same assay plate. A standard curve was generated for each assay. A schematic representation of this protocol is shown in **Fig. 3-2**.

3-2-8. An improved enzymatic, fluorometric assay to quantitate 2-deoxyglucose and 2-deoxyglucose-6-phosphate for in vitro and in vivo

To quantitate glucose, 2DG, G6P and DG6P separately, we proposed using four independent, single reaction mixtures containing G6PDH from *Leuconostoc mesenteroides* and *Candida utilis* (tolura yeast) [159]. However, several years later, Sigma-Aldrich stopped selling *C. utilis* G6PDH and a substitute distributor did not exist. So, we improved our assay method by incorporating minor modifications for the use of *L. mesenteroides* G6PDH. We prepared four independent reaction mixtures, as shown in **Table 3-3**. All the reactions were performed in a 384-well white assay plate at 37°C, and incubation time was set to 45–90 min for cocktails A and C, and 30 min for cocktails B and D. In this case, a smaller amount of G6PDH can be used by increasing the incubation time. At the end of each incubation, fluorescence at 615 nm (excitation at 530 nm) was monitored on a MTP-800 microplate reader.

3-3. Results

3-3-1. Determination of glucose, 2DG, G6P and DG6P

In our previous work [159] (***see Chapter 2***), where we measured 2DG uptake in cultured cells, we used a single assay solution containing HK, Mg^{2+}, ATP, *L. mesenteroides* G6PDH, NADP, diaphorase and resazurin, and used 2DG as standard. However, in this *in vitro* study, although the above assay solution could react with glucose, 2DG, G6P and DG6P, the assay almost exclusively only detected DG6P in cells because the cells had been treated with only 2DG and stable DG6P had accumulated in cells. Because glucose is present in the body, 2DG and glucose, or DG6P and G6P

needed to be measured separately in order to use the 2DG uptake assay in an in vivo study. Therefore, we used two kinds of G6PDH with different substrate specificity. When the reactivities of commercial G6PDHs towards DG6P were investigated, the enzyme from *C. utilis* (tolura yeast) showed the lowest reactivity towards DG6P. Thus, low numbers of units of the *C. utilis* enzyme reacted only with G6P whilst high numbers of units of the enzyme from *L. mesenteroides* reacted with both G6P and DG6P (**Fig. 3-3**). A further step that was required was to improve the assay to allow determination of low concentrations of glucose and 2DG in a 96-well or 384-well microplate format. It was found that just by decreasing the concentration of resazurin in the reaction solution, it became possible to measure low-concentrations of glucose and 2DG. Based on the above, reaction solutions to measure each target molecule were developed as shown in **Table 3-1**. Since measurement sensitivity was raised, the 2DG uptake period in the in vitro study could be shortened to 5 min from about 20 min.

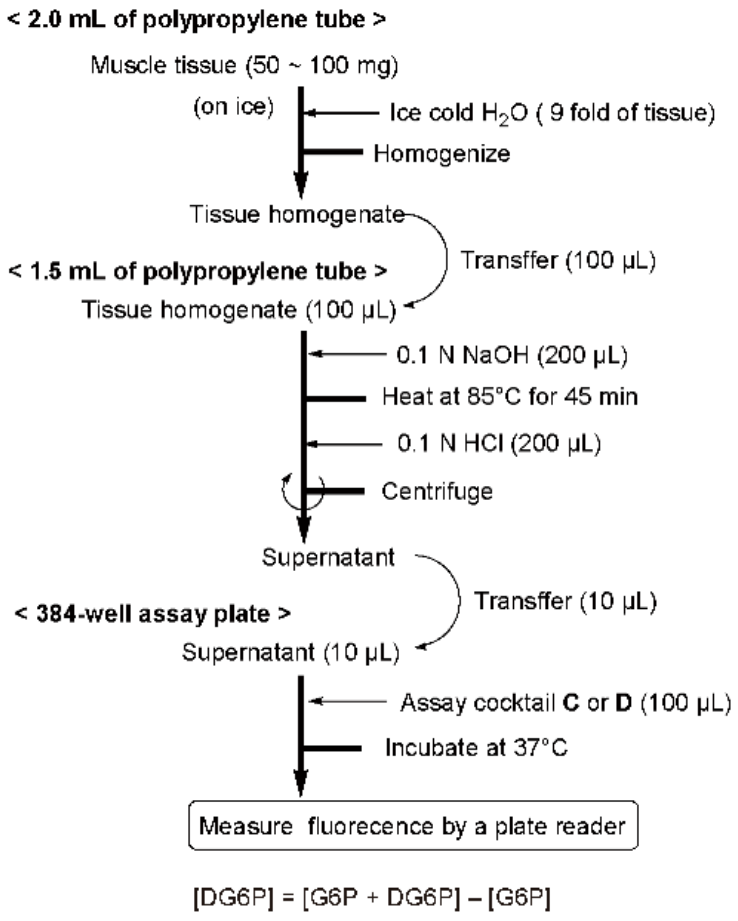

Fig. 3-2 Schematic representation of the determination of DG6P in muscle tissue. Protocol of sample preparation is described in Method. [G6P + DG6P] are measured using Cocktail **C**, and [G6P] is measured with Cocktail **D**. [DG6P] is calculated as the difference between [G6P + DG6P] and [G6P] assay values.

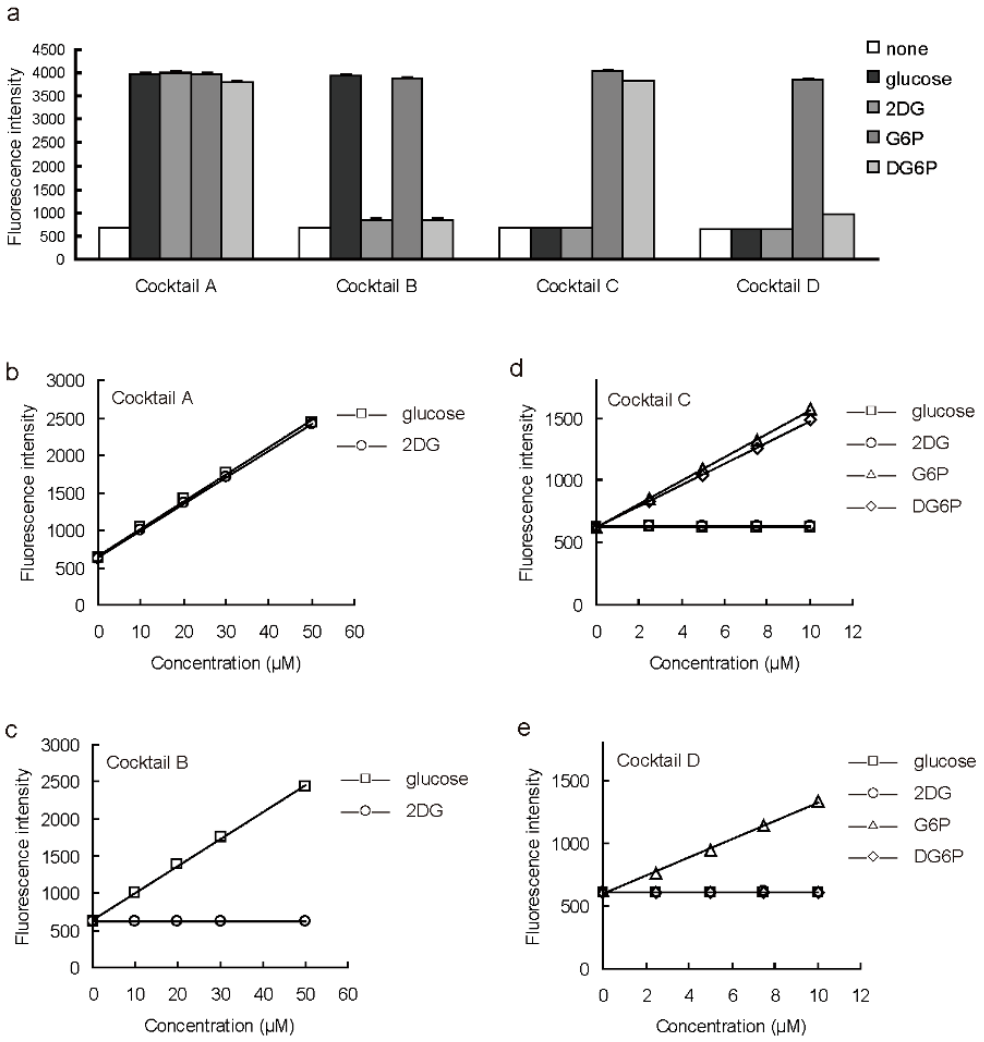

Fig. 3-3. Detection of glucose, 2DG, G6P, and DG6P by assay solutions. (**A**) Comparison of detection of target molecules by each assay solution. The standard solutions (5 μL) of glucose, 2DG, G6P, and DG6P (100 μM each) were reacted with each assay cocktail (100 μL). After incubation of the plate at 37°C for 1 h, fluorescence (ex. 530 nm, em. 615 nm) was measured on a plate reader. The composition of each assay solution is described in the text and the concentration of resazurin in each assay solution was set to 5 μM. (**B, C**) The standard solutions of glucose and 2DG (~50 μM, 5 μL) were reacted with assay cocktails A and B (100 μL), respectively. The reaction time was set to 60 min for cocktail A and 30 min for cocktail B. (**D, E**) The standard solutions of glucose, 2DG, G6P, and DG6P (~10 μM, 10 μL) were reacted with assay cocktails C and D (100 μL). The reaction time was set to 60 min for cocktail C and 30 min for cocktail D. Each data point is the mean ± SD from triplicate determinations.

The glucose oxidase method is used widely by measuring blood sugar. Then, the glucose oxidase method was employed to measure 2DG. Since GOD reacted to both of glucose and 2DG, it was not able to measure separately glucose and 2DG. (**Fig. 3-4**). In other words, the GOD method was able to measure the total amount of glucose and 2DG. Because a resazurin–diaphorase amplifying method has a higher sensitivity to detect glucose than GOD method, we thought that our assay cocktail

A would be useful to detect blood glucose in study using small animals, such as a mouse. The amount of blood could be lessened

3-3-2. Determination of glucose and 2DG in plasma

Glucose and 2DG in plasma from mice which had been injected with 2DG or DG with glucose were measured using this enzymatic assay (**Fig. 3-5**). Since this method was highly sensitive, the amount of blood needing to be collected was less than 10 μL. For this assay, we used only 1 μL of plasma and 5μL of 500 fold diluted plasma. The diluted plasma (5 μL) was reacted with assay cocktail A for determination of total of glucose and 2DG and was reacted with assay cocktail B for determination of glucose. The concentration of 2DG in plasma could be calculated from the data from these two independent reactions. As shown in **Fig. 3-5**, it was observed that the blood glucose level decreased and the concentration of 2DG also fell upon stimulation with insulin. In the absence of insulin stimulation, blood glucose increased slightly upon injection of 2DG.

3-3-3. Determination of insulin-stimulated DG6P accumulation in muscle tissue

To confirm that our assay system could evaluate the uptake of 2DG in response to insulin stimulation in muscle tissue, we injected 2DG and insulin into mice, and determined 2DG accumulation in femoral muscle tissue using our enzymatic assay. The femoral muscle was taken 30 min after injection of 2DG and insulin and stored in a freezer (–85°C). The frozen tissue was homogenized in ice-cold water, the homogenate heat-treated with alkali and the accumulation of DG6P in muscle tissue detected using assay cocktails C and D (**Fig. 3-5 and 3-6**). Because a portion of the glucose which contaminated the tissue sample could potentially be converted into G6P during the pre-treatment of the sample tissue, the value of DG6P was corrected with the value obtained from the assay using cocktail C. Using this method, we could detect the enhanced DG6P accumulation (2DG uptake) caused by insulin-stimulation in muscle tissue.

Table 3-3. Composition of reaction mixtures

		Improved Assay Cocktails [162]				Previous Assay Cocktails [160]			
		A	B	C	D	A	B	C	D
Triethanolamine hydrochloride [a]	(mM)	50	50	50	50	50	50	50	50
Potassium chloride	(mM)	50	50	50	50	50	50	50	50
Magnesium acetate [b]	(mM)	0.5	0.5	---	---	0.5	0.5	---	---
Bovine serum albumin [c]	(%)	0.02	0.02	0.02	0.02	0.02	0.02	0.02	0.02
β-NADP	(mM)	0.1	---	0.1	---	0.1	0.1	0.1	0.1
β-NAD	(mM)	---	0.1	---	0.1	---	---	---	---
ATP	(mM)	0.5	0.5	---	---	0.5	0.5	---	---
Diaphorase	(units/mL)	0.2	0.2	0.2	0.2	0.2	0.2	0.2	0.2
Resazurin sodium salt [d]	(μM)	2~10	2~10	2~10	2~10	2~10	2~10	2~10	2~10
Hexokinase	(units/mL)	2	2	---	---	2	2	---	---
C. utilis G6PDH	(units/mL)	---	---	---	---	---	0.1~0.3	---	0.1~0.3
L. mesenteroides G6PDH [e]	(units/mL)	15~20	0.1~0.3	15~20	0.1~0.3	15~20	---	15~20	---
Target compounds	glucose	●	●	-	-	●	●	-	-
	2DG	●	-	-	-	●	-	-	-
	G6P	●	●	●	●	●	●	●	●
	DG6P	●	-	●	-	●	-	●	-

[a] The buffered pH value of all reaction mixture is 8.1.
[b] Magnesium chloride or magnesium sulfate can be used.
[c] Concentration can be raised up to 0.1%.
[d] The concentration of resazurin was lowered to detect the low concentration of the target compound with low background and high sensitivity.
[e] Recombinant G6PDH is recommended strongly because it is only slightly contaminated with other enzymes and a high number of units of G6PDH are required in the present assay.

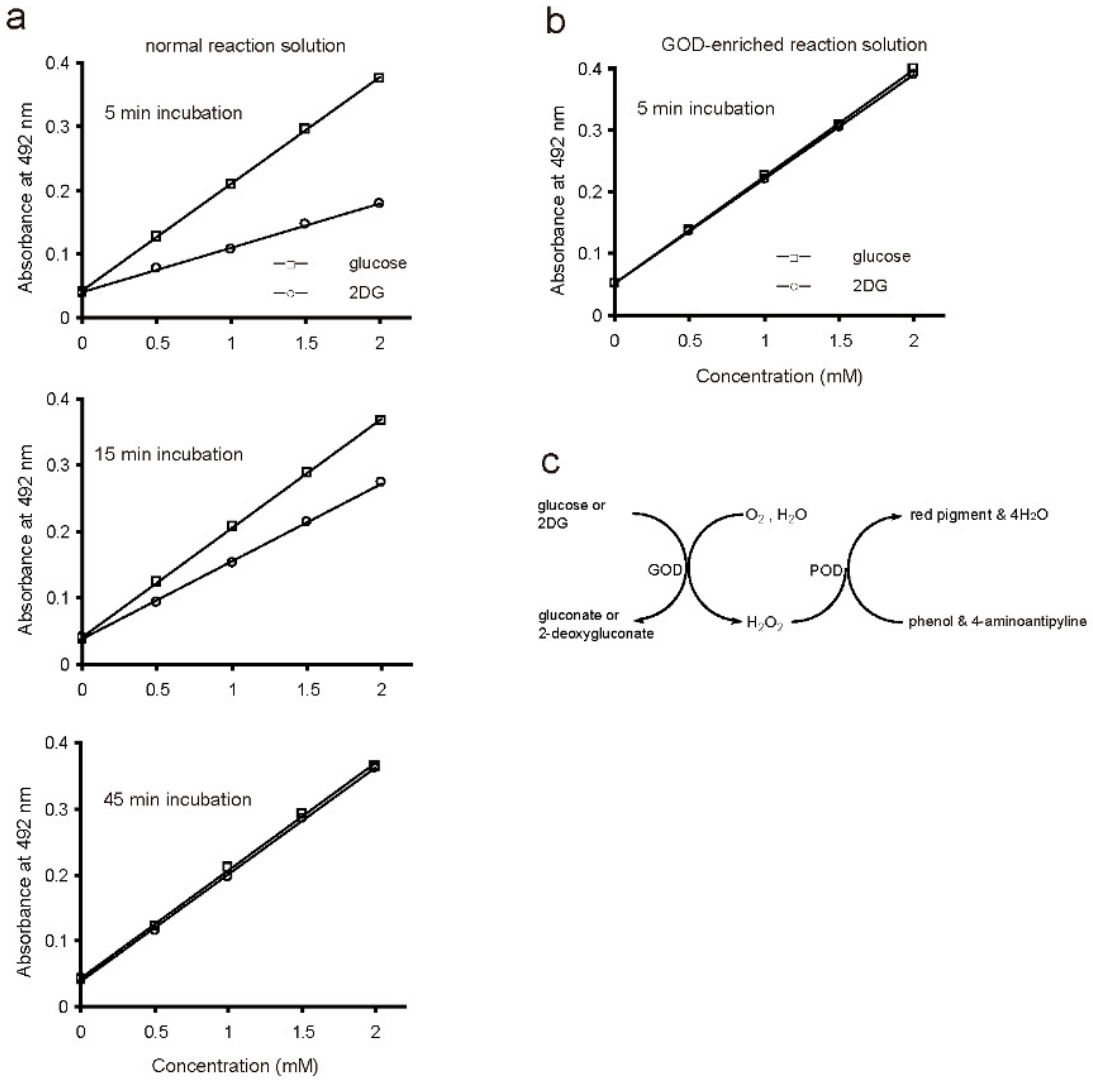

Fig. 3-4. 2DG determination by glucose oxidase (GOD) method. (**a**) 2DG determination by a normal assay solution. (**b**) 2DG determination by a GOD-enriched assay solution. (**c**) Schematic representation of GOD method. POD, horse radish peroxidase. A commercial available kit, Glucose-CII-Test-Wako (Wako Pure Chemical) was used for a normal assay solution, and a GOD-enriched assay solution was prepared by adding GOD to the kit (**Table 3-2**). Although 2DG determination was analyzed by GOD method, its sensitivity did not match resazurin-diaphorase-amplified hexokinase-G6PDH method.

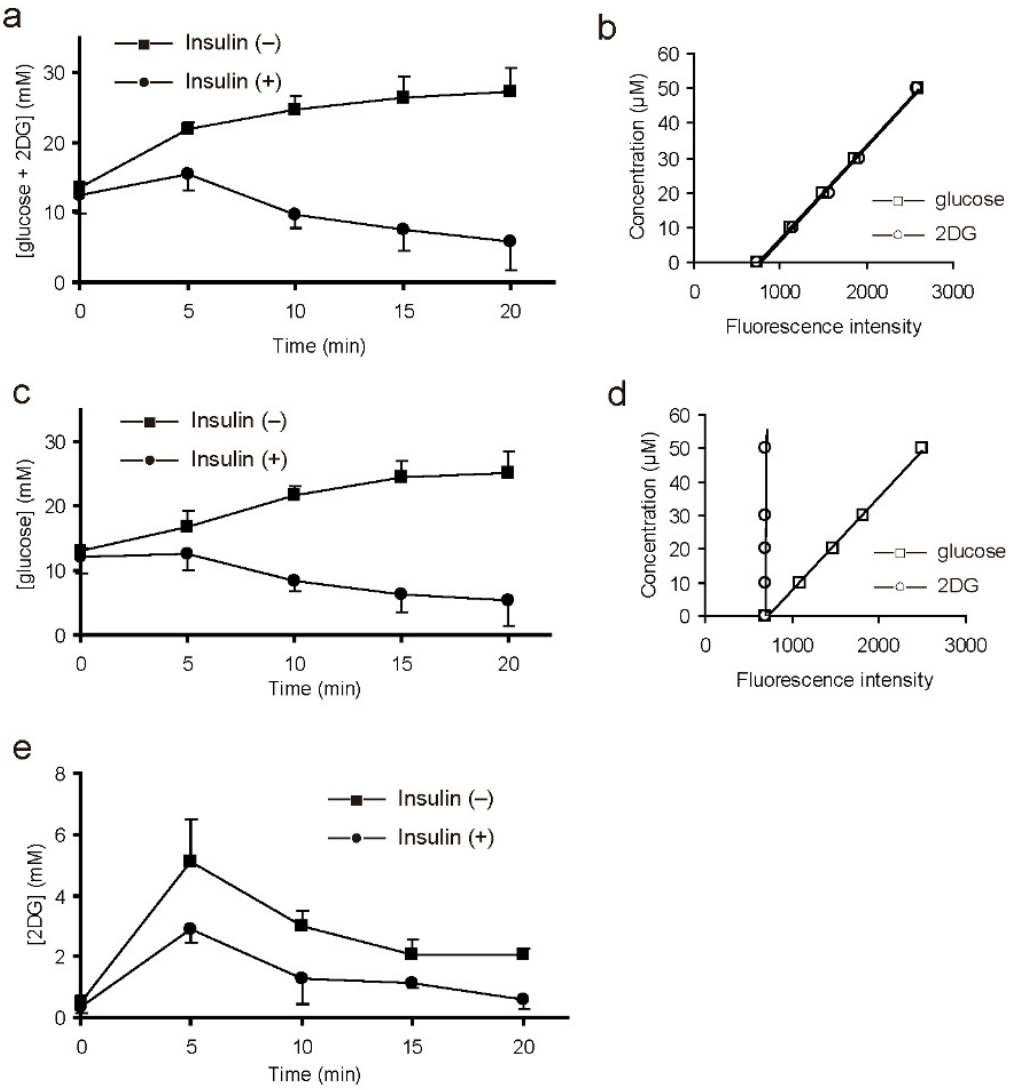

Fig. 3-5. Time course of glucose and 2DG in mouse blood after intravenously injection of 2DG and insulin. 2DG (2 mmol/kg body weight) and insulin (1.5 units/kg body weight) were intravenously injected into the tail vein at the same time (*N*=3). Control mouse was injected only 2DG (*N*=3). Plasma sample was diluted (×500) and was measured 2DG and glucose by enzymatic assay. (**a**) Time course of [glucose + 2DG]. The total concentration of [glucose + 2DG] was measured by using assay cocktail A and was determined from the standard curve of 2DG (**b**). (**c**) Time course of [glucose].The concentration of [glucose] was measured by using assay cocktail B and was determined from the standard curve of glucose (**d**). (**e**) Time course of [2DG].The concentration of 2DG was calculated as the difference between [glucose + 2DG] and [glucose] assay values. Composition of each assay cocktail is described in Table 1 and the concentration of resazurin in each assay solution was set to 5 μM.

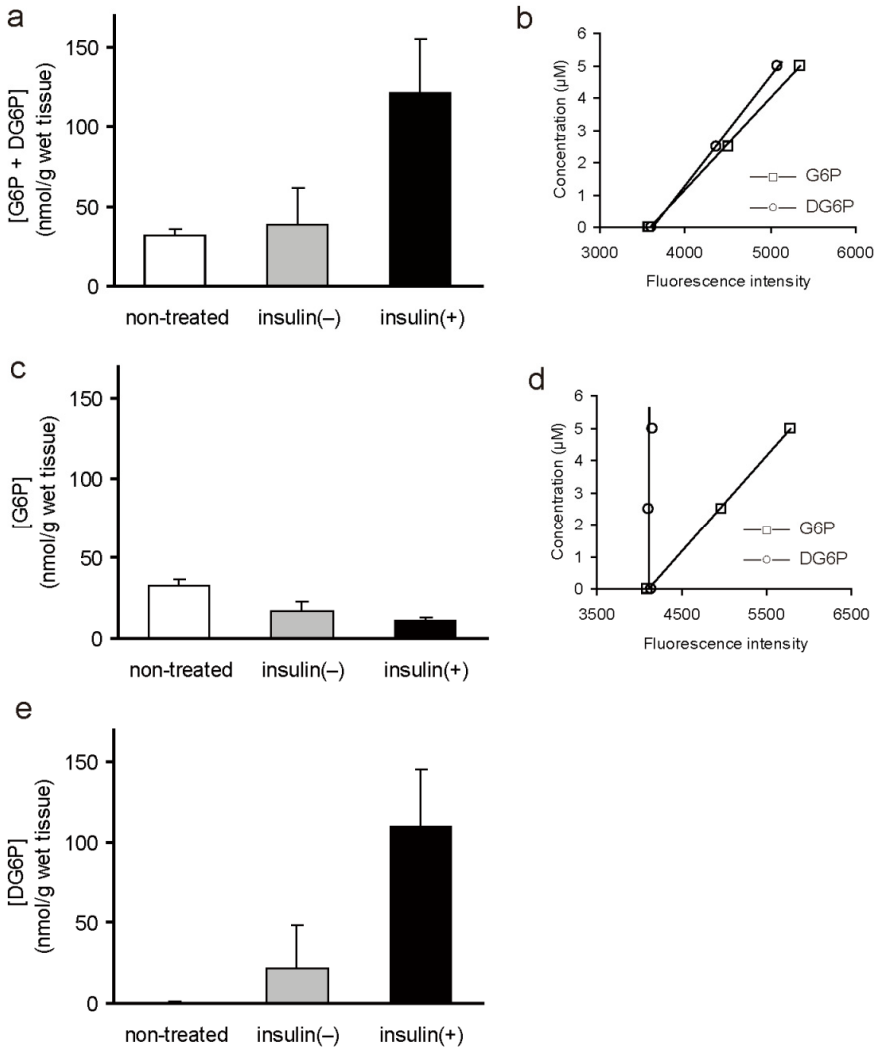

Fig. 3-6. Insulin stimulated DG6P accumulation in muscle tissue of mouse. 2DG (2 mmol/kg body weight) and insulin (1.5 units/kg bodyweight) were intravenously injected into the mouse tail vein (*N*=3). Control mouse was injected only 2DG (*N*=3). At 30 min after the injection, femoral muscle was removed and directly snap-frozen in liquid N_2. Frozen femoral muscle was treated as described in Methods and as shown in **Fig. 3-2**. (**a**) The concentration of [G6P + DG6P] was measured by using assay cocktail C and was determined from the standard curve of G6P (**b**). (**c**) The concentration of [G6P] was measured by using assay cocktail D and was determined from the standard curve of G6P (**d**). (**e**)The concentration of 2DG6P was calculated as the difference between [DG6P + G6P] and [G6P] assay values. Composition of each assay cocktail was shown in **Table 3-1** and the concentration of resazurin in each assay solution was set to 2 μM. Each data point is the mean ± SD.

3-3-4. An improved enzymatic, fluorometric assay

G6PDH catalyzes the conversion of G6P to 6-phospho-gluconolactone, coupled with the conversion of $NADP^+$ to NADPH. *L. mesenteroides* G6PDH can catalyze the conversion of 2DG to 6-phospho-2-deoxygluconolactone and can use $NADP^+$ and NAD^+ as a coenzyme [149]. Thus, the

enzyme can bind $NADP^+$, NAD^+, G6P, and DG6P, but the reaction rates are different when the enzyme-G6P and enzyme-DG6P complexes with coenzyme and when the enzyme binds to NAD^+ and $NADP^+$ alone [149]. In brief, the order of the reaction speed of the complexes with coenzymes is: [enzyme-G6P with $NADP^+$] > [enzyme-G6P with NAD^+] >> [enzyme-DG6P with $NADP^+$] > [enzyme-DG6P with NAD^+]. Taking advantage of the fact that two forms of the enzyme exhibit differences in reactivities, we prepared four independent reaction mixtures, as shown in **Table 3-3**. Assay cocktail A is the same as that reported previously, but cocktails B, C, and D are modified from the previous method [160]. The previous report differs in that only one type of enzyme is used along with NAD^+ and $NADP^+$. In our assay, to prepare cocktails B and D, NAD^+ was used instead of $NADP^+$ and low units of *L. mesenteroides* G6PDH were used instead of using *C. utilis* G6PDH. The addition of ATP and hexokinase allows the detection of glucose and 2DG. Hexokinase catalyzes the conversion of glucose to G6P, and the conversion of 2DG to DG6P. For the reaction addition of Mg^{2+} is needed, because ATP binds to the enzyme as a complex with Mg^{2+}, which provides charge compensation and promoting a favorable conformation of ATP at the active site. Scheme and principle of the assay are described in detail in previous report [159]. Theoretically, the amount of resorufin derived should be equal to the amount of target compounds if the reaction goes to completion.

All assay cocktails were prepared in a buffered solution (pH 8.1) with 50 mM TEA adjusted with HCl. The addition of fetal bovine albumin stabilizes the enzymes in each assay solutions. Magnesium chloride or magnesium sulfate can be used instead of magnesium acetate in the assay cocktails A and C. The reason that we selects magnesium acetate is its lower hygroscopicity than other salts for easy handling. As shown in **Fig. 3-7**, cocktail A could determine [glucose, 2DG, G6P, and DG6P] simultaneously and without distinction; cocktail B, [glucose and DG6P]; cocktail C, [G6P and DG6P]; and cocktail D, [G6P] only. The obtained results were in agreement with results previously reported though the composition of reaction mixture was different. The linearity (linearity coefficient from 0.994 to 0.999) of each standard curve was excellent and intra-assay (percentage coefficient of variation values < 0.5) reproducibility of the method was very satisfactory, and intra-assay reproducibility was also satisfactory.

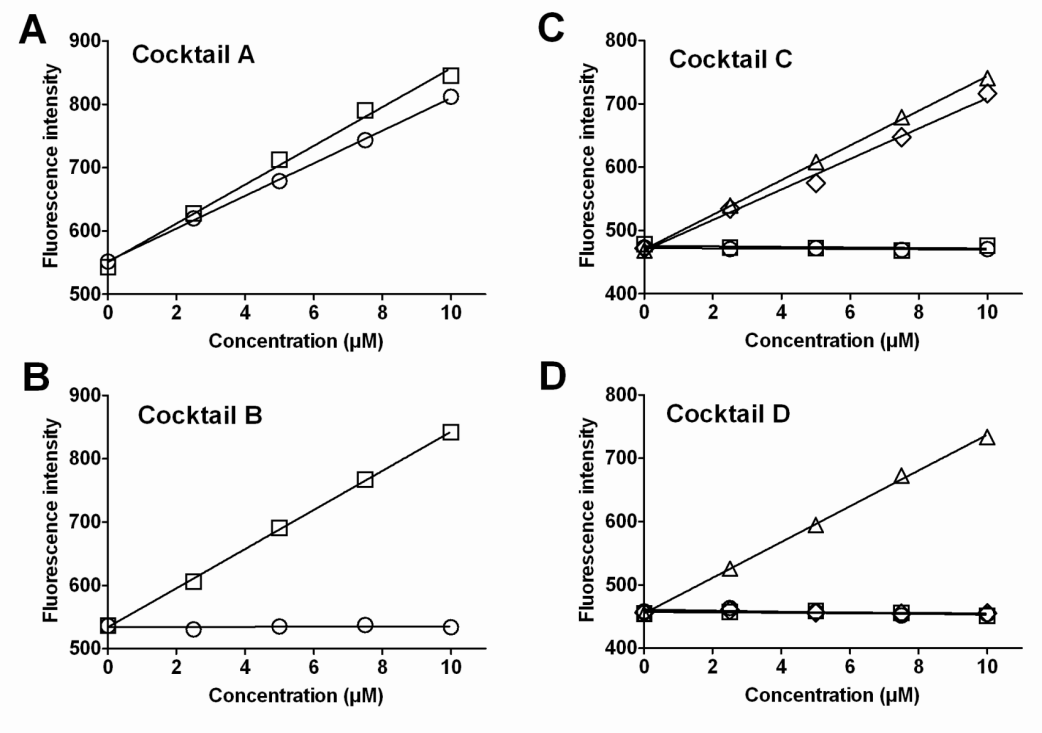

Fig. 3-7. Estimation of the concentrations of glucose, 2DG, G6P, and DG6P by assay solutions. The standard solution of glucose, 2DG, G6P, and DG6P (5 μL) were reacted with 100 μL of assay cocktails A , B , C and D (graph **A**, **B**, **C** and **D**, respectively). After incubation of the plate at 37 °C for 90 min, fluorescence (ex. 530 nm, em. 615 nm) was measured on a plate reader. The composition of each assay solution is shown in Table 1, and the concentration of resazurin in each assay solution was set to 5 μM. The concentration of G6PDH was 150 units/mL in cocktails A and C and 0.1 units/mL in cocktails B and D. All data was acquired after incubation for 90 min. When using cocktails B and D, each reaction was completed in 30 min and no change was observed until 90 min. Each data point is mean ± SD of triplicate measurements.

3-4. Discussion

Facilitative glucose transport systems are ubiquitous in animal cells and are responsible for transporting glucose across the cell surface membrane. Uptake of glucose into cultured cells and tissues is commonly determined using non-metabolizable radioactive hexoses, such as 3MG or 2DG. Assaying the uptake of [^{3}H or ^{14}C]2DG is more convenient than assaying the uptake of [^{3}H]3MG because 2DG is converted to a stable and impermeable derivative (DG6P) through phosphorylation by HK or glucokinase. Although new radiolabeled glucose analogues for use as tracers of glucose uptake have been synthesized, none of these molecules has been found to show the same biological behavior as 2DG [145]. Therefore, 2DG is often considered to be the gold standard of reference tracers of glucose transport and phosphorylation. Manchester *et al*. [139] and Sasson *et al*. [131] developed enzymatic assays for evaluating 2DG uptake into tissues and cultured cells that avoid the need for radioisotopes. Their methods were based on the assay of DG6P, which is monitored by detection of

NADPH produced during the oxidation of DG6P to 6-phosphoglucuronic acid by G6PDH. The NADPH produced in their assays could be detected by direct fluorescent measurements of the stoichiometric amount of NADPH generated or by amplification of this NADPH by enzymatic cycling [163].

Resazurin, which is the *N*-oxide of the fluorescent dye resorufin which is also known under the name AlamarBlue™, is useful for detecting reductive activities in cells and has been widely used for measuring cell proliferation [164,165] and mitochondrial metabolic activity [166]. The "resazurin reduction test" has been used for about 50 years to monitor bacterial and yeast contamination of milk and also for assessing semen quality [167]. Resazurin itself is non-fluorescent until it is reduced to the highly red fluorescent resorufin. Usually, NADPH or NADH is the reductant that converts resazurin to resorufin in the presence of the enzyme diaphorase. Thus, resazurin can be used to detect NAD(P)H or diaphorase levels. Furthermore, the resazurin-diaphorase system can be used to detect any biochemical or enzyme activity that is involved in a biochemical reaction generating NAD(P)H [168-173].

Based on the above information, we considered the resazurin-diaphorase system to be suitable to facilitate measurement of NADPH in the 2DG uptake assay, and we reported the protocol for measurement of 2DG uptake in cultured cells [159] (***see Chapter 2***). The principle of the methods can be summarized as described below and in **Fig 3-1a**. In the first reaction, HK catalyzes the conversion of 2DG to DG6P. In the second reaction, G6PDH catalyzes the conversion of 'DG6P to 2-deoxy-6-phosphoglucuronate', coupled with the conversion of 'NADP to NADPH'. In the third reaction diaphorase catalyzes the conversion of 'resazurin to resorufin', coupled with the conversion of 'NADPH to NADP'. This reaction should continue until 2DG and DG6P are consumed. Thus, detection of the reaction would be recorded at the endpoint and the amount of generated resorufin should be equivalent to the amount of 2DG and DG6P In these reactions, glucose and G6P are similarly distinguished. By using this method, we reported a 2DG uptake assay in L6 skeletal muscle cells cultured in 96 well microplates [159] and we also demonstrated a 2DG uptake assay in cultured 3T3-L1 adipose cells

To evaluate 2DG uptake in an in vivo study using the enzymatic method, separate detection of glucose, 2DG, G6P and DG6P was needed because the tissue levels of glucose are much higher than those of 2DG and DG6P. To determine 2DG and DG6P, Chi *et al*. [174,175] and Akabayashi *et al*. [176] have developed enzymatic assays. Their methods are based on a HK-G6PDH assay in the same way as our method, and directly detect NADPH derived from the reactions or detect NADPH by amplification with a NADP cycling reagent. They also use elimination reaction steps in their methods. To eliminate glucose, Chi *et al*. [174] used GOD and mutarotase, which convert glucose to glucono-δ-lactone. To eliminate glucose and G6P, Akabayashi *et al*. [176] used a glucose-elimination-reagent containing HK, glucosephosphate isomerase and phosphofructokinase. In the reaction mixture glucose plus G6P were converted to fructose 1,6-bisphosphate and 2DG was converted to DG6P. Using these elimination reagents involves many steps and the operations are complicated. In our present method we do not use such elimination reagents but instead use four

independent assay solutions (cocktail A, B, C and D as shown in **Table 3-1**). The components of each assay solution are similar to each other and each assay solution can be prepared easily by mixing stock solutions. Furthermore, the actual reaction step is very simple, involving only a single incubation with the assay solution followed by the reading of fluorescence. The same authors also developed an assay for glucose and G6P in which the above elimination reactions were omitted and the concentration of G6PDH reduced to about 1/250 of that used in the assay of 2DG and DG6P. The authors noted that DG6P was not oxidized at this low concentration of G6PDH. We initially used their strategy, but the long incubation time caused a slight reaction with DG6P. Thus, we screened for a commercially available G6PDH enzyme suitable for our assay. Using this screen we confirmed that *C. utilis* G6PDH has much lower reactivity towards DG6P than *L mesenteroides* G6PDH. We also confirmed that using low numbers of units of *C. utilis* G6PDH didn't cause increasing fluorescence during a long incubation when DG6P was reacted. HK can convert both glucose and 2DG to G6P and DG6P respectively and the reaction needs Mg^{2+} and ATP. This reaction had been utilized effectively for analyzing separately the phosphorylated sugar and free sugar in both of the Chi and Akabayashi methods. We also utilized this reaction. In brief, cocktail C and D do not contain HK, Mg^{2+} and ATP and do not react with non-phosphorylated glucose and 2DG.

Finally, we prepared four assay solutions (cocktail A, B, C and D as shown in **Table 3-1**) to allow the separate determination of glucose, 2DG, G6P and DG6P. Briefly, assay cocktail A detects total glucose, 2DG, G6P and DG6P, cocktail B detects glucose plus G6P, cocktail C detects G6P plus DG6P and cocktail D detects only G6P. Therefore, glucose, G6P and DG6P can be calculated using the values from each assay. If the sample solution contains vanishingly small amounts of G6P and DG6P, assay cocktail A and B may also be used for determination of levels of glucose and 2DG, and if the sample solution doesn't contain glucose or 2DG, cocktail A may be used for determination of DG6P. For example, we could use assay cocktail A in a 2DG uptake assay in cultured cells because the cells were washed before enzymatic determination of DG6P, and we could use assay cocktails A and B without using C and D for detection of glucose and 2DG in blood.

We also investigated the GOD method, which is widely used for measuring blood glucose, as a means of determining glucose and 2DG levels. Since GOD reacts with both glucose and 2DG, the GOD method cannot be used to separately measure glucose and 2DG. Thus, given that a resazurin-diaphorase amplifying method gives a much higher sensitivity towards glucose than the GOD method. In in vitro studies, investigators usually wish to make several physiological measurements from small volumes of blood to decrease the stress on the laboratory animals and improve the quality of their experiments. We are of the opinion that assay cocktail A would be of use in studies of small animals such as mouse because the amount of blood needed would be decreased.

Using our assay system, we demonstrated the detection of 2DG in blood and the detection of DG6P accumulation in muscle tissue with our new assay method. After the administration of 2DG (2 mmol/kg body weight), blood glucose was elevated approximately 10 millimolar above the base level in spite of blood 2DG being several millimolar. It was thought that this phenomenon depended on

inhibition of glucose uptake in peripheral tissue by non-tracer amount of 2DG. However, at this time, insulin decreased blood glucose and 2DG and increased DG6P accumulation in muscle tissue. Thus, our assay system was clearly able to evaluate the effects of insulin in a mouse study.

In the present study, we describe application of this classical enzymatic method to an in vivo mouse study. Prior to the animal experiment, we developed methods to allow measurement of glucose, 2DG, G6P and DG6P separately. This was achieved using four different reaction solutions, the composition of which changed depending on the compound being assayed. Using this assay system, we demonstrate the detection of 2DG in blood and the detection of DG6P accumulation in muscle tissue. To quantitate glucose, 2DG, G6P and DG6P separately, we proposed using four independent, single reaction mixtures containing G6PDH from *L. mesenteroides* and *C. utilis*. Since *C. utilis* G6PDH was no longer sold by Sigma-Aldrich and a substitute distributor did not exist, we needed to improve our assay method without using *C. utilis* G6PDH. Then, we achieved the improvement of our assay method by incorporating minor modifications. Assay cocktail A is the same as that reported previously, but cocktails B, C, and D are modified from the previous method [160] (shown in **Table 3-3**). We found assay cocktail C most suitable for the determination of 2DG uptake in cultured cells. Because the process of 2DG uptake in cultured cells is usually carried out in the absence of glucose, the treated cells show accumulation of DG6P and contain little or no glucose and G6P [159]. Thus, the use of cocktail C detects cellular DG6P. When the cell is assumed to contain glucose and G6P, the difference between the measurements obtained using cocktail C and D is determined. Before the assay, cells are lysed, intracellular enzymes are inactivated and coenzymes are decomposed [159] (***see Chapter 2***).

To determine the concentration of glucose and 2DG in a blood sample (serum or plasma), the combination of cocktail A and B is used because blood sample contains little or no G6P and DG6P [160]. The independent concentration of glucose and 2DG can be calculated by using measurements obtained by two independent reactions. It is necessary to dilute blood samples before they can be used in the assay. To determine the concentration of DG6P in tissues such as muscle, the combination of cocktail C and D is used because G6P is present in low abundance in tissue samples and it is possible that the accumulation of G6P is an artifact that can be introduced during tissue processing (e.g., homogenization) [160]. The concentration of DG6P is calculated as the difference between [DG6P + G6P] and [G6P] assay values, which is obtained by two independent reactions. To evaluate 2DG uptake in an in vivo study using our enzymatic method, separate detection of glucose, 2DG, G6P, and DG6P was needed because glucose levels in tissues are much higher than those of 2DG and DG6P. Some methods [174-176] have been previously reported, but these methods involve many steps such as elimination and amplification steps and the operations are complicated. In our method, the components of each assay solution can be prepared easily by mixing stock solutions. The actual reaction step is very simple, involving only a single incubation step with the assay solution followed by the reading of fluorescence. Furthermore, our assay is based on direct fluorometric measurement of stoichiometric amounts of resorufin generated and can be performed in the 96-well or 384-well

format.

In conclusion, our assays for DG, DG6P and glucose are based on direct fluorometric measurement of stoichiometric amounts of resorufin and can be performed in 96-well or 384-well formats. This direct assay is simpler than previous assays. Furthermore, the processing of the sample is also simplified. In addition, our method does not require radiolabeled 2DG or a specialized institution registered for using radioactive isotopes. In the present study, the proposed methods have been aimed at measurement in muscle in general. Methods for evaluation of glucose uptake are applied in a wide range of fields because facilitative glucose transport systems are ubiquitous in animal cells and are responsible for transporting glucose across the cell membrane. There is no reason for why these methods should be limited to evaluate glucose uptake only in muscles and adipocytes. We believe that we have devised a simple and reliable method for in vitro and in vivo evaluation of glucose uptake in cells and that it can be applied in a wide range of fields.

Chapter 4

Artemisia princeps extract promoted glucose uptake in cultured L6 muscle cells *via* glucose transporter 4 translocation

4-1. Introduction

Insulin resistance is defined as reduced ability of tissues to respond to physiological levels of insulin. It is characteristic of non-insulin-dependent diabetes mellitus (NIDDM). Skeletal muscle constitutes the major mass of peripheral tissue, accounting for about 40% of total body mass and > 30% of total energy expenditure, and it is the primary tissue responsible for postprandial uptake of glucose from blood [122]. One of the major factors regulating glucose uptake into muscle is the quantity of glucose transporter (GLUT) protein on the cell surface. In muscle cells and adipocytes, GLUT1 mediates basal and nonstimulated transport, whereas an insulin responsive GLUT, GLUT4, facilitates increased glucose transport in the presence of insulin. Hence, to survey for agents that increase glucose uptake by enhancing GLUT4 translocation is one of the major strategies for discovering new therapeutic agents for NIDDM.

On this basis, we developed a non-radioisotopic, high-throughput enzymatic assay to evaluate glucose uptake in cultured skeletal muscle cells [159] (***see Chapter 2***). Using our method, we surveyed herbal extracts that promote uptake of 2-deoxyglucose (2DG) in cultured L6 myotubes because there is growing interest in natural sources of nutrients and health-promoting compounds. (**Fig. 4-1**). This search is continuing now, and we have evaluated 600 plant materials or more so far. Among them, we discovered an ethanol extract of *Artemisia princeps* Pampan (*Asteraceae*) was a promising stimulator of glucose uptake.

A. princeps is an ingredient in kusa-mochi (also known as yomogi-mochi), a Japanese confectionery, to which it imparts its fresh, springlike fragrance and vivid green coloring. In Korea, it is used for making tteok (rice cakes), jeon (Korean-style pancakes), ssuk kimchi, ssukguk (soup made with ssuk), and so forth. It is also used in traditional Asian medicine in the treatment of inflammation, diarrhea, and many circulatory disorders. In the present study, we investigated to determine whether APE-stimulated glucose uptake is accompanied by translocation of GLUT4 in cultured skeletal muscle.

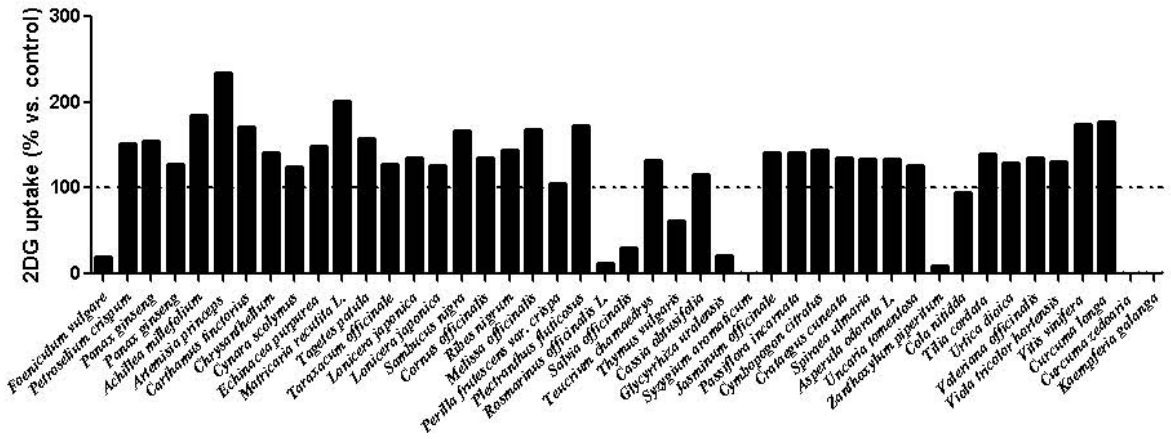

Fig. 4-1. A part of data of screening of plant extract using 2DG uptake assay in cultured L6 muscle cells. L6 myotubes were grown in a monolayer in a 96-well plate and treated with herval extract. This shows the data when the concentration of plant extract was 5 mg/mL as the equivalent of dried herb. The data of *A.princeps* is the 6th column from the left.

4-2. Materials and methods

4-2-1. Plant material

A. princeps, harvested in Japan and marketed as a raw dried herbal material, was obtained from Mikuni (Osaka, Japan). The herbal plant (2.0 g) was extracted with ethanol (30 mL) at 5°C for 24 h and filtered through no.2 paper filter (Toyo Advantech, Tokyo). The extract obtained was evaporated and dissolved in ethanol to yield a 1:1 fluid extract (1 mL of fluid extract is equivalent to 1,000 mg of dry whole plant), and stored at 4°C. The sample solvent was replaced by DMSO just before analysis. The 1:1 fluid extract obtained was 1.4% w/v dry matter.

4-2-2. Chemicals and reagents

Glucose-6-phosphate dehydrogenase (G6PDH), 2DG, 2-deoxyglucose-6-phosphate (DG6P), and insulin were purchased from Sigma-Aldrich (St. Louis, MO). Resazurin sodium salt and triethanolamine hydrochloride (TEA) were from Wako Pure Chemicals (Osaka, Japan). Diaphorase, ATP, and NADP were from Oriental Yeast (Tokyo). For western blot analysis, anti-GLUT4 goat IgG, anti-GLUT1 goat IgG, anti-IRβ rabbit IgG, anti-goat IgG, anti-p-PI3K goat IgG, and anti-rabbit IgG antibody were from Santa Cruz Biotechnology (Santa Cruz, CA). Anti-phospho-Akt (Thr-308) rabbit IgG, anti-phospho-PKCλ/ζ rabbit IgG, anti-Akt rabbit IgG, and anti-AMPKα rabbit IgG were from Cell Signaling Technology (Danvers, MA). Anti-phospho-Akt (Ser-473) rabbit IgG was from Sigma-Aldrich. Anti-PI3K mouse IgG, and anti-PKCλ mouse IgG were from BD Transduction Laboratories (San Jose, CA). All other reagents used were of the highest commercially available grade.

4-2-3. HPLC analysis of polyphenol profiles

The polyphenol profiles of APE were analyzed by an HPLC system, as previously described [177]. Briefly, ethanol extract was filtered through a Millex-LG 0.2-μm membrane filter (Millipore, Bedford, MA). The extract was analyzed by a Hitachi HPLC series D-7000 (Tokyo) equipped with Hitachi model D-7000 chromatography data station software and diode array detection system D7450 to monitor at all wavelengths from 200 to 600 nm. Chromatographic separation was carried out on a Capcell pak C18 UG120 (250 × 4.0 mm i.d., S-5, 5 μm, Shiseido, Tokyo) by a gradient elution of 50 mM sodium phosphate (pH 3.3) containing either 10% v/v methanol (solution A) or 70% methanol (solution B). The gradient program was as follows: 100% solution A; 70% solution A for the following 15 min; 65% solution A for 20 min; 60% solution A for 20 min; 50% solution A for 5 min; and 0% solution A for the final 25 min. The flow rate was 1 mL/min, the injection volume was 10 μL, and the oven temperature was 35°C. Phenolic compound quantification was determined by the absorbance at 250 and at 320 nm recorded in the chromatograms relative to external standards or previously generated calibration curves in the system library.

4-2-3. Cell culture

L6 skeletal muscle cells and 3T3-L1 adipose cells were purchased from Dainippon Pharmaceuticals (Osaka, Japan). L6 myoblasts were cultured in α-minimal essential medium (α-MEM) supplemented with 10% heat-inactivated fetal bovine serum (FBS) at 37°C in 5% CO2. The cells were grown in a 96-well plate for the 2DG uptake assay and in a 35-mm diameter dish for western blot analysis. Differentiation of L6 myoblasts to myotubes was performed as previously described.[159] Briefly, cells were cultured in α-MEM supplemented with 2% FBS and maintained in this medium post-differentiation. Myotubes were used in experiments 5–7 d after differentiation. Differentiation of 3T3-L1 fibroblasts to adipocytes was performed as described previously [178]. Briefly, confluent cells in a 24-well culture plate were incubated for 2 d in Dulbecco's Modified Eagle's Medium (DMEM) supplemented with 10% FBS, 0.5 mM 3-isobutyl-1-methylxanthine, 1 μM dexamethasone, and 5 μg/mL of insulin. After differentiation, the medium was replaced every other day with DMEM containing 10% FBS and 5 μg/mL of insulin.

4-2-4. 2DG uptake assay

Glucose uptake was determined by non-radioisotopic, enzymatic fluorescence assay for 2DG uptake in cultured cells, as described previously.[159,160] In brief, L6 myotubes in a 96-well format were incubated for 4 h in a medium containing herbal extract or DMSO (0.1% v/v) as vehicle control. After induction, the cells were washed twice with Krebs-Ringer-Phosphate-Hepes (KRPH) buffer containing 0.1% BSA, and 2DG uptake was initiated by incubation with KRPH buffer containing 1 mM 2DG and 0.1% BSA. After 20 min, the cells were washed twice with KRPH buffer containing 0.1% BSA, followed by the addition of 50 μL of 0.1 M NaOH, and the culture plate was heated at

85°C for 50 min. The component in the wells was neutralized by the addition of 50 μL of 0.1 M HCl, followed by the addition of 50 μL of 150 mM TEA buffer (pH 8.1). The cell lysate (10 μL) was transferred to a 96-well assay plate and incubated for 45 min with 100 μL of assay cocktail, which contained 50 mM KCl, 0.1 mM NADP, 20 units/mL of G6PDH, 0.2 units/mL of diaphorase, 5 μM resazurin sodium salt, and 50 mM TEA buffer (pH 8.1). The resorufin generated was measured with a plate reader (ex. 530 nm and em. 615 nm). A standard curve was generated by measuring DG6P standard solution in the wells of the assay plate. For the 3T3-L1 adipose cells (24 well format plate), cell lysate treated with 2DG was prepared in a 24-well format culture plate, and an aliquot was transferred to a 96-well plate for measurement of DG6P, as described above.

4-2-5. Western blot analysis

L6 myotubes were serum-starved for 18 h and treated with 5 mg/mL of APE for the indicated durations, and plasma membrane or whole cell lysate was prepared, as described previously [179]. In summary, proteins (5–20 μg) were separated with 7.5 or 10% SDS-PAGE gels and electrophoretically transferred to a polyvinylidene fluoride (PVDF) membrane. The membranes were blocked with Blocking-one™ (Nacalai Tesque, Kyoto, Japan) and washed with TBST (10 mM Tris-HCl, pH 8.0, 150 mM NaCl, and 0.05% Tween 20) 6 times. Antibodies were diluted in Can Get Signal® Immunoreaction Enhancer Solution (Toyobo, Osaka, Japan) and incubated overnight at 4°C. Membranes were incubated with primary antibody for 1 h at room temperature, and then incubated with secondary antibody conjugated to horseradish peroxidase at room temperature for 1 h. Antibody-bound proteins were visualized using Lumi-Lightplus Western Blotting Substrate (Roche Applied Science, Mannheim, Germany) following the manufacturer's protocol.

Table 4-1. Polyphenols in APE Identified by an HPLC System

Name[a]	Conc. in a 1:1 fluid extract (nmol/mL)	Retention time of peak (min)
Protocatechuic acid	20[b]	9.7
Chlorogenic acid	33[b]	13.7
3,5-di-*O*-caffeoylquinic acid	380[c]	31.6
Luteolin	75[b]	80.0

[a] The phenolic content of APE was determined using an HPLC system constructed for simultaneous determination of polyphenols in foods.[3)] The names of the compounds that were identifiable using this system are shown.
[b] Quantities of protocatechuic acid, chlorogenic acid, and luteolin were calculated using previously generated calibration curves in the system library.
[c] The quantity of 3,5-di-*O*-caffeoylquinic acid was calculated using the standard curve generated from an external standard. An unknown compound peak, thought to be a flavone (r.t., 84.0 min), with a spectrum similar to luteolin, was detected at a concentration comparable to luteolin.

4-2-6. Statistical analysis

Statistical significance was determined by analysis of variance (ANOVA), followed by the Tukey multiple comparison test (GraphPad Prism 5 for Windows Version 5.01, GraphPad Software). *p*-Values < 0.05 were considered statistically significant.

4-3. Results

4-3-1. Polyphenol analysis

The polyphenolic profile of APE was analyzed using a HPLC system constructed for simultaneous determination of polyphenols in food stuffs (**Table 4-1**). Comparison with the library in the HPLC system identified the presence of luteolin (20 nmol/mL in a 1:1 fluid extract), chlorogenic acid (33 nmol/mL), and protocatechuic acid (20 nmol/mL) in APE. 3,5-di-*O*-caffeoylquinic acid (380 nmol/mL), which was one of the major components, was analyzed by comparison with a standard chromatogram. A previous study reported that one of the flavones, eupatilin, is an active compound in *A. princeps* [180,181]. We checked the amount of eupatilin in our APE as compared with standard compounds obtained from PhytoLab (Vestenbergsgreuth, Germany), and confirmed that our APE did not contain eupatilin. We could not identify some peaks because they were absent from our polyphenolic library data, but one of the unidentified peaks was assumed to be a flavone on the basis of its spectrum.

4-3-2. Effects of APE on 2DG uptake in L6 myotubes and 3T3-L1 adipocytes

Treatment of L6 myotubes with APE for 4 h resulted in dose-dependent increases in 2DG uptake, similarly to the insulin-stimulated cells (**Fig. 4-2A**). APE increased 2DG uptake in 3T3-L1 adipocytes, too (**Fig. 4-2B**). However, the high concentrations of APE (10 mg/mL for L6 cells and 5 mg/mL for 3T3L1 cells) tended to result in less activity. This suggests that the high concentration of extract affected the viability of the cells. Hence, in the following experiments, L6 cells were stimulated at a concentration of 5 mg/mL.

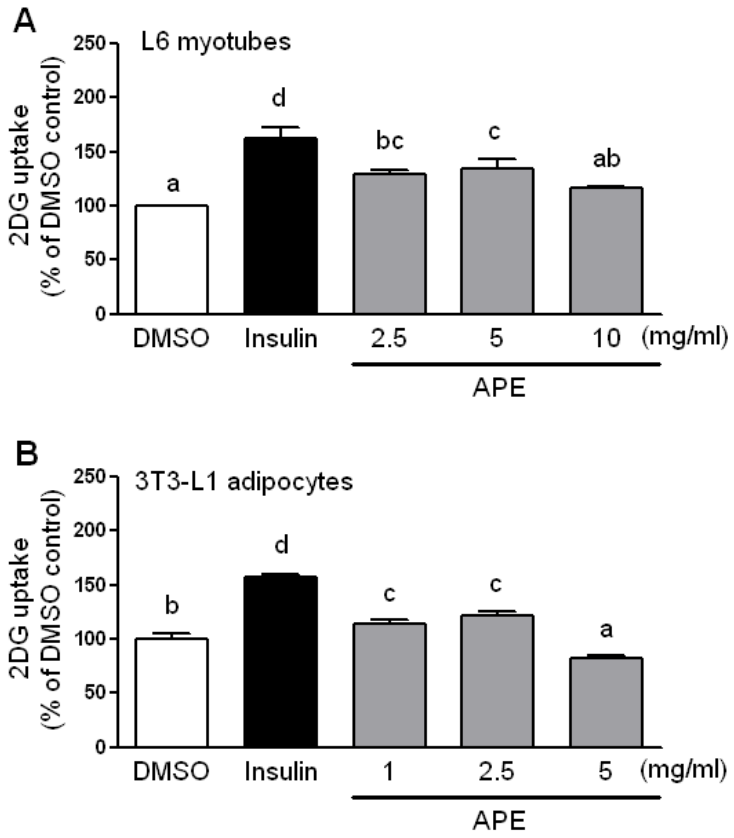

Fig. 4-2. Effects of APE on 2DG Uptake in L6 Myotubes (**A**) and 3T3-L1 Adipocytes (**B**). L6 myotubes were grown in a monolayer in a 96-well plate and 3T3-L1 adipocytes were grown in a monolayer in a 24-well plate, as described in "*Materials and Methods*." Cells were treated with increasing doses of APE for 4 h prior to 2DG uptake assay. Cells were treated with DMSO (0.1% v/v) or insulin (100 nM) as negative and positive control respectively. 2DG uptake was measured for a period of 20 min. Values are the mean ± SD of triplicates. Different letters indicate statistically significant differences. *The dose value of APE is expressed as the equivalent of dried herb.

4-3-3. Effects of APE on GLUT4 translocation

To assess the potential activity of APE on glucose metabolism and insulin action, we first examined the effect of APE on the translocation of GLUT4 to plasma membrane, an essential step in inducible glucose uptake into muscle cells and adipocytes. The effects of APE on the translocation of the GLUT1 and GLUT4 isoforms were analyzed by western blot in L6 cells (**Fig. 4-3**). APE raised plasma membrane levels of GLUT4 from 15 to 60 min. On the other hand, APE did not affect the level of GLUT1 in the plasma membrane. This suggests that GLUT4 translocation contributes to APE-stimulated glucose uptake.

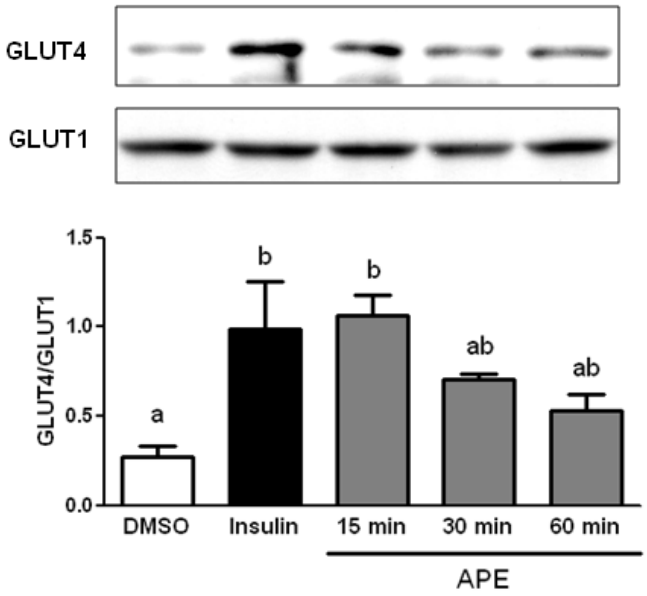

Fig. 4-3. Effects of APE on GLUT4 Translocation in L6 Myotubes. L6 myotubes were serum-starved for 18 hours prior to treatment with APE at 5 mg/ml* for the indicated durations. A plasma membrane fraction was prepared from the cells, and western blot analysis was performed to detect GLUT4 and GLUT1. Cells treated with 100 nM insulin or 0.1% v/v DMSO for 15 min served as positive and negative control respectively. Values are the mean ± SE of three independent experiments.*The dose value of APE is expressed as the equivalent of dried herb.

4-3-4. Effects of PI3K inhibitor on APE-stimulated 2DG uptake

The phosphatidyl inositol 3'-kinase (PI3K) pathway plays a major regulatory role in the insulin action pathway, and PI3K inhibitors inhibit insulin-stimulated glucose uptake. We used LY294002, a potent and selective PI3K inhibitor, to examine the contribution of PI3K to APE-induced glucose uptake. As shown in **Fig. 4-4**, the stimulatory effect of APE on glucose uptake was inhibited by 25 μM of LY294002, indicating that PI3K is a key molecule in APE-stimulated glucose uptake, but inhibition by LY294002 was not complete, although insulin-stimulated 2DG uptake was inhibited completely.

4-3-5. Effects of APE on the PI3K downstream pathway

Next we explored the effects of APE on two important downstream targets of the PI3K signaling pathway, serine/threonine kinase Akt, also known as protein kinase B (PKB), and atypical protein kinase C (aPKC). These two targets of PI3K have been found to play roles in insulin-stimulated GLUT4 translocation in muscle and fat cells. Cell lysate was immunoblotted with antibodies raised against p-PI3K, p-Akt (Thr-308), p-Akt (Ser-473), and p-PKC (**Fig. 4-5**). Phosphorylation of PI3K, Akt (Thr-308), and aPKC was observed in cells stimulated with APE for 15 min, but APE did not induce phosphorylation of the Ser-473 residue of Akt. APE-stimulated

phosphorylation decreased to control levels in the cells after 60 min. Insulin stimulated phosphorylation of all these kinases.

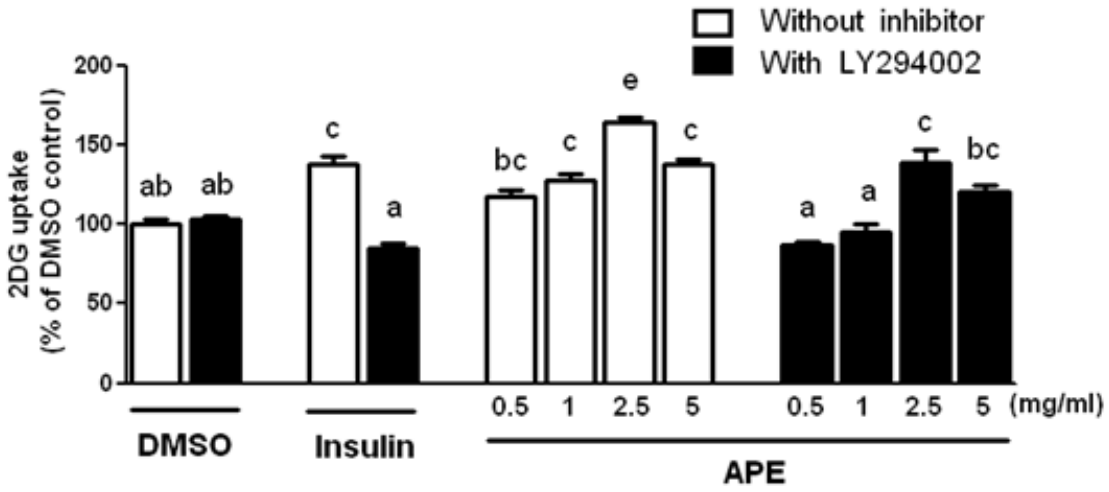

Fig. 4-4. Effects of the PI3K Inhibitor LY294002 on APE-Induced 2DG Uptake. Differentiated L6 cells in a 96-well plate were treated with and without 25 μM LY294002 for 30 min. They were then incubated with APE or 100 nM insulin for 4 h. After incubation with stimuli, 2DG uptake was assayed as described in "Materials and Methods." Values are the mean ± SD of tripricate. Different letters indicate statistically significant differences. *The dose value of APE is expressed as the equivalent of dried herb.

4-3-6. Effects of APE on AMPK phosphorylation

We also investigated to determine whether APE stimulates phosphorylation of AMPK, a stress kinase that has been found to regulate GLUT4 translocation. As shown in **Fig. 4-6**, APE-induced phosphorylation of AMPK was observed by western blot analysis at 60 min, at a level similar to that observed in AICAR-stimulated cells.

4-4. Discussion

In the present study, we found that an ethanol extract of *A. princeps* (APE) increased glucose uptake activity in cultured L6 myotubes and 3T3-L1 adipocytes. This increased activity was accompanied by stimulation of GLUT4 translocation to the cell surface in APE-stimulated L6 myotubes *via* activation of both PI3K and its downstream factors, and AMPK. Peripheral resistance to

insulin is a prominent feature of NIDDM. One of the major factors regulating glucose uptake into muscle is the quantity of GLUT protein on the cell surface [128]. Insulin resistance is believed to result from defects in insulin-post-receptor signals that induce translocation of GLUT4 to the plasma membrane [182,183] Hence, surveying for agents that increase glucose uptake *via* stimulation of GLUT4 translocation is one of the major strategies for discovering new therapeutic agents for NIDDM. We have developed a method of evaluating glucose uptake into cultured cells [159,160] and have surveyed the herbal extracts that promote uptake of 2DG in cultured L6 myotubes. We found that APE promoted 2DG uptake into the cells. This is the first report that APE stimulates GLUT4 translocation and increases glucose uptake activity in insulin-sensitive peripheral tissues.

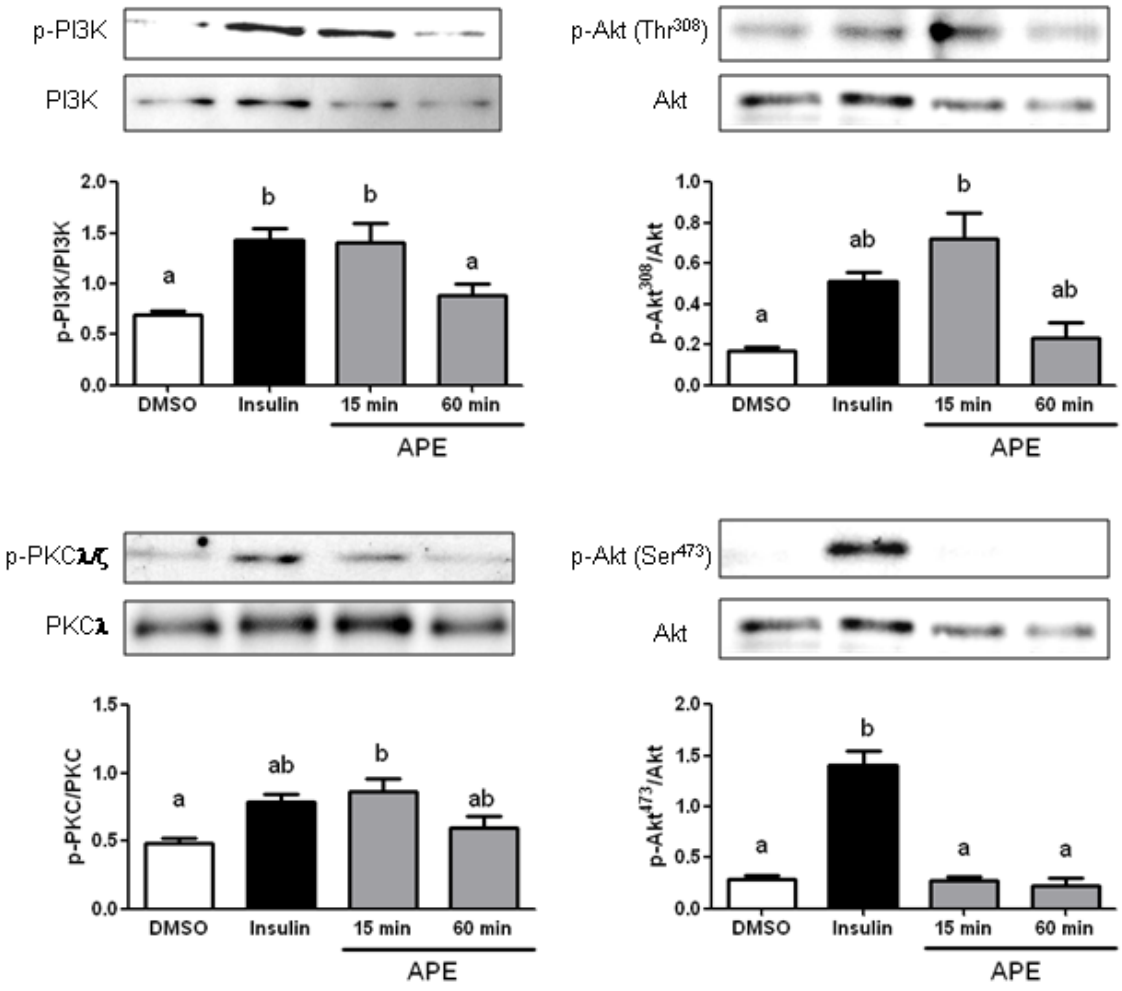

Fig. 4-5. Effects of APE on the Insulin-Signaling Pathway in L6 Myotubes. L6 myotubes were serum-starved for 18 h prior to treatment with 5 mg/ml* of APE for 15 and 60 min. Whole-cell lysates were subjected to western blots to detect the phosphorylation status of PI3K, Akt, and aPKCλ/ζ. Values are the mean ± SE of triplicates. Different letters indicate statistically significant differences. *The dose value of APE is expressed as the equivalent of dried herb.

Recently, an anti-diabetic effect of Korean *A. princeps* in type-2 diabetic mice was reported [180,181]. The active constituent is thought to be a flavone, eupatilin, which had a functional anti-diabetic effect by enhancing hepatic and plasma glucose metabolism [181]. Hence, we analyzed the amount of eupatilin in our APE by HPLC analysis, and confirmed that our APE did not contain eupatilin. The *A. princeps* used in the previous studies were variants cultivated in Korea, and may have had a different composition of phytochemicals than Japanese *A. princeps*. Furthermore, the anti-diabetic effects of Korean *A. princeps* appeared to be mediated through stimulation of glucokinase activity, inhibition of glucose-6-phosphatase activity in the liver, and enhanced pancreatic insulin secretion [181], but the regulation of glucose uptake in muscle and adipose tissues through GLUT4 translocation was not examined in these previous studies.

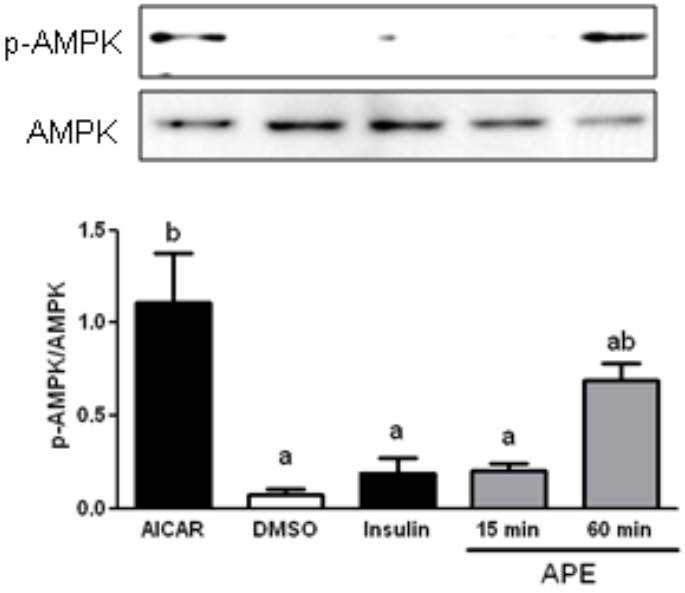

Fig. 4-6. Effects of APE on Phosphorylation of AMPK in L6 Myotubes. Serum-starved L6 myotubes were treated with 5 mg/ml* of APE extract for 15 and 60 minutes. Whole-cell lysates were subjected to western blots with anti- anti-phospho-AMPK (Thr-172) and anti-AMPK. L6 myotubes were treated with 2 nM AICAR for 4 h as a positive control. Values are the mean ± SE of three independent experiments. Different letters indicate statistically significant differences.*The dose value of APE is expressed as the equivalent of dried herb.

The compound with the highest concentration in APE, 3,5-di-*O*-caffeoylquinic acid, did not promote glucose uptake at a concentration equivalent to its quantity in APE. The other chemicals

identified by HPLC did not induce glucose uptake (data not shown). It has been reported that Artemisia plants contain β-sitosterol and scopoletin [184]. TLC analysis revealed that our APE contained β-sitosterol and scopoletin, but these compounds did not induce glucose uptake at concentrations equivalent to their levels in APE (data not shown). *A. princeps* contains sesquiterpenoid lactones [185,186] and number of volatile chemicals [187]. Some individual components may have synergistic effects, while some particular components may have strong independent effects.

Insulin stimulates glucose uptake into muscle cells and adipocytes by inducing the redistribution of insulin-responsive GLUT4 from intracellular stores to the plasma membrane. Treatment with APE promoted translocation of GLUT4 to the plasma membrane of L6 myotubes. To determine the mechanisms of GLUT4 translocation and glucose uptake by APE, we examined the effects of APE on cellular signaling pathways known to modulate these processes. The ability of APE to induce 2DG uptake was inhibited by a potent and selective PI3K inhibitor, LY294002. Hence, the downstream action of PI3K on glucose uptake is thought to contribute to this up-regulation, but the inhibition by LY294002 was not complete even though insulin-stimulated 2DG uptake was inhibited completely. It is generally accepted that PI3K has an essential regulatory role in the insulin-signaling pathway, and that it is primarily activated through insulin receptor substrates, IRS-1 and IRS-2. It is further thought that downstream effectors PI3K, Akt [188-192], and aPKCλ/ζ [80,81,193,194] serve as major distal regulators of glucose transport in response to insulin. Hence, we examined to determine whether APE would activate these downstream effectors of the insulin-signaling pathway. Insulin stimulated the phosphorylation of PI3K, Akt (Thr-308 and Ser-473), and aPKCλ/ζ in L6 muscle cells. In comparison, APE stimulated the phosphorylation of PI3K, Akt (Thr308), and aPKCλ/ζ, but did not stimulate the phosphorylation of the Ser-473 residue of Akt. The PI3K/Akt pathway plays an important role in the metabolic effects of insulin [195]. Full activation of Akt requires phosphorylation of the Thr-308 and Ser-473 residues [196]. Although Ser-473 phosphorylation clearly contributes to Akt activation, Ser-473 phosphorylation does not necessarily correlate with Akt kinase activity. For example, in cells engineered to lose the PDK1 function, Thr-308 is not phosphorylated in response to insulin, and Akt kinase activity does not increase [197]. In contrast, insulin does increase Ser-473 phosphorylation in PDK1 –/– cells without affecting Akt activity. Monitoring of Ser-473 alone can therefore incorrectly assess Akt activity [198]. Kotani *et al*. reported that aPKC was required for insulin stimulation of glucose uptake, but not for Akt activation [193]. They suggested that insulin-elicited signals that pass thorough PI3K are subsequently transmitted by at least two independent pathways: an Akt pathway and an aPKC pathway. Akt is phosphorylated at the Thr-308 residue in the activation loop by PDK1, and is phosphorylated at the Ser-473 residue in the hydrophobic motif near the COOH terminus by PDK2, but the identity of PDK2 is uncertain. Several investigators have suggested that PDK2 is a rictor-mTOR complex (rapamycin-insensitive mTOR complex 2, or mTORC2) or another unknown kinase, or that Akt is PDK2, and that phosphorylation of Ser-473 occurs *via* Akt autophosphorylation [199,200]. We suggest that the phosphorylation of the Ser-473 residue of Akt by APE is implicated in the activation of PDK2, but it is uncertain whether this

activation of PDK2 takes part in the uptake of glucose. Similarly to Akt, another PDK1 substrate, the atypical aPKCλ/ζ family, has been implicated in GLUT4 transfer to the plasma membrane [201]. APE induced phosphorylation of aPKCλ/ζ and the Thr-308 residue of Akt, but did not induce phosphorylation of the Ser-473 residue of Akt. These results suggest that APE stimulates aPKC activity thorough the activation of PI3K. Phosphorylation of aPKC was observed transiently at 15 min, and returned to basal levels by 60 min. The observed GLUT4 translocation 15 min after APE-treatment suggests that transient activation of these pathways contributed to GLUT4 translocation.

In skeletal muscle, glucose transport is activated by distinct pathways mediated by insulin and muscle contraction [202]. AMPK regulates GLUT4-dependent glucose transport in response to diverse forms of cellar stress, including contraction, hypoxia [100], and agents that disrupt the intracellular ATP:AMP ratio [183]. An early study using non-specific pharmacological activators such as AICAR, a compound taken up into skeletal muscle and metabolized by adenosine kinase to form 5-aminoimidazole-4-carboxamide-1-β-D-ribofluranotide, the monophosphorylated derivative that mimics the effect of AMP on AMPK, suggested that AMPK regulated glucose transport [115]. Treatment of skeletal muscle with AICAR *in vitro* increased glucose uptake, which was unaffected by inhibition of the insulin-dependent PI3-kinase pathway [115,203], mimicking the effect of muscle contraction to increase glucose transport. APE- and AICAR-stimulated cells showed similar levels of AMPK phosphorylation. Therefore, activation of AMPK by APE must also contribute to increases in glucose uptake *via* translocation of the GLUT4 protein, but the question remains which component of APE is the most effective inducer of AMPK. AMPK is regulated by the AMP:ATP ratio and upstream kinases, including calcium-dependent protein kinase kinase, or LKB1 [204-208]. This suggests that APE contains a compound that modulates the cellular AMP:ATP ratio or an upstream kinase of AMPK.

In conclusion, APE facilitated glucose uptake in cultured muscle cells *via* GLUT4 translocation. The results of the present study indicate that *A. princeps* stimulated the PI3K-dependent aPKC pathway and the AMPK pathway and had insulin-mimetic activity, suggesting that an insulin-independent pathway is the major mechanism by which APE exerts anti-diabetic potential.

There is growing interest in natural sources of nutrients and health-promoting compounds. Although the active components and their precise mechanisms of action remain to be clarified, these promising in vitro results indicate a need for *in vivo* testing of *A. princeps* in diabetic animals. Moreover, the identification of active compounds in *A. princeps* might result in the discovery of promising new anti-diabetic molecules.

Chapter 5

Anti-obesity and anti-diabetic effects of ethanol extract of *Artemisia princeps* in C57BL/6 mice fed a high-fat diet

5-1. Introduction

Obesity is a metabolic disorder resulting from an imbalance between energy uptake and expenditure. Dietary fat is considered to be one of the most important factors in the pathophysiology of obesity, and shows an almost linear relationship with body weight and glucose tolerance [209]. C57BL/6 mice are commonly used for obesity research, because they are lean when fed a low-fat diet, but show obese characteristics, including increased body-fat mass, hyperglycemia and hyperinsulinemia, when fed a high-fat (HF) diet [210,211].

An HF diet may induce hepatic triglyceride accumulation as a result of the import of excess amounts of fatty acids into the liver [210,212]. Hepatic triglyceride accumulation has been directly linked to systemic insulin resistance [213,214]. The hepatic triglyceride level increases when the rate of fatty acid input exceeds that of their output. The triglyceride level in hepatocytes thus represents complex interactions among the uptake of fatty acids, their derivation from non-esterified fatty acids (NEFA), *de novo* fatty acid synthesis, fatty acid oxidation, and fatty acid export as very low-density lipoprotein (VLDL)-triglyceride [215].

The genus *Artemisia* (Asteraceae) includes approximately 250 species of mostly perennial plants distributed in the northern hemisphere. They have a range of uses, including in medicines, foods, and spices, and as ornaments. Several *Artemisia* species have been reported to help prevent hyperglycemia and inflammation [216-218]. *A. princeps* (Japanese mugwort, or yomogi) is the best known *Artemisia* species in Japan, where it comprises a fundamental ingredient of the Japanese confection, kusa-mochi. This plant has been also used in traditional Asian medicine for the treatment of inflammation, diarrhea, and many circulatory disorders. Recent studies have shown it to have anti-atherosclerotic, anti-oxidant, and anti-inflammatory effects [219,220]. Previously, we reported that an ethanol extract of *A. princeps* facilitated glucose uptake in cultured muscle cells *via* GLUT4 translocation [221] (***see Chapter 4***). The results of the prvious study indicated that *A. princeps* stimulated the PI3K-dependent aPKC pathway and the AMPK pathway and had insulin-mimetic activity, suggesting that an insulin-independent pathway is the major mechanism by which APE exerts anti-diabetic potential. The present study investigated the effects of an ethanol extract of *A. princeps* (APE) on obesity and hyperglycemia in C57BL/6 mice fed an HF diet, and analyzed the obesity factors and hepatic enzyme activities involved in fatty acid oxidation and synthesis.

5-2. Materials and methods

5-2-1. Plant material

Dried powder of the aerial part of *A. princeps* (Kazuzaki yomogi), which had been cultivated as a food ingredient in a properly managed field, was obtained from Uenochu (Osaka, Japan). The powder (1,200 g) was soaked in ethanol (18 L) at 4°C for 3 days. The obtained fluid was filtered through a cotton cloth and GA-200 glass-fiber filter paper (Advantec Toyo, Tokyo, Japan), stirred with 1% (w/v) activated charcoal for 2 h, and filtered again using GA-200 glass-fiber filter. The filtrate was concentrated and the remaining paste (15.6 g, 1.3%) was mixed with three times its weight of cellulose powder (Ceolus ST, Asahi Kasei Chemical, Tokyo, Japan) until uniformly dispersed.

5-2-2. HPLC analysis of polyphenols

Polyphenol profiles of the APE were analyzed using an HPLC system, as previously described [177]. Briefly, the ethanol extract was filtered through a Millex-LG 0.2-μm membrane filter (Millipore, Bedford, MA), then analyzed using a Hitachi HPLC series D-7000 (Tokyo, Japan) equipped with Hitachi model D-7000 chromatography data station software and diode array detection system D7450 to monitor all wavelengths from 200–600 nm. Chromatographic separation was carried out on a Capcell pak C18 UG120 (250 mm × 4.0 mm internal diameter, S-5, 5 μm, Shiseido Co., Ltd., Tokyo, Japan) by a stepwise elution with 50 mM sodium phosphate (pH 3.3) containing 10% (v/v) methanol (solution A) and 70% methanol (solution B). The gradient program was as follows: 0–15 min ratio of solution A to solution B 100:0 (v/v), 15-45 min 70:30, 45-65 min 65:35, 65-70 min 60:40, 70-85 min 50:50, 85-110 min 0:100. The flow rate was 1 mL/min, the injection volume was 10 μL, and the oven temperature was 35°C. Phenolic compounds were quantified on the basis of their absorbance at 250 or 320 nm, relative to external standards or to previously generated calibration curves in the system library.

5-2-3. Animal treatment

Male C57BL/6 mice aged 4 weeks (Japan SLC, Shizuoka, Japan) were maintained at 22 ± 3°C under an automatic lighting schedule (09:00–21:00 h light). Food and water available *ad libitum*. On the day after the 7-days acclimatization, they were randomly divided into eight groups (n = 5), and fed with control diet (C) or HF diets containing 30% w/w lard for 14 weeks. The compositions of the diets and their energy contents are listed in **Table 5-1**. Body weight and food intake were measured weekly. At the end of the experiment, the tissues were collected, and frozen immediately using liquid nitrogen and kept at -80°C until use. All animal treatments were approved by the Institutional Animal Care and Use Committee (Permission number 19-5-32) and carried out according to the Guidelines of Animal Experimentation of Kobe University Animal Experimentation Regulations.

5-2-4. Oral glucose tolerance test

An oral glucose test (OGTT) was performed using an oral dose of glucose (2 g/kg body weight) at week 12. Animals were food restricted for 12 h prior to the OGTT. Blood samples were collected from a tail vein into heparinized tubes at the indicated times after the glucose load. Plasma glucose concentration was measured using a commercial assay kit (Glucose CII-test, Wako Pure Chemical, Osaka, Japan).

5-2-5. Measurement of plasma parameters related to glucose and lipid metabolism and adipocytokines

After 14 weeks, the mice were fasted for 12 h and sacrificed by collecting blood *via* cardiac puncture using a heparinized syringe, under anesthesia with sodium pentobarbital. The plasma was stored at –80°C until use. Plasma triacylglycerol, total cholesterol, free fatty acid, and glucose were measured using appropriate commercial assay kits (Triglyceride-E test, Cholesterol-E test, NEFA-C test, and Glucose CII-test, Wako Pure Chemical). Plasma insulin, adiponectin, and leptin were measured by assay kits, according to the manufacturer's directions (mouse insulin ELISA kit, Shibayagi, Gunma, Japan; mouse/rat adiponectin ELISA kit, Otsuka Pharmaceutical, Tokyo, Japan; and mouse leptin ELISA kit, Morinaga, Yokohama, Japan, respectively.) The index of the homeostasis model assessment of insulin resistance (HOMA-IR) was calculated using the relationships between the plasma glucose and insulin levels, according to the following formula [222].

HOMA-IR = fasting glucose (mg/100 mL) × fasting insulin (μU/mL)/405.

5-2-6. Measurement of hepatic lipid levels

Approximately 100 mg of liver was homogenized with 0.35 mL of distilled water, and the homogenate was extracted three times with 0.7 mL of chloroform-methanol (2:1, v/v) solution. The chloroform layer was collected by centrifugation at 1,800 × g for 10 min, and washed with a 1/4 volume of 0.88% (w/v) KCl. The obtained chloroform layer was evaporated, and measured the weight of the residue as total lipids. The residue was dissolved in isopropanol containing 10% (v/v) Triton-X 100, and triglyceride and cholesterol levels were measured using commercial kits, as described above.

5-2-7. Hepatic enzyme activities related to lipid metabolism

Approximately 300 mg of liver was homogenized in 2 mL of 3 mM Tris buffer (pH 7.4) containing 1mM ethylenediaminetetraacetic acid (EDTA), 0.25 M sucrose, 1 mM dithiothreitol (DTT) and protease inhibitors (25 μM calpain inhibitor I (ALLN), 100 μM phenylmethylsulfonylfluoride, 5 μg/mL eupeptin, and 10 μM (L-3-trans-carboxyoxirane-2- carbonyl)-L-leucylagmatine hemihydrate (E-64)) with 10 strokes of a motor-driven Teflon pestle in a 5-mL glass vessel. An aliquot of the

homogenate was stored at –80°C as crude homogenate fraction until enzymatic analysis. The remaining homogenate was centrifuged at 9,000 × *g* at 4°C for 15 min and the supernatant was stored at –80°C as an S9 fraction until enzymatic analysis. Fatty acid synthase (FAS) was determined spectrophotometrically, as described previously [223,224]. Acyl-CoA oxidase (ACO) was determined using a previously described method [225]. Carnitine palmitoyltransferase (CPT) was determined using 96-well plates, according to a previously described method [226].

5-2-8. Statistical analysis

Data are expressed as mean ± SE. Statistical analysis (ANOVA) was carried out using the Tukey-Kramer multiple comparison test. Differences were considered significant when *P* values were < 0.05.

Table 5-1. Composition of the experimental diets

	Control diet				HF diet			
	0% APE	0.2% APE	0.5% APE	1.0% APE	0% APE	0.2% APE	0.5% APE	1.0% APE
APE[a] (%)	–	1.19	0.48	0.96	–	1.19	0.48	0.96
Cellulose (%)	8.66	8.47	8.18	7.70	8.66	8.47	8.18	7.70
Lard (%)	–	–	–	–	28.85	28.85	28.85	28.85
Cornstarch (%)	44.81	44.81	44.81	44.81	15.96	15.96	15.96	15.96
Casein (%)	13.46	13.46	13.46	13.46	13.46	13.46	13.46	13.46
L-Cystine (%)	0.19	0.19	0.19	0.19	0.19	0.19	0.19	0.19
Dextrin (%)	14.90	14.90	14.90	14.90	14.90	14.90	14.90	14.90
Sucrose (%)	9.62	9.62	9.62	9.62	9.62	9.62	9.62	9.62
Soybean oil (%)	3.85	3.85	3.85	3.85	3.85	3.85	3.85	3.85
Mineral mix (AIN-93M) (%)	3.37	3.37	3.37	3.37	3.37	3.37	3.37	3.37
Vitamin mix (AIN-93) (%)	0.96	0.96	0.96	0.96	0.96	0.96	0.96	0.96
Choline bitartrate (%)	0.29	0.29	0.29	0.29	0.29	0.29	0.29	0.29
Tertiary butyl hydroxy quinone (%)	0.0008	0.0008	0.0008	0.0008	0.0008	0.0008	0.0008	0.0008
Total (%)	100	100	100	100	100	100	100	100
Energy[b] (MJ/100 g diet)	1400	1400	1400	1400	2084	2084	2084	2084

APE-containing diets were prepared by adding APE-containing cellulose powder to the control or HF diet.
[a]APE, ethanol extract of *A. princeps*.
[b]The energy was calculated by counting out the energy of APE.

5-3. Results

5-3-1. Polyphenol Analysis

The polyphenol profile of APE was analyzed using a HPLC system constructed for simultaneous determination of polyphenols in food stuffs (**Table 5-2**). Comparison with the library in the HPLC system identified the presence of chlorogenic acid (19.0 mg/g), protocatechuic acid (38.2 mg/g), and trace of luteolin in APE. 3,5-di-*O*-caffeoylquinic acid (278.1 mg/g), which was one of the major phenolic components, was analyzed by comparison with a standard chromatogram. A previous study reported that one of the flavones, eupatilin (5,7-dihydroxy-3,4,6-trimethoxyflavone), is an active compound in *A. princeps* [181]. We checked the amount of eupatilin in our APE as compared with standard compound obtained from PhytoLab (Vestenbergsgreuth, Germany), and confirmed that our APE did not contain eupatilin.

Table 5-2. Polyphenols in an ethanol extract of *A. princeps* (APE) identified by high-performance liquid chromatography (HPLC)

Name[a]	Concentration in APE (mg/g)	Retention time of peak (min)
Protocatechuic acid	19.0[b]	9.7
Chlorogenic acid	38.2[b]	13.7
3,5-di-*O*-caffeoylquinic acid	278.1[c]	31.6
Luteolin	trace[b]	80.0

[a] The phenolic content was determined using an HPLC system constructed for the simultaneous determination of polyphenols in foods.13
[b] These values were calculated using previously generated calibration curves available in the system library.
[c] This value was calculated using a curve generated from an external standard.

5-3-2. Effects of APE on body weight and adipose tissue weight

At the end of 14-week HF diet feeding, body weights were significantly higher than that of those in the control diet group. However, the body weights of APE-supplemented groups (HF-0.2%APE, HF-0.5%APE and HF-1.0%APE) were 8.6%, 20.4%, and 20.4% lower compared with the HF-0%APE group (**Table 5-3**). Both 0.5% and 1.0% APE supplementation significantly decreased HF diet-induced body weight gain from week 11 (**Fig. 5-1**). There were no significant differences in body weights among the control diet groups. The weights of all the white adipose tissues were significantly increased in the HF-0%APE group, compared with the C-0%APE group (**Table 5-3**). APE suppressed the HF diet-induced increase in adipose tissue weight. Supplementation of the HF diet with 1.0% APE significantly reduced the weights of almost all white adipose tissues, except for epididymal adipose tissue, compared with the HF-0%APE group. The weights of mesenteric adipose

tissue of APE-supplemented groups (HF-0.2%APE, HF-0.5%APE, and HF-1.0%APE) were 29.3%, 49.7%, and 62.1% lower compared with the HF-0%APE group. APE supplementation tended to reduce body weight and adipose tissue weights in the control diet groups, but the differences were not significant. These results suggest that dietary APE has the potential to counteract obesity.

5-3-3. Preventive effect of APE on HF diet-induced hyperglycemia

An OGTT was performed after feeding the mice with APE for 12 weeks (**Fig. 5-2A**). Plasma glucose levels in the HF-0 group remained high between 15 and 120 min, but supplementation of the HF-diet with APE (HF-0.5%APE and HF-1.0%APE) significantly improved glucose tolerance compared with the HF-0 group. There were no significant differences in OGTT results throughout the experiment in the control diet groups. The area under the curve (AUC) in the HF-0%APE group was 37% higher than that in the C-0%APE group ($P < 0.05$), while that in the HF-0.5%APE group was 32% lower than that in the HF-0%APE ($P < 0.05$) (**Fig. 5-2B**).

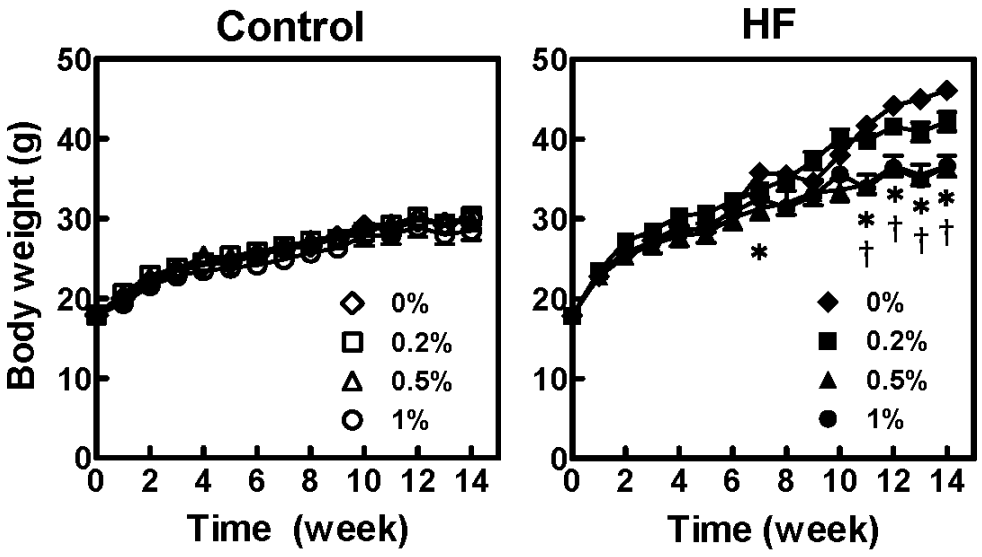

Fig. 5-1. Changes in body weight of mice fed with control and high-fat (HF) diets containing an ethanol extract of A. princeps for 14 weeks. Closed symbols represent the HF-diet groups and open ones represent the control-diet groups. Values are the means ± SE (n=5). Significant differences between the 0% group and 1.0% (*) or 2.0% (†) groups are indicated (P<0.05 by the Tukey-Kramer multiple comparison test).

Table 5-3. Effects of an ethanol extract of *A. princeps* (APE) on body weight, adipose tissue weights, and plasma lipid levels of mice fed control and the high-fat diets.

	Control diet				High-fat diet			
	0% APE	0.2% APE	0.5% APE	1.0% APE	0% APE	0.2% APE	0.5% APE	1.0% APE
Total energy intake (MJ/mouse)	4,895	4,519	4,397	4,071	5,690	5,803	5,456	5,941
Body weight (g)	28.2 ± 0.9^{a}	28.3 ± 0.9^{a}	28.0 ± 1.1^{a}	27.1 ± 1.2^{a}	44.2 ± 0.7^{b}	40.4 ± 1.2^{b}	35.2 ± 1.2^{c}	35.2 ± 1.1^{c}
Tissue weight (g/100 g body weight)								
Liver	3.72 ± 0.12^{ab}	3.79 ± 0.11^{ab}	3.72 ± 0.19^{ab}	3.78 ± 0.05^{ab}	4.01 ± 0.12^{a}	3.32 ± 0.27^{b}	3.32 ± 0.06^{ab}	3.47 ± 0.09^{ab}
White adipose tissue								
Total	8.10 ± 1.53^{ab}	8.08 ± 1.38^{ab}	7.26 ± 1.16^{a}	6.64 ± 0.79^{a}	23.1 ± 0.71^{c}	21.8 ± 1.69^{c}	19.3 ± 2.13^{cd}	14.0 ± 1.33^{bd}
Epididymal	1.94 ± 0.31^{a}	2.20 ± 0.35^{a}	1.96 ± 0.2^{a}	2.09 ± 0.50^{a}	4.80 ± 0.37^{b}	5.47 ± 0.36^{b}	5.17 ± 0.51^{b}	4.11 ± 0.30^{b}
Mesenteric	0.90 ± 0.10^{ab}	0.97 ± 0.14^{ab}	0.77 ± 0.14^{a}	0.84 ± 0.25^{a}	3.62 ± 0.30^{c}	2.56 ± 0.31^{d}	1.82 ± 0.29^{bd}	1.37 ± 0.13^{ab}
Retroperitoneal	1.35 ± 0.27^{ab}	1.36 ± 0.23^{ab}	1.10 ± 0.21^{a}	1.19 ± 0.32^{ab}	3.80 ± 0.28^{c}	3.33 ± 0.28^{cd}	3.26 ± 0.37^{cd}	2.41 ± 0.21^{bd}
Subcutaneous	3.91 ± 0.90^{ab}	3.55 ± 0.69^{ab}	3.43 ± 0.57^{ab}	2.53 ± 0.34^{a}	10.9 ± 0.31^{c}	10.5 ± 0.97^{c}	9.02 ± 1.07^{cd}	6.09 ± 0.76^{bd}
Brown adipose tissue	0.53 ± 0.03^{abc}	0.63 ± 0.06^{abcd}	0.47 ± 0.05^{a}	0.58 ± 0.12^{abcd}	0.94 ± 013^{ed}	1.07 ± 0.11^{e}	0.83 ± 0.06^{bce}	0.66 ± 0.05^{acd}
Plasma lipid levels								
Total cholesterol (mg/dL)	105 ± 3^{a}	105 ± 4^{a}	109 ± 10^{a}	115 ± 8^{ab}	180 ± 6^{c}	144 ± 9^{b}	144 ± 10^{b}	122 ± 3^{ab}
NEFA (meq/L)	0.91 ± 0.05^{a}	0.70 ± 0.06^{abc}	0.74 ± 0.07^{abc}	0.79 ± 0.12^{ab}	0.63 ± 0.04^{abc}	0.65 ± 0.05^{abc}	0.49 ± 0.02^{c}	0.53 ± 0.04^{bc}
Triglyceride (mg/dL)	134 ± 5^{a}	120 ± 4^{ab}	116 ± 5^{b}	119 ± 1^{ab}	107 ± 1^{b}	110 ± 2^{b}	113 ± 3^{b}	108 ± 2^{b}

Mice were fed with control or a high-fat diets containing APE for 14 weeks. At the end of experiment, body weight, tissue weights, and plasma lipid levels were measured after fasting for 12 h. Values are the mean ± SE (n=5). Values without common letters in a row indicate significant differences ($P<0.05$) by the Tukey-Kramer multiple comparison test.

The plasma glucose level at the end of the experiment was significantly higher in the HF-0 group, compared with the C-0%APE group (**Fig. 5-3A**). Supplementation of the HF diet with APE reduced plasma glucose levels in a dose-dependent manner. The plasma insulin level was also higher in the HF-0%APE group than in the C-0%APE group (**Fig. 5-3B**). Insulin levels in the HF-0.5%APE and HF-1.0%APE groups were normalized, and equivalent to that in the control diet group. Neither glucose nor insulin levels changed in the control diet groups. HOMA-IR is a good predictor of total insulin sensitivity, and was significantly higher in the HF-0 than in the C-0%APE group (**Fig. 5-3C**). Supplementation of the HF diet with 0.5% and 1.0% APE significantly attenuated the HF diet-induced increase in HOMA-IR.

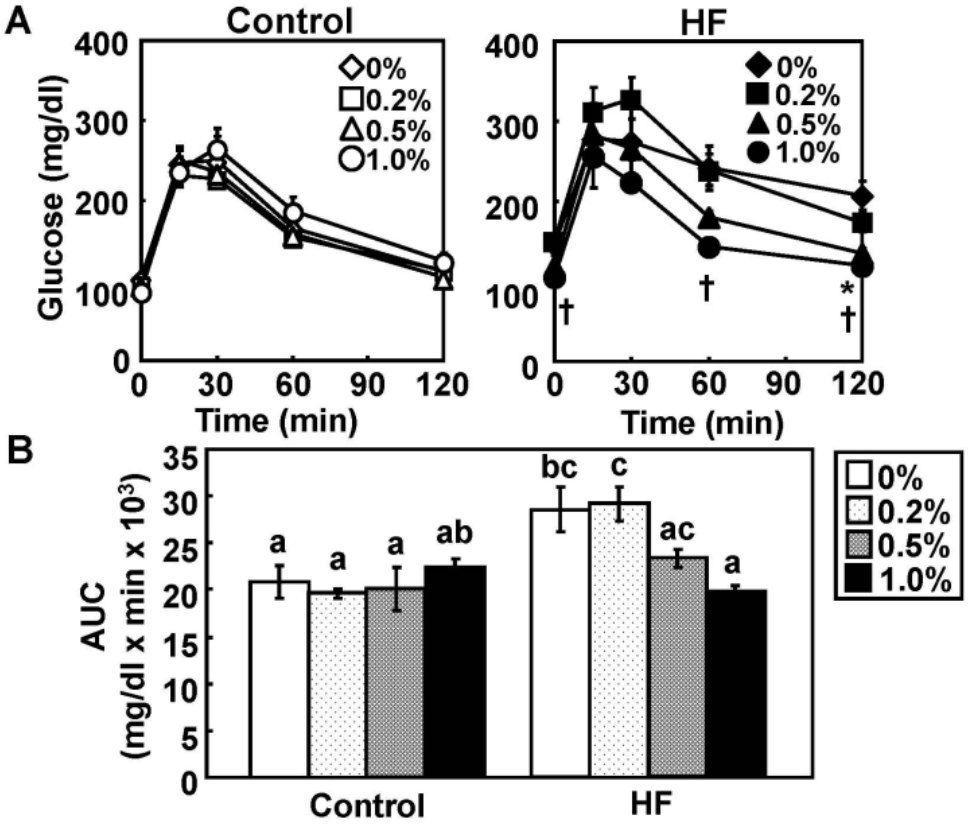

Fig. 5-2. Oral glucose tolerance test (OGTT) in mice fed control and high-fat (HF) diets containing an ethanol extract of A. princeps (APE) at week 12. (A) Fasting plasma glucose levels after oral glucose administration (2.0 g/kg body weight). Closed symbols represent the HF-diet groups and open ones represent the control-diet groups. Values are the mean ± SE (n=6). Significant differences between 0% group and 1.0% (*) or 2.0% (†) group are indicated ($P<0.05$ by the Tukey-Kramer multiple comparison test). (B) Area under the curve (AUC) from the values of (A). Values are the mean ± SE (n=5). The same letters indicate no significant differences according to the Tukey-Kramer multiple comparison test. $P<0.05$ was considered significant.

APE suppressed hyperglycemia and insulin resistance, as described above, and α-glucosidase activities in the small intestine were measured to clarify the mechanisms behind the antihyperglycemic effect. Both maltase and sucrase activates tended to decrease in the HF-diet groups, compared with the control groups, though the differences were not significant (data not shown). APE did not inhibit maltase or sucrase activities in the small intestine.

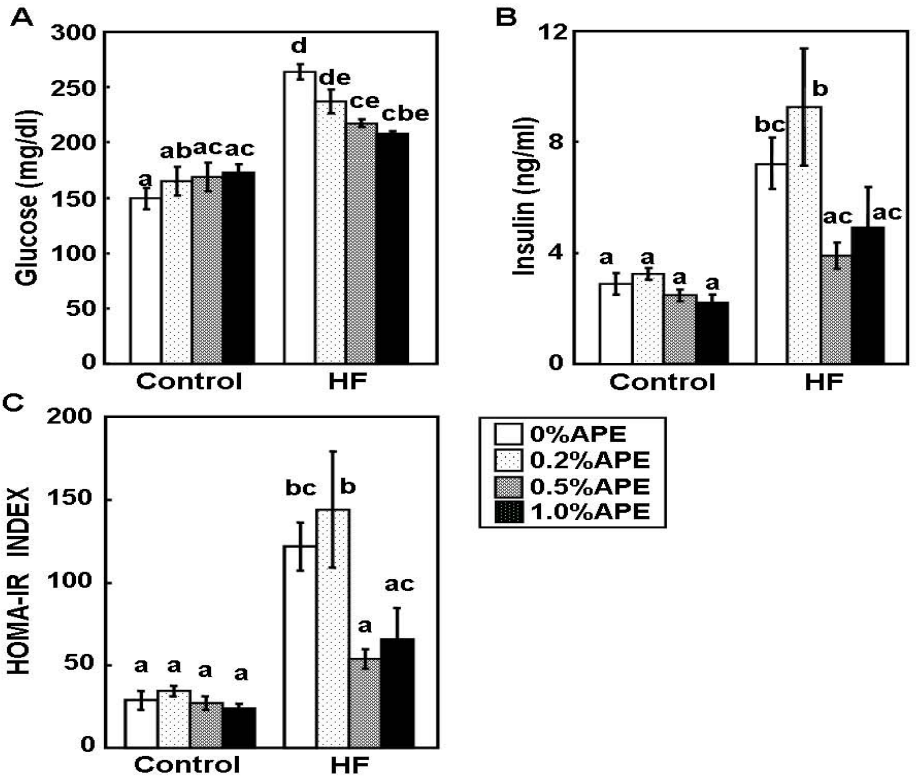

Fig. 5-3. Effect of an ethanol extract of *A. princeps* (APE) on plasma glucose and insulin levels in mice fed control and high-fat (HF) diets for 14 weeks. Plasma levels of glucose (**A**) and insulin (**B**) were measured, and the homeostasis model assessment of insulin resistance index (HOMA-IR) was calculated (**C**). Values are the mean ± SE (n=4). The same letters represent no significant differences according to the Tukey-Kramer multiple comparison test. P<0.05 was considered significant.

5-3-4. Effect of APE on lipid metabolism

Intake of a HF diet induces fatty liver and hepatic lipid accumulation, which are involved in systemic insulin resistance [213,214]. The hepatic total lipid level was significantly higher in the HF-0%APE group than in the C-0%APE group (**Fig. 5-4**). APE suppressed the HF diet-induced

hepatic lipid accumulation in a dose-dependent manner, and the hepatic total lipid level was significantly lower in HF-1.0%APE group than in the HF-0%APE group. The hepatic triglyceride level in the HF-0%APE group was also higher than that in the C-0%APE group, and this higher value was significantly lowered by supplementation with 1.0% APE (**Fig. 5-4**). The hepatic cholesterol level was significantly higher in the HF-0 group than in the C-0 group, and this was also significantly lowered by supplementation with 1.0% APE (**Fig. 5-4**). These results suggest that APE has the ability to prevent fatty liver induced by an HF diet.

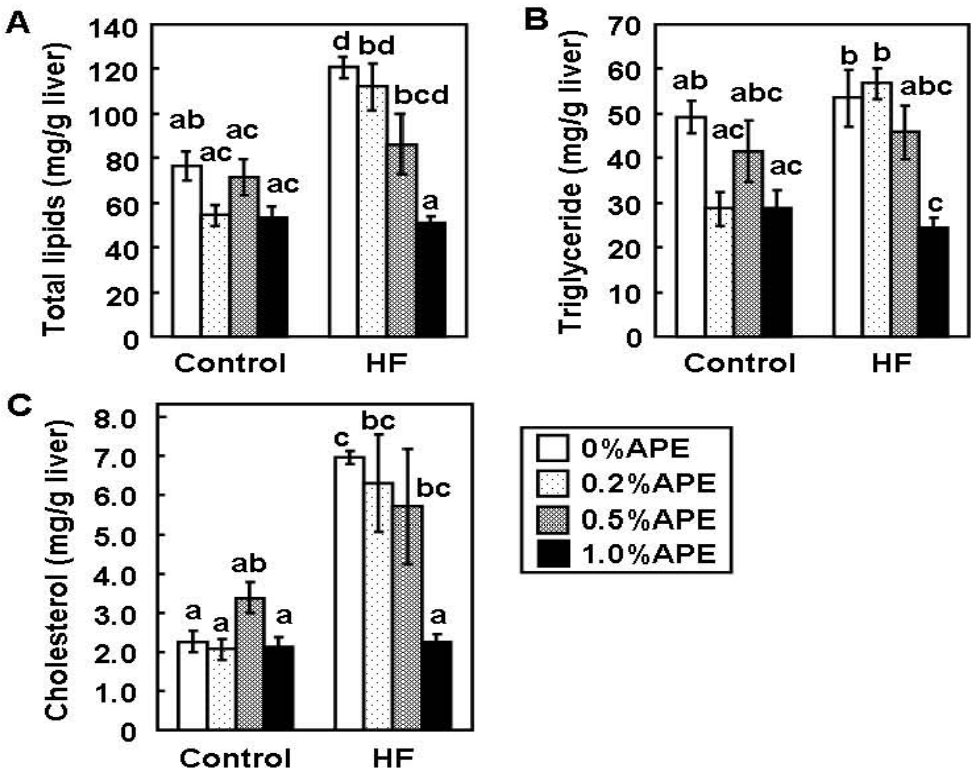

Fig. 5-4. Effects of an ethanol extract of *A. princeps* (APE) on hepatic lipid levels in mice fed control and high-fat (HF) diets for 14 weeks. Total lipid (**A**), triglyceride (**B**) and cholesterol (**C**) levels were measured. Values are the mean ± SE (n=5). The same letters represent no significant differences according to the Tukey-Kramer multiple comparison test. $P<0.05$ was considered significant.

APE suppressed hepatic lipid levels, and plasma lipid levels were therefore also measured. The total plasma cholesterol level was significantly higher in the HF-0%APE group, compared with the C-0%APE group (**Table 5-3**), but was significantly lower in the HF-0.2%APE, HF-0.5%APE, and HF-1.0%APE groups, compared with the HF-0%APE group. The cholesterol level in the

HF-1.0%APE group was similar to that in the control diet groups. Plasma NEFA and triglyceride levels in the HF diet groups were lower than those in the control diet groups (**Table 5-3**). APE tended to decrease NEFA levels in both the control and HF-diet groups.

The activities of the hepatic enzymes related to lipid metabolism were also measured (**Fig. 5-5**). CPT, ACO and FAS activities were lower in the HF-diet groups than in the control groups. CPT and ACO are responsible for β-oxidation in mitochondria and peroxisomes, respectively [227], APE did not affect CPT or ACO activities in either control or HF-diet groups. FAS is a key enzyme that catalyzes fatty acid biosynthesis [228,229], APE significantly reduced FAS activity in the HF-diet groups in a dose-dependent manner.

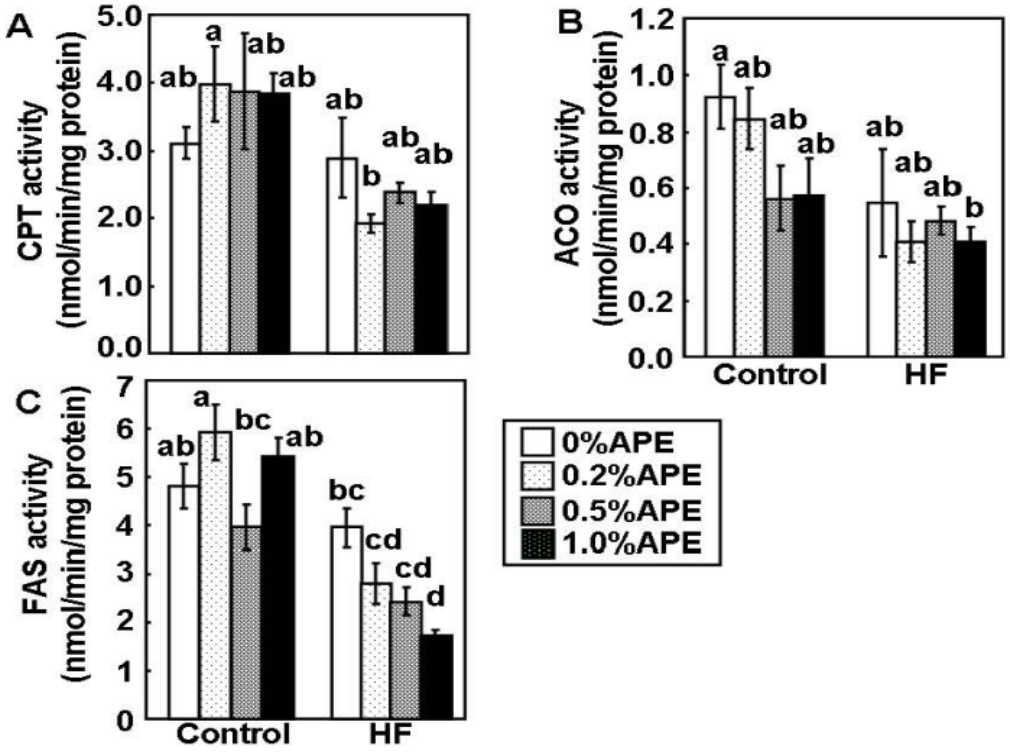

Fig. 5-5. Effects of an ethanol extract of *A. princeps* (APE) on the activities of hepatic enzymes related to lipid metabolism in mice fed control and high-fat (HF) diets for 14 weeks. Carnitine palmitoyltransferase (CPT) (**A**), acyl-CoA oxidase (ACO) (**B**), and fatty acid synthase (FAS) (**C**) activities in the liver were measured. Values are the mean ± SE (n=5). The same letters represent no significant differences according to the Tukey-Kramer multiple comparison test. P<0.05 was considered significant.

5-3-5. Effect of APE on adipocytokines

White adipose tissue is a major endocrine tissue that releases various adipocytokines into the bloodstream. Because leptin and adiponectin are major adipocytokines associated with maintaining

glucose homeostasis [230], we measured the plasma levels of these adipocytokines (**Fig. 5-6**). The plasma leptin level was 13.5-fold greater in the HF-0%APE than in the C-0%APE group, and APE significantly and dose-dependently reduced HF diet-induced leptin levels. Plasma leptin levels were 34.7%, 51.4%, and 73.3% lower in the HF-0.2%APE, HF-0.5%APE, and HF-1.0%APE groups, respectively, compared with the HF-0%APE group. There were no significant differences in leptin levels among the control diet groups. In contrast, plasma adiponectin levels were similar in all groups in this study, despite the fact that circulating adiponectin levels are reportedly reduced in obese states [230].

5-4. Discussion

The genus Artemisia comprises numerous diverse species, many of which are used as medical plants to alleviate human conditions including hyperglycemia and diabetes [216-218]. This study investigated the use of an ethanol extract of *A. princeps* as a potential dietary supplement for the management of hyperglycemia and obesity in HF diet-induced obese C57BL/6 mice. A regular HF-diet is generally accepted to cause obesity, and prevention of obesity and fat accumulation is important for the promotion of human health. APE suppressed fat accumulation without reducing food intake, suggesting that dietary APE has the potential to counteract obesity.

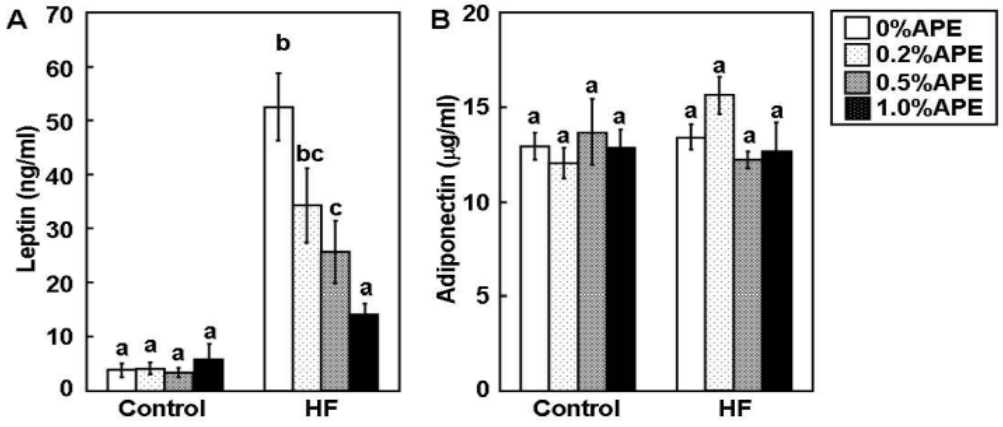

Fig. 5-6. Effect of an ethanol extract of *A. princeps* (APE) on plasma leptin and adiponectin levels in mice fed control and high-fat (HF) diets for 14 weeks. Plasma leptin (**A**) and adiponectin (**B**) were measured. Values are the mean ± SE (n=5). The same letters represent no significant differences according to the Tukey-Kramer multiple comparison test. P<0.05 was considered significant.

Obesity is strongly associated with insulin resistance, and improved insulin resistance is important in preventing the development of type 2 diabetes (T2DM). The results of this study suggest that dietary APE can prevent HF diet-induced insulin resistance and hyperglycemia. Inhibition of carbohydrate-hydrolyzing enzymes in the small intestine represents an effective method of preventing and treating hyperglycemia [231]. Synthetic α-glucosidase inhibitors such as acarbose and miglitol are widely for treating T2DM patients [226]. These inhibitors block the action of the α-glucosidase enzymes in the small intestine, thereby delaying glucose absorption [231]. Certain plant extracts have been reported to inhibit α-glucosidase activities [232,233]. Although HPLC analysis identified chlorogenic acid and 3,5-di-*O*-caffeoylquinic acid, both compounds with reported α-glucosidase inhibitory activities [234], as components of APE in this study, APE had no effect on α-glucosidase activities in this study. The suppression of hyperglycemia and insulin resistance by APE is therefore to the result of α-glucosidase inhibition.

Previously, an anti-diabetic effect of Korean *A. princeps* in type-2 diabetic mice was reported [180,181]. The active constituent is thought to be a flavones, eupatilin, which had a functional anti-diabetic effect by enhancing hepatic and plasma glucose metabolism [181]. Hence, we analyzed the amount of eupatilin in our APE by HPLC analysis, and confirmed that our APE did not contain eupatilin. The *A. princeps* used in the previous studies were variants cultivated in Korea, and may have had a different composition of phytochemicals than Japanese *A. princeps*.

APE significantly suppressed the accumulation of white adipose tissue, including visceral adipose tissue. Visceral adipose tissue is an important predictor of insulin resistance, hyperglycemia and other metabolic risk factors [21,235]. Increased adipose tissue weights are accompanied by the induction of inflammatory cytokines involved in insulin resistance [236-238], and inhibition of fat accumulation by APE may therefore also contribute to its prevention of hyperglycemia.

APE normalized liver weight and hepatic lipid content in the HF-diet groups, suggesting that it could prevent HF diet-induced fatty liver. Visceral adipose tissue has recently been correlated with intrahepatic triglyceride content, and an increase in intrahepatic triglycerides is associated with the metabolic abnormalities [213,214,239]. The prevention of fatty liver by APE may thus also contribute to the prevention of hyperglycemia. The activities of hepatic enzymes related to lipid metabolism were measured, to clarify the mechanisms whereby APE prevented hepatic lipid accumulation. APE inhibited FAS activity in mice fed an HF-diet. FAS catalyzes the final step in fatty acid synthesis, and is believed to be a determinant of the capacity for *de novo* fatty acid synthesis [229]. APE thus inhibited fatty acid synthesis through inhibition of FAS, a rate-limiting enzyme in fatty acid synthesis, resulting in a decrease in hepatic lipid content. FAS activities were higher in the control diet groups than in the HF-diet groups. Lipogenic enzyme activities are reduced by fasting or by intake of an HF-diet, and increased by intake of a carbohydrate-rich diet or by re-feeding [240,241]. Inhibition of FAS by APE could therefore help to prevent HF diet-induced fatty liver.

Jung and Kang *et al*. reported that ethanol extracts of *A. princeps* improved glucose and insulin tolerance *via* enhancing hepatic and plasma glucose metabolism [180] and reduced FAS in

diabetic animals, db/db mice [242]. Inhibition of hepatic activity of glucose-6-phosphatase, a rate-limiting enzyme of gluconeogenesis may partly contribute to the anti-hyperglycemic effect of APE. Furthermore their groups reported that eupatilin isolated from their APE played the role of an antidiabetic functional component in *A. princeps* by enhancing hepatic and plasma glucose metabolism as well as by increasing insulin secretion in type 2 diabetic mice [181]. We observed the anti-diabetic and anti-obese effects in the absence of eupatilin in our APE. The regulation of FAS activity by APE might be the one with another compound that is not eupatilin. *Artemisia* plant contain various phytochemicals, such as β-sitosterol [184], scopoletin [184], sesquiterpenoid lactones [185,186] and number of volatile chemicals [187]. Some individual components may have synergistic effects, while some particular components may have strong independent effects. The previous observation in the db/db mice, a genetic model of diabetes and the present observation in the environmentally-induced diabetic model is sure to make the effect of *A. princeps* certain regardless of whether the active ingredient is eupatilin.

The down-regulation of FAS activity by APE may, in turn, result from prevention of hyperleptinemia. Lipogenesis has recently been shown to be controlled by leptin *via* signal transducer and activator of transcription 3-independent central mechanisms [243]. Furthermore, intraperitoneal leptin administration in C57BL/6 mice was able to directly suppress the expression of FAS in the liver and white adipose tissue, accompanied by reduced liver triglyceride levels [244]. Prevention of leptin secretion by APE may therefore contribute to the inhibition of FAS activity and triglyceride accumulation in the liver.

The hepatic triglyceride content is determined by the balance between fatty acid input (e.g., by *de novo* fatty acid synthesis) and output (e.g., by oxidation and export of VLDL-triglycerides). Measurements of hepatic CPT and ACO activities indicated that APE supplementation had no effect on the activities of these enzymes. The oxidation of intrahepatocellular fatty acids occurs mainly in mitochondria, and to a much lesser extent in peroxisomes and microsomes. CPT regulates the transport of fatty acids from the cytoplasm to the mitochondrial matrix across the membrane [227], while ACO is the initial enzyme in the peroxisomal β-oxidation system [245,246]. The results in this study suggest that APE does not affect β-oxidation in either the mitochondria or peroxisomes.

Han *et al*. reported the antiatherosclerotic and anti-inflammatory activities in LDLR(–/–) mice [219]. Chronic inflammation in fat plays a crucial role in the development of obesity-related insulin resistance and endothelial dysfunction is an early event in atherosclerosis, and large-vessel atherosclerotic disease is the major cause of morbidity and mortality in diabetes. Not only metabolizing glucose and lipid but also these functions might have contributed effectively.

The dosage of APE in mice fed a HF-diet containing 1.0% of APE becomes about 100 mg/man/day as 60 kg in weight to human according to conversion based on body surface area. However, it is not appropriate to apply dosage from a present result in the study of mice to the dosage to the human. Further study will be needed to clarify its effect on the health of human.

In conclusion, we investigated the effects of APE on obesity and hyperglycemia in C57BL/6

mice fed an HF diet. Dietary APE prevented body weight gain, fat accumulation, and hyperglycemia in mice fed an HF diet. APE supplementation suppressed hyperleptinemia, which may prevent hepatic lipid accumulation through inhibition of FAS activity in the liver. This inhibition of hepatic lipid accumulation will thus contribute to the prevention of hyperglycemia. The results also suggested that *A. princeps* might be an excellent natural food additive because of its antiobesity and antidiabetic properties, and that it could be useful for the development of a more potent and selective agent.

Chapter 6

Cardamonin stimulates glucose uptake through translocation of glucose transporter 4 in L6 myotubes

6-1. Introduction

Natural products provide a rich resource for the development of novel therapeutic agents used to treat a variety of human diseases. There is currently a growing interest in the use of nutrients and health-promoting compounds from natural sources. Chalcones were originally isolated from natural plant sources and have been reported to have a variety of biological properties, including antioxidant, antiinflammatory and anticancer activities [247]. Several synthetic chalcone derivatives are known to inhibit diabetic complications [248,249].

Insulin resistance is a characteristic feature of non-insulin-dependent diabetes mellitus and an important contributory factor in the pathophysiology of this disorder. It can be associated with a number of complications, including cardiovascular disease and renal failure. Insulin resistance is defined as a reduced ability of tissue to respond to physiological levels of insulin. Skeletal muscle constitutes the major mass of peripheral tissue, accounting for about 40% of total body mass and > 30% of total energy expenditure; it is the primary tissue responsible for postprandial uptake of glucose from the blood [39]. The availability of glucose transporter (GLUT) protein on the cell surface is a major factor regulating glucose uptake into muscle. GLUT1 mediates basal or nonstimulated transport in muscle cells and adipocytes, whereas the insulin-responsive GLUT4 facilitates increased glucose transport in the presence of insulin.

Previously a non-radioisotopic, high-throughput enzymatic assay was developed to evaluate glucose uptake in cultured cells [159,160,162] (***see Chapter 2 and 3***). Recently our group used this assay to screen for phytochemicals promoting the uptake of 2-deoxyglucose (2DG) in L6 myotubes, and we identified several compounds having high activity (**Fig. 6-1**). Among them, 4-hydroxyderricin and xanthoangelol (**Fig. 6-2**), prenylated chalcones abundant in Ashitaba (*Angelica keiskei* Koidzumi, Apiaceae), significantly increased 2DG uptake in L6 cells by 1.9-fold at 10 μM, compared with the level in DMSO-treated control cells [4], and we investigated the effect of these chalcones on the translocation of GLUT4 and its underlying mechanisms. The chalcones increased the GLUT4 level in the plasma membrane of L6 cells, but activated neither protein kinase C λ/ζ, Akt, nor adenosine monophosphate-activated protein kinase, all of which regulate the GLUT4 translocation. This suggests that chalcones are promising compounds for the maintenance of blood glucose levels through their stimulation of skeletal-muscle-associated glucose uptake. The chemistry and biological activities of chalcones have been of interest for some time, and their wide range of biological activities has been well documented in the literature. These include antituberculous activity [250], tyrosine kinase

inhibition [251] and cytotoxicity against murine and human cancer lines [252].

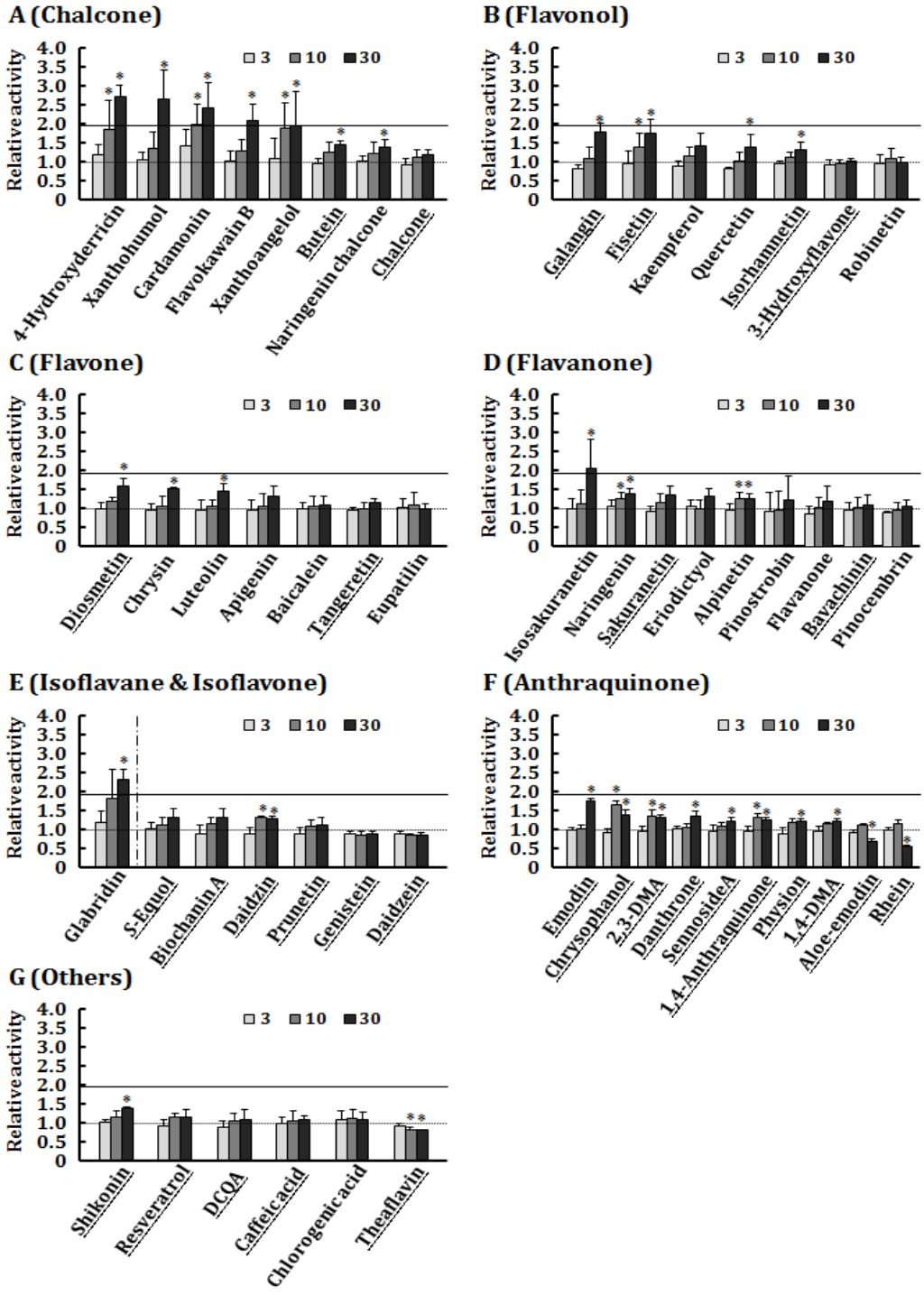

Fig. 6-1. Effects of 54 phytochemicals on glucose uptake in L6 myotubes. After incubation in 0.2% (w/v) BSA/MEM for 18 h, L6 myotubes were treated with DMSO (thin line), insulin (0.1 μM, thick line) or phytochemicals (3, 10 and 30 μM) for 4 h, and then incubated in 2DG-containing buffer for a further 20 min. The uptake of 2DG was determined as described in ***Chapter 2***. (A) Chalcone; (B) flavanone: (C) flavonol; (D) flavones; (E) isoflavane and isoflavone; (F) Anthraquinone; Other phytochemical. Relative activity was calculated as the ratio of 2DG uptake in polyphenol-treated L6 myotubes to that in DMSO-treated cells. Data are shown as the mean ± SD from 3 independent experiments. Asterisk indicates a statistically significant difference ($p < 0.05$) from the DMSO-treated cells by Dunnet's test. A part of this work were published previously [4]

Among the phytochemicals which was screened (**Fig. 6-1**), the chalcone cardamonin (2',4'-dihydroxy-6'-methoxychalcone) and the flavanone alpinetin (7-hydroxy-5- methoxyflavanone) (**Fig. 6-3**), which are two of the main constituents of the seeds of *Alpinia katsumadai* Hayata (Zingiberaceae), also promoted glucose uptake in L6 myotubes. They demonstrate antibacterial, antiinflammatory and other important therapeutic activities of significant potency, with low systemic toxicity. Medicinally, plants of this family are reputed to have values such as antihepatotoxic, antiinflammatory and stomachic properties, and *A. katsumadai* Hayata has been utilized as a traditional Chinese herbal antiemetic and stomachic drug [253]. However, the effects of cardamonin or *A. katsumadai* Hayata on glucose uptake in muscle cells have not yet been reported. This study investigated the effects of cardamonin, isolated from *A. katsumadai* Hayata, and its related chemicals on 2DG uptake in cultured L6 myotubes.

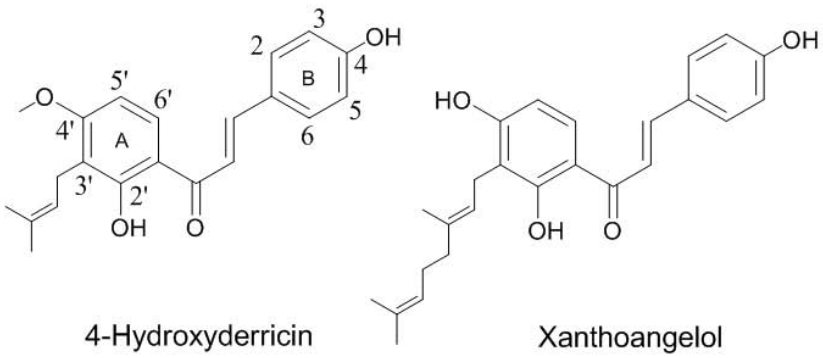

Fig. 6-2. Chemical structure of 4-hydroxyderricin and xanthoangelol.

6-2. Materials and methods

6-2.-1. Reagents

Pinostrobin, glucose-6-phosphate dehydrogenase (G6PDH), 2DG, 2-deoxyglucose-6-phosphate (DG6P) and insulin were purchased from Sigma-Aldrich (St Louis, MO). Resazurin sodium salt and triethanolamine (TEA) hydrochloride were from Wako Pure Chemical Industries (Osaka, Japan), diaphorase, ATP and NADP were from Oriental Yeast (Tokyo, Japan), and WST-1 was from Roche Diagnostics (Mannheim, Germany). For western blot analysis, anti-GLUT4 goat IgG, anti-GLUT1 goat IgG, anti-IRß rabbit IgG, anti-goat IgG, anti-phospho-phosphatidylinositol 3'-kinase (PI3K) goat IgG, and anti-rabbit IgG antibodies were purchased from Santa Cruz Biotechnology

(Santa Cruz, CA), anti-phospho-Akt (Thr-308) rabbit IgG, antiphospho-PKCλ/ζ rabbit IgG, anti-Akt rabbit IgG and anti-AMP-activated protein kinase (AMPK)α rabbit IgG were from Cell Signaling Technology (Danvers, MA), anti-phospho-Akt (Ser-473) rabbit IgG was from Sigma-Aldrich, and anti-PI3K mouse IgG and anti-PKCλ mouse IgG were from BD Biosciences (San Jose, CA). All other reagents used were of the highest grades commercially available.

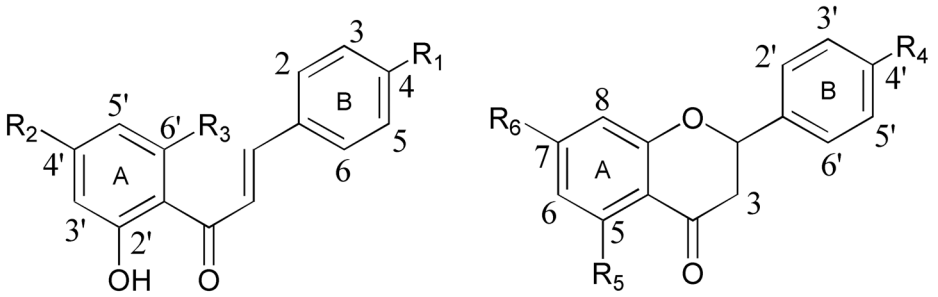

	-R_1	-R_2	-R_3
Cardamonin	-H	-OH	-OMe
Flavokawain B	-H	-OMe	-OMe
Naringenin chalcone	-OH	-OH	-OH

	-R_4	-R_5	-R_6
Alpinetin	-H	-OMe	-OH
Pinostrobin	-H	-OH	-OMe
Pinocembrin	-H	-OH	-OH
Naringenin	-OH	-OH	-OH

Fig. 6-3. Chemical structure of phenolic compounds tested in this study.

6-2-2. Isolation and synthesis of flavonoids

Cardamonin, alpinetin and pinocembrin were isolated from the seeds of *A. katsumadai* Hayata, which was cultivated in Hainan Island in Southern China and purchased from Mikuni & Co. (Osaka, Japan). Powdered seed (100 g) was defatted with hexane (1 L × 2) and extracted in ethyl acetate (EtOAc) (1 L × 3). The EtOAc extract was dried using MgSO4 and adsorbed to a neutral alumina column (activity grade 3, 50–200 μm, 5 × 7 cm; MP Biomedicals, Eschwege, Germany), washed with EtOAc until the eluted substance disappeared, and eluted with 300 mL of EtOAc–90% formic acid (95:5). The obtained fluid was washed with water 10 times, dried with $MgSO_4$, and concentrated in a vacuum. White precipitate was formed during the concentration and the residue remaining on the filter paper following filtration was crystallized from 1, 4-dioxane to pure alpinetin (yield 201.8 mg). The permeate was subjected to a silica gel column (64–210 μm, 3 × 20 cm), eluted with EtOAc, and the yellow eluate was then evaporated and dissolved in 1,4-dioxane. Pure

cardamonin (163.7 mg) and pinocembrin (249.2 mg) were refined by reverse‐phase medium‐pressure liquid chromatography on a Wakosil 40C18 column (40 μm, 15 × 300 mm; Wako Pure Chemical Industries) eluted with methanol–H2O 80:20 at 5 mL/min, and were then crystallized from EtOAc solution.

Flavokawain B was synthesized by direct aldol condensation of acetophenone with benzaldehyde. Briefly, an ethanol solution (8 mL) of 4',6'-dimethoxy-2'-hydroxyacetophenone (200 mg; Tokyo Chemical Industry, Tokyo, Japan) and benzaldehyde (150 μL) was added to 40% NaOH (200 μL) and stirred at room temperature for 15 h. The reaction mixture was added 0.1 N HCl (150 mL) and extracted with EtOAc (150 mL). The EtOAc layer was washed with water four times, dried with $MgSO_4$, and concentrated in a vacuum. The obtained residue was purified by silica gel chromatography (64–210 μm, 2 × 15 cm, Wako Pure Chemical Industries) using CH_2Cl_2-acetone 100:1, and crystallized from EtOAc-hexane to give flavokawain B (158.0 mg).

Naringenin chalcone was obtained by isomerization from naringenin (Tokyo Chemical Industry). Briefly, naringenin (100 mg,) was dissolved in 95% ethanol (5 mL) and stirred at room temperature for 15 min after addition of KOH powder (100 mg). The solution was then acidified by adding dilute HCl, and was extracted with EtOAc. The EtOAc layer was washed with water four times, dried using $MgSO_4$ and concentrated in a vacuum. The residue was submitted to silica-gel column chromatography (64–210 μm, 2 × 20 cm) using $CHCl_3$-methanol (MeOH) 85:15. Fractions were monitored by TLC (silica gel 60, Merck; $CHCl_3$-MeOH 85:15, H2SO4) and pure naringenin chalcone (yield 21.6 mg) was obtained by crystallization from MeOH.

The structures of the obtained chemicals were identified by ^{1}H nuclear magnetic resonance spectroscopy (^{1}H-NMR), in comparison with previously published data. ^{1}H-NMR was recorded using an ECP-500 spectrometer (JEOL, Tokyo, Japan) at 300 K. The spectral data are shown below. **Cardamonin** (2',4'-dihydroxy-6'-methoxychalcone) [253], ^{1}H-NMR (DMSO-d6, 500 MHz) δ 13.68 (1H, s, 2'-OH), 10.6 (1H, s, 4'-OH), 7.81 (1H, d, J=15.7, H-8), 7.70 (2H, m, H-2/6), 7.65 (1H, d, J=15.7, H-7), 7.43 (3H, m, H-3-5), 6.02 (1H, d, J=2.1, H-3'), 5.93 (1H, d, J=2.2, H-5'), 3.87 (3H, s, 6'-OMe). **Alpinetin** (5-methoxy-7-hydroxyflavanone) [253], ^{1}H-NMR (DMSO-d6, 500 MHz) δ 10.54 (1H, s, 7-OH), 7.49 (2H, m, H-2'/6'), 7.37 (3H, m, H-3'-5'), 6.06 (1H, d, J=2.0, H-8), 5.99 (1H, d, J=2.1, H-6), 5.48 (1H, d, J=3.0, H-2), 3.73 (1H, s, 5'-OMe), 2.97 (1H, dd, J=16.4, 12.4, H-3), 2.62 (1H, dd, J=16.4, 3.0, H-3). **Flavokawain B** (2'-hydoroxy-4',6'-dimethoxyflavanone) [254], ^{1}H-NMR ($CDCl_3$, 500 MHz), δ 7.90 (1H, dd, J=15.6, 1.6, H-8), 7.78 (1H, d, J=15.6, H-7), 7.61 (2H, d, J=7.3, H-2/6), 7.40 (3H, m, H-3-5), 6.11 (1H, m, H-3'), 5.97 (1H, d, J=2.3, H-5'), 3.92 (3H, d, J=1.6, 6'-OMe), 3.84 (3H, d, J=1.4, 4'-OMe). **Pinocembrin** (5,7-dihydroxyflavanone) [254], ^{1}H-NMR (DMSO-d6, 500 MHz), δ 12.1 (1H, s, 5-OH), 10.8 (1H, s, 7-OH), 7.50 (2H, m, H-2'/6'), 7.39 (3H, m, H-3'-5'), 5.92 (1H, d, J=2.0, H-8), 5.89 (1H, d, J=2.0, H-6), 5.57 (1H, dd, J=12.6, 3.0, H-2), 3.24 (1H, dd, J=17.1, 12.6, H-3), 2.78 (1H, dd, J=17.0, 3.1, H-3). **Naringenin chalcone** (4,2',4',6'-tetrahydroxychalcone) [255], ^{1}H-NMR (CD_3OD, 500 MHz), δ 8.11, (1H, d, J=15.6, H-8), 7.74 (1H, d, J=15.6, H-7), 7.54 (2H, m, H-2/6), 6.86 (2H, m, H-3'/5').

6-2-3. Cell culture

L6 skeletal muscle cells were purchased from DS Pharma Biomedical (Osaka, Japan). L6 myoblasts were cultured in minimal essential medium (MEM) supplemented with 10% heat-inactivated FBS at 37°C in 5% CO_2. Cells were grown in a 96-well plate for the 2DG uptake assay or in a 60-mm diameter dish for western blot analysis. The differentiation of L6 myoblasts into myotubes was performed as previously described [159]. Briefly, cells were cultured in MEM supplemented with 2% FBS and were maintained in this medium post-differentiation. Myotubes were used for experiments 5–7 days after differentiation.

6-2-4. 2DG uptake assay

Glucose uptake was determined using a non-radioisotopic, enzymatic fluorescence assay for 2DG uptake in cultured cells, as described previously [159,160,162] (***see Chapter 2 and 3***). In brief, L6 myotubes in a 96-well format were incubated for 4 h in medium containing a test compound or DMSO (0.1% v/v) as vehicle control. To examine the contribution of PI3K to cardamonin-induced glucose uptake, the cells were treated with the PI3K inhibitor wortmannin (1 μM) for 30 min before induction. After induction, the cells were washed twice with Krebs-Ringer-HEPES (KRH) buffer (50 mM HEPES, pH 7.4, 137 mM sodium chloride, 4.8 mM potassium chloride, 1.85 mM calcium chloride, 1.3 mM MgSO4) containing 0.1% BSA. 2DG uptake was initiated by incubation with KRH buffer containing 1 mM 2DG and 0.1% BSA. After 20 min, the cells were washed twice with KRH buffer containing 0.1% BSA, followed by the addition of 50 μL 0.1 M NaOH, and the culture plate was heated at 85°C for 50 min. The components in the wells were neutralized by the addition of 50 μL 0.1 M HCl, followed by 50 μL of 150 mM TEA buffer (pH 8.1). The cell lysate (10 μL) was transferred to a 96-well assay plate and incubated for 45 min with 100 μL of assay cocktail, containing 50 mM KCl, 0.1 mM NADP, 20 U/mL of G6PDH, 0.2 units/mL of diaphorase, 5 μM resazurin sodium salt and 50 mM TEA buffer (pH 8.1). The generated resorufin was measured using a plate reader (excitation wavelength 530 nm and emission wavelength 615 nm). A DG6P standard solution in the wells was used to generate a standard curve.

6-2-5. Cytotoxicity

The cytotoxicities of the polyphenols were determined using the WST-1 assay and crystal violet staining. Following the treatment of L6 myotubes in a 96-well plate with DMSO or polyphenols (3, 10 and 30 μM) in 0.2% (w/v) BSA/MEM for 24 h, the cells were incubated in 0.2% (w/v) BSA/MEM containing WST-1 and mPMS for 4 h. The absorbance of the medium was measured at 450 nm, with a reference wavelength of 630 nm. The cells were then fixed and stained with 2% ethanol containing 0.2% (w/v) crystal violet for 10 min. The wells were washed three times with tap water, and the stained cells were extracted with 50% ethanol containing 0.5% (w/v) SDS. The absorbance at 570 nm was measured, with a reference wavelength of 630 nm.

6-2-6. Western blot analysis

After L6 myotubes were serum-starved for 18 h, the myotubes were treated with the test compound dissolved in DMSO for the indicated time, and were subjected to plasma membrane preparations or whole cell lysates, as described previously [179]. In summary, proteins (5–20 μg) were separated by 7.5 or 10% SDS-PAGE gels, and electrophoretically transferred to a PVDF membrane. The membranes were blocked with Blocking-one (Nacalai Tesque, Kyoto, Japan) and washed six times with TBST (10 mM Tris-HCl, pH 8.0, 150 mM NaCl and 0.05% Tween 20) for 5 min. All antibodies were diluted in Can Get Signal Immunoreaction Enhancer Solution (Toyobo, Osaka, Japan), and incubated overnight at 4°C. Membranes were incubated with primary antibody for 1 h at room temperature, and incubated with horseradish peroxidase-conjugated secondary antibody at room temperature for 1 h. Antibody-bound proteins were visualized using Lumi-Lightplus Western Blotting Substrate (Roche Applied Science, Mannheim, Germany), according to the manufacturer's protocol.

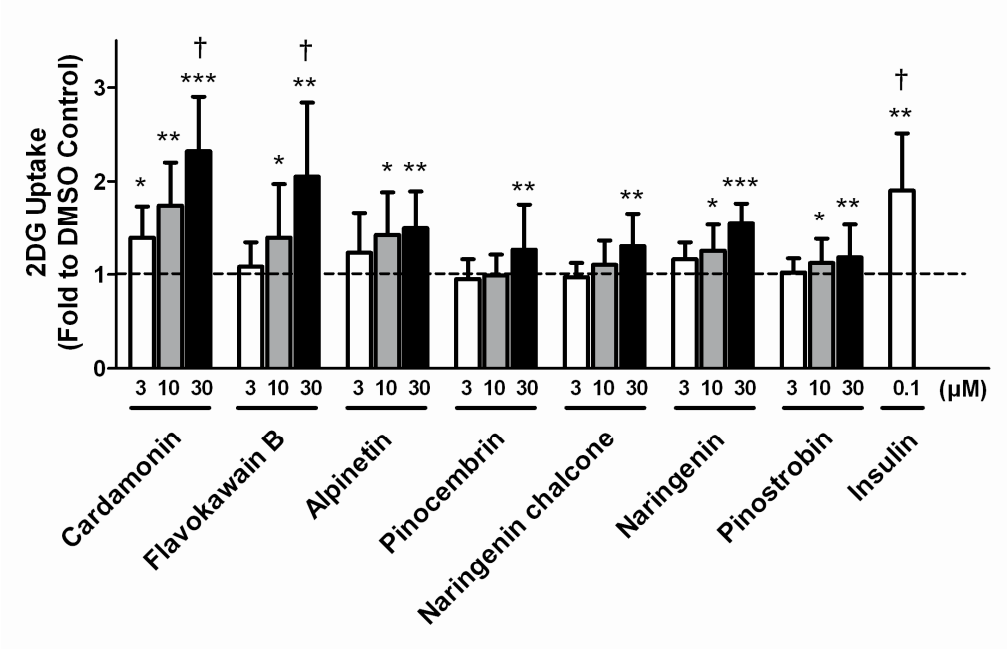

Fig. 6-4. Effects of cardamonin and related compounds on uptake of 2-deoxyglucose in L6 myotubes. After incubation in MEM containing 0.2% BSA for 18 h, L6 myotubes were treated with DMSO (0.1%, control), insulin (100 nM, positive control) or polyphenols (3, 10 and 30 μM) for 4 h, and then incubated in 2DG-containing buffer for a further 20 min. The uptake of 2DG was determined using an enzymatic, fluorescent method. Relative activity was calculated as the ratio of 2DG uptake in polyphenol-treated L6 myotubes to that in DMSO-treated cells. Data are shown as the mean ± SD from more than three independent triplicate experiments. Statistical analysis was performed using two-tailed unpaired Student's *t*-tests (*$p < 0.05$; **$p < 0.01$; ***$p < 0.001$) and Tukeys' multiple comparison tests (†$p < 0.05$) compared with DMSO-treated cells. 2DG, 2-deoxyglucose.

6-2-7. Statistical analysis

The results were analyzed using Student's t-test and Tukey's multiple comparison test. Values of $p < 0.05$ were considered to be statistically significant.

6-3. Results

6-3-1. Effect of cardamonin and related compounds on 2DG uptake in L6 myotubes

The study initially investigated the glucose uptake-inducing ability of cardamonin and its related chemicals in L6 myotubes. Treatment of L6 myotubes for 4 h with cardamonin and the 4'-O-methoxylated cardamonin analog, flavokawain B, resulted in dose-dependent increases in 2DG uptake (**Fig. 6-4**), similar to that in insulin‐stimulated cells. The cardamonin isomer, alpinetin, provoked 2DG uptake at concentrations of 10 and 30 μM ($p < 0.05$ vs. DMSO control by Student's t-test), but its activity was lower than that of cardamonin (not significant by Tukey's test). Other tested compounds also increased 2DG uptake at concentrations of 30 μM ($p < 0.05$ vs. DMSO control by Student's t-test), but their activities were weak and the results were not statistically significant by Tukey's test.

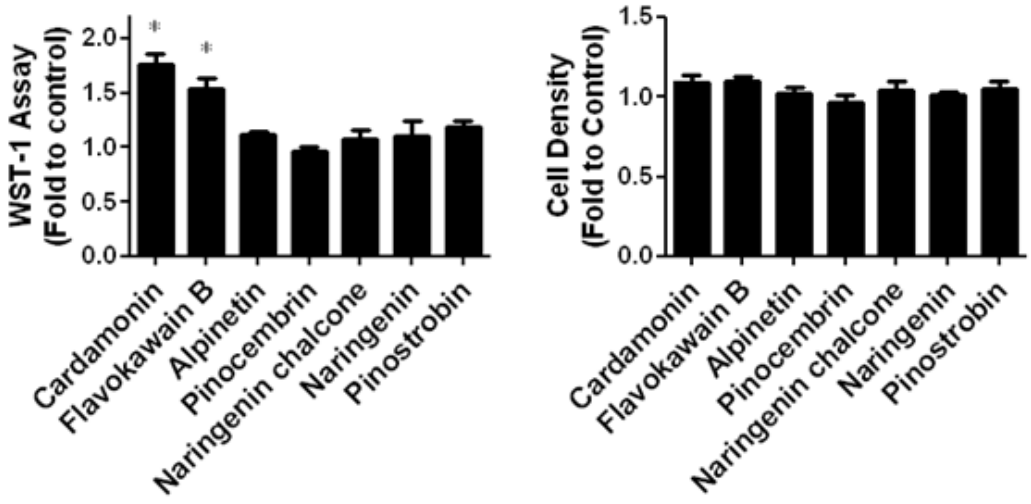

Fig. 6-5. Effect of cardamonin on cell viability and cell density of L6 myotubes. L6 myotubes were treated with DMSO or cardamonin for 24 h, and cell viability (**A**) and cell density (**B**) were evaluated by WST-1 assay and crystal violet staining, respectively. Data were normalized to the value for DMSO-treated cells and shown as the mean ± SD from three independent experiments. Asterisk indicates a statistically significant difference ($p < 0.05$ by Tukey's multiple comparison test) compared with DMSO-treated cells. There were no significant differences among the values for crystal violet staining.

6-3-2. Effects of cardamonin and its related compounds on viability of L6 myotubes

The cytotoxicity of the test compounds was determined by measuring cell viability and density using the WST-1 assay and crystal violet staining, respectively. No compounds showed any cytotoxic effects at a concentration of 30 μM. In contrast, cardamonin and flavokawain B resulted in increased WST-1-reducing activity, without affecting cell density (**Fig. 6-5**).

6-3-3. Cardamonin-stimulated GLUT4 translocation in L6 myotubes

GLUT4 is a major transporter of glucose, and its translocation from the cytosol to the plasma membrane is induced by insulin under postprandial conditions. Therefore the effect of cardamonin on the translocation of GLUT4 in L6 myotubes was investigated. The level of GLUT4 in the plasma membrane fraction of insulin-treated cells increased at 1–4 h, compared with that in the control cells (**Fig. 6-6**). Cardamonin induced the translocation of GLUT4 at 1 h and sustained the same level until 4 h.

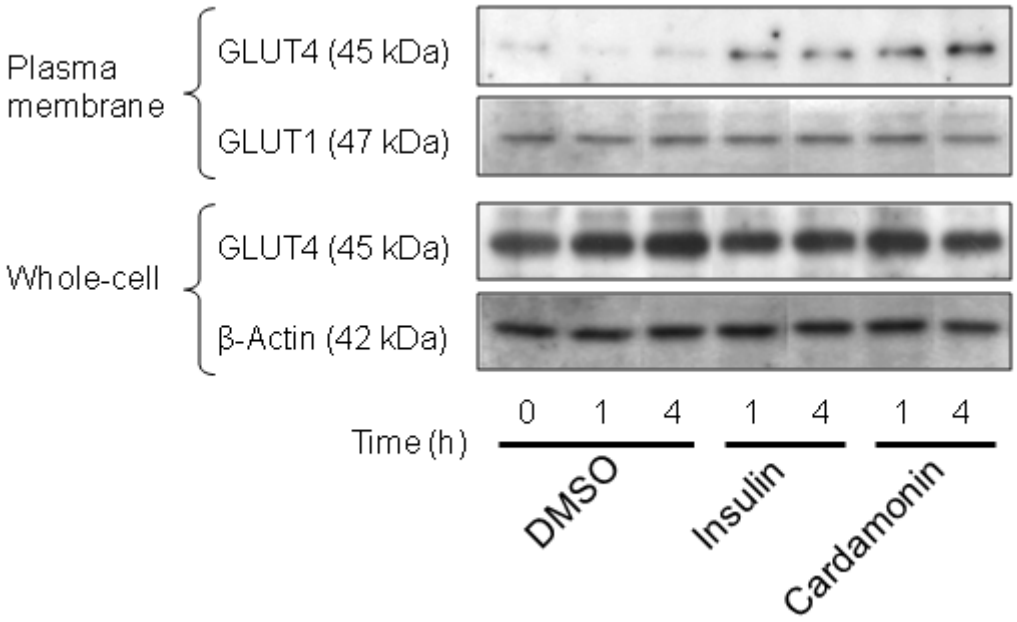

Fig. 6-6. Cardamonin induced GLUT4 translocation in L6 myotubes. Following incubation in MEM containing 0.2% BSA for 18 h, L6 myotubes were treated with DMSO, insulin (100 nM) or cardamonin (30 μM) for 1–4 h. Thereafter the plasma membrane fraction and whole protein were subjected to western blotting, as described in Materials and Methods. Results shown are representative of three independent experiments.

6-3-4. Effect of PI3K inhibitor, wortmannin, on glucose uptake

The PI3K pathway plays a major regulatory role in the insulin action pathway, and PI3K inhibitors inhibit insulin-stimulated glucose uptake. Therefore the contribution of PI3K to cardamonin-induced glucose uptake was examined. As shown in **Fig. 6-7**, insulin-stimulated 2DG uptake, but not cardamonin-stimulated uptake, was inhibited by wortmannin, indicating that PI3K is not a key molecule in cardamonin-stimulated glucose uptake.

6-3-5. Effect of cardamonin on PI3K downstream targets

The effects of cardamonin were investigated on two important downstream targets of the PI3K signaling pathway, serine/threonine kinase Akt, also known as PKB, and atypical PKC. These targets of PI3K have been found to play roles in insulin-stimulated GLUT4 translocation in muscle and fat cells [256]. Cell lysate was immunoblotted with antibodies raised against p-Akt (Ser-473) and p-PKCλ/ζ (Thr-410/403) (**Fig. 6-8**). No phosphorylation of Akt or PKCλ/ζ was observed in cells stimulated with cardamonin for 1–4 h, although phosphorylation of both was stimulated by insulin.

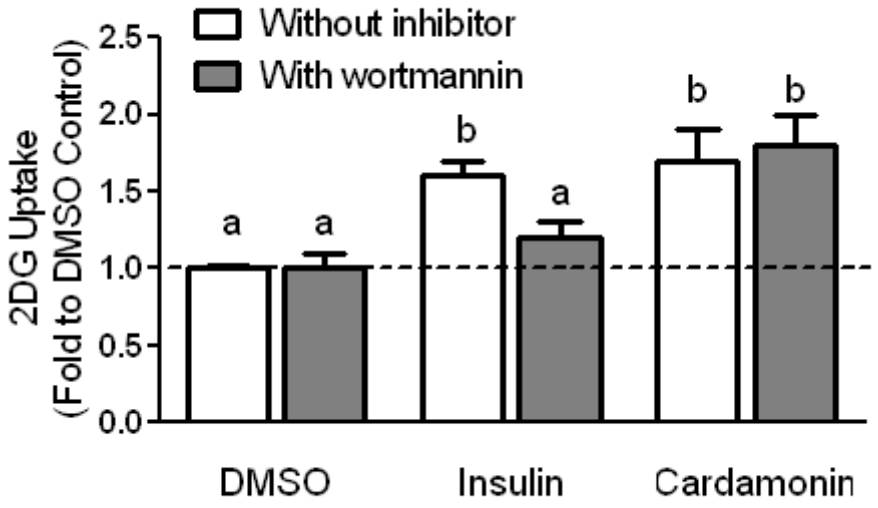

Fig. 6-7. Effects of the PI3K inhibitor, wortmannin, on cardamonin-stimulated uptake of 2-deoxyglucose. Differentiated L6 cells in a 96-well plate were treated with 1 μM wortmannin for 30 min. They were then incubated with 30 μM cardamonin or 100 nM insulin for the indicated time. After incubation, 2DG uptake was assayed as described in Materials and Methods. Values are mean ± SD of triplicate experiments. Different letters indicate statistically significant differences by Tukey's test. 2DG, 2-deoxyglucose.

6-3-6. Effect of cardamonin on AMPK phosphorylation

The study determined the effect of cardamonin on phosphorylation of AMPK, a stress kinase that has been found to regulate GLUT4 translocation [257]. Cardamonin failed to induce AMPK phosphorylation, as shown by western blot analysis (**Fig. 6-8**). However, AMPK phosphorylation did occur in cells stimulated with 5'-amino-5-imidazolecarboxamide-riboside (AICAR) under the same conditions.

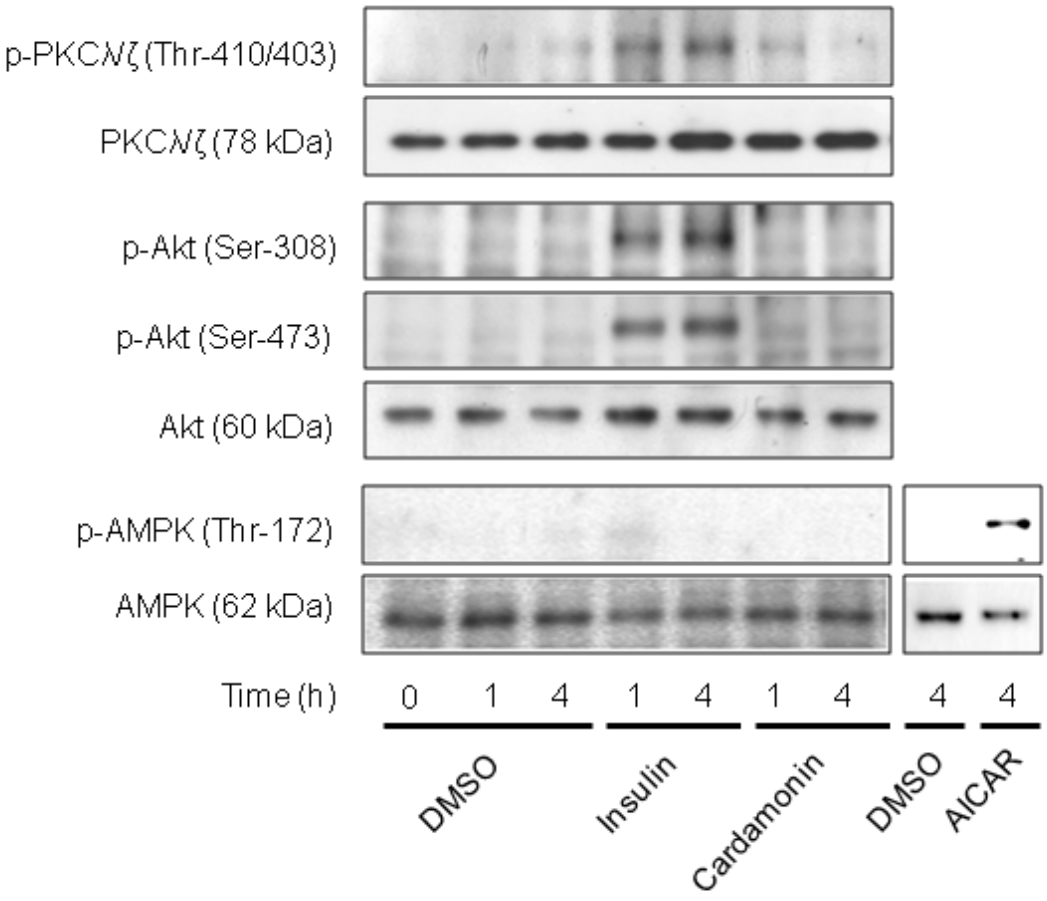

Fig. 6-8. Effects of cardamonin on PI3K downstream and AMPK phosphorylation. Serum-starved L6 myotubes were treated with 30 μM cardamonin or 100 nM insulin. Cell lysates were subjected to western blotting to detect the phosphorylation status of aPKCλ/ζ, Akt, and AMPK. Results shown are representative of three independent experiments. AICAR was used as a positive control for AMPK phosphorylation, under

6-4. Discussion

Their wide range of biological activities, including antioxidant, antiinflammatory, anticancer, antihyperglycemic and antidiabetic activities, have made polyphenols important targets associated with the growing interest in natural sources of nutrients and health‐promoting compounds. Stimulating glucose uptake into peripheral tissues may reduce the level of glucose in the circulation. Skeletal muscle is the primary tissue responsible for the postprandial uptake of glucose [135] (***see Chapter 1***). Therefore a high-throughput enzymatic assay was developed that can be used assess the effects of active compounds and natural products on glucose uptake into cultured cells [159,162] (***see Chapter 2 and 3***).

The results of the present study showed that cardamonin and its 4'-*O*-methylated analog, flavokawain B, enhanced glucose uptake into L6 myotubes, while other tested compounds showed weaker activity ($p < 0.05$ vs. control by Student's t-test, but not significant by Tukey's test, at concentrations of 30 μM). In our previous study, 2DG uptake in cultured L6 myotubes was stimulated by chalcones containing a 2'-hydroxy group (4-hydroxyderricin, xanthoangelol, xanthohumol and butein), but not by chalcones lacking a 2'-hydroxyl group [4]. A wider range of polyphenols needs to be investigated using this screening method to determine the structure–activity relationship, though the current and previous results suggest that the α,β-unsaturated carbonyl group and the 2'-hydroxyl group in the chalcone structure are both important. The reactive α,β-unsaturated carbonyl group in chalcones is known to regulate cell functions, such as the NF-E2-related factor 2/Kelch-like ECH-associated protein system [258], and may influence glucose uptake in muscle cells, while the low activity of naringenin chalcone suggests the functional importance of the hydrophobic moiety.

The current study also demonstrated the induction of GLUT4 translocation by cardamonin in L6 myotubes. GLUT4 is the primary mediator of glucose uptake into insulin‐stimulated and contraction-stimulated skeletal muscle cells. Regulation of glucose uptake into muscle cells *via* GLUT4 is a fundamental action of insulin, a process that is impaired in type 2 diabetes [259]. The binding of insulin to its receptor activates PI3K, which induces the activation of PKCλ/ζ and Akt through the downstream kinase phosphoinositide-dependent protein kinase-1. PKCλ/ζ and Akt mediate the translocation of GLUT4 from the cytosol to the plasma membrane by actin remodeling and activation of the exocytosis regulator Rab, respectively [260] The study examined the actions of cardamonin on two cellular signaling pathways that are known to mediate GLUT4 translocation, but cardamonin had no effect on the phosphorylation of either PKCλ/ζ or Akt, and its glucose uptake‐promoting activity was unaffected by treatment with a PI3K inhibitor. Recent studies have reported roles for conventional/novel PKC [261], sirtuin [262], extracellular signal-regulated kinase (ERK) 1/2 and p38 [263] in GLUT4 translocation. However, cardamonin-stimulated 2DG uptake was not inhibited by the PKC inhibitor (bisindolylmaleimide), nor by the sirtuin inhibitor (nicotinamide), and ERK1/2 and p38 phosphorylation were unaffected in cardamonin-treated L6 myotubes (data not shown). Furthermore, the sirtuin activator resveratrol showed no activity during screening of

phytochemicals to identify polyphenols promoting 2DG uptake in L6 muscle cells [4]. The AMPK pathway is a major regulator of GLUT4 translocation in response to some antidiabetic agents such as AICAR and metformin [264,265]. The activation of AMPK by energy depletion and elevated intracellular Ca^{2+} levels leads to induction of GLUT4 translocation [266]. Therefore the effect of cardamonin on AMPK activation was investigated. Cardamonin failed to increase AMPK phosphorylation, suggesting that the AMPK signaling pathway is not responsible for the stimulation of GLUT4 translocation by cardamonin The structurally related chalcones, 4-hydroxyderricin and xanthoangelol, caused GLUT4 translocation in L6 myotubes with no insulin-like or AMPK-inducing effects, similar to the situation for cardamonin [4]. A comprehensive analysis of the signaling components affected by these chalcones is needed to determine their mechanisms of action.

Tetrazolium salts, including MTT and WST-1, are used widely in cell biology for measuring the metabolic activity of cells from a wide range of organisms [267,268]. WST-1 produces a highly water‐soluble formazan upon cellular reduction [269] and its ease of use means it is widely applied in colorimetric cell viability assays. A WST-1 assay was used to determine the cytotoxicity of the test compounds. Cardamonin and flavokawain B, both of which showed glucose uptake-enhancing activities, increased WST-1 reduction without increasing cell density. Flavonoids have been reported to reduce MTT in the culture medium in the absence of cells [270]. However, no direct reduction of WST-1 by cardamonin or flavokawain B occurred in our assay, indicating that WST reduction was mediated by cells stimulated with these compounds. The glucose-uptake activity and the WST-reducing activity are thought to be correlated. Fractionation studies using mammalian cells indicated that the reduced pyridine cofactor, NADH, was responsible for most MTT reduction, a result supported by studies with whole cells. The main reduction of MTT is believed to occur directly on the surface of the mitochondrial membrane. However, second-generation tetrazolium dyes that form water-soluble formazans and require an electron acceptor such as mPMS for reduction are characterized by a net negative charge, and are therefore largely cell-impermeable. Evidence indicates that their reduction occurs at the cell surface, or at the level of plasma membrane electron transport [268]. These results suggest that a currently unknown mechanism may be responsible for the up-regulation of glucose uptake by cardamonin.

Cardamonin is a chalcone that exists in many medicinal herbs [271] and possesses a wide spectrum of pharmacologic effects, including antitumor-promoting [272], antiinflammatory [273], antituberculous [250], platelet aggregation inhibitory [274] and vasorelaxant effects [275], as well as significant microbial resistance. Liao *et al*. recently suggested that cardamonin may play a role in ameliorating insulin resistance and smooth muscle hyperplasia of major vessels in fructose-induced rats, possibly *via* a mechanism involving the modulation of insulin/mTOR signaling [276]. Although the current study did not reveal the detailed mechanisms of cardamonin action, the results confirmed that cardamonin enhanced glucose uptake in cultured muscle cells *via* translocation of GLUT4. A previous, preliminary study showed that glucuronide/sulfate conjugated cardamonin was found in the plasma of mice administered cardamonin (data not shown). This suggests that chalcones involving

cardamonin are active products and promising compounds for the maintenance of blood glucose levels through their stimulation of skeletal muscle-associated glucose uptake. The pathogenesis of diabetes is complicated, and the development of safe and effective antidiabetic agents remains a challenge. Researchers continue to search for new drugs by targeting key compounds or pathways involved in the disease. The complex structure of natural products leads to greater target diversity, and natural molecules therefore offer good candidates for drug discovery strategies aimed at novel targets or pathways involved in disease. The results of the current study suggest that further studies on the in vivo effects and metabolism of cardamonin are necessary.

The regulation of glucose uptake into muscle and fat cells *via* GLUT4 is a fundamental action of insulin and is impaired in type 2 diabetes, which is currently spreading with epidemic proportions. Understanding the molecular basis of GLUT4 regulation is therefore of paramount importance. Ishiki and Klip previously reviewed the complexities of GLUT4 traffic and its regulation, and elucidation of the roles of the different regulatory inputs on GLUT4 compartment biogenesis, storage, cycling and membrane retention will be essential for pinpointing defects in insulin resistance and creating approaches to improve insulin action and glucose uptake [259].

In conclusion, it was shown that cardamonin enhanced glucose uptake through inducing GLUT4 translocation in L6 myotubes. These results suggest that chalcones may provide the basis for the development of novel hypoglycemic substances, though more studies are needed to evaluate their in vivo effects in humans.

Chapter 7

General discussion

Development of non-radioisotopic glucose uptake assay

Glucose is the main fuel for most cells and its importance as an energy substrate has led to intense research on its actions as a cellular metabolite and into the mechanisms controlling its uptake. A number of diseases are associated with glucose transport and metabolism defects, such as myocardial ischemia, Type 2 diabetes, or cancer. Facilitative glucose transport systems are ubiquitous in animal cells and are responsible for transporting glucose across the cell surface membrane. Essentially, glucose can be transported across membranes by two different mechanisms: an Na^+-coupled active carrier system, and a growing family of structurally related Na^+-independent glucose transporter glycoproteins. It has long been established that the plasma membranes of virtually all mammalian cells possess a transport system for glucose of the facilitative diffusion type; these transporters allow the movement of glucose across the plasma membrane down its chemical gradient either into or out of cells. These transporters are specific for the D-enantiomer of glucose and are not coupled to any energy-requiring components, such as ATP hydrolysis or H^+ gradient. The facilitative glucose transporters are distinct from the Na^+-dependent transporters, which actively accumulate glucose.

A vast number of studies have been conducted on glucose uptake mechanisms in cultured cells. All mammalian cells contain one or more members of the facilitative glucose transporter family named GLUT [5,41]. These transporters have a high degree of stereoselectivity, providing for the bidirectional transport of substrate, with passive diffusion down its concentration gradient. GLUTs function to regulate the movement of glucose between the extracellular and intracellular compartments maintaining a constant supply of glucose available for metabolism.

Glucose transport is generally assumed to present the rate-limiting step for lipogenesis in adipose tissue in vivo and adipocytes in vitro, at least under conditions of low to moderate concentrations of glucose in plasma and incubation medium, respectively. Skeletal muscle is the primary tissue responsible for the postprandial uptake of glucose from the blood in humans. Two major transporters expressed in adipose tissue/skeletal muscle are the fat/muscle-specific glucose transporter GLUT4 and ubiquitous transporter GLUT1. The insulin-stimulated acute activation of glucose transport mainly occurs by one of two mechanism: translocation of GLUT4 and GLUT1 from intracellular vesicles to the plasma membrane and augmentation of the intrinsic catalytic activities of the transport. The molecular mechanisms underlying the glucose transport and its regulation are similar for adipose and muscle cells.

The physiological function of GLUTs depend on their kinetic and substrate specificities. Several studies have examined the kinetic properties of the isoforms. However, the facts that glucose is rapidly metabolized and that transport is not always rate-limiting, means that nonmetabolizable glucose analogues, such as fluoro-deoxyglucose (FDG), 2-deoxy-D-glucose (2DG) and 3-*O*-methyglucose (3MG), have to be used as glucose tracers. Uptake of glucose in cultured cells is commonly determined by using radioactive hexose, such as 3MG or 2DG. 3MG is a non-phosphorylatable glucose analog which can be used for the accurate measurement of true initial glucose transport rate without interference with the subsequent glucose-metabolizing steps (e.g. phosphorylation to glucose-6-phosphate). Isotopic labels provide a good "signal to noise" ratio and higher specificity than fluorescent or enzymatic labels. The strong and unique signal emitted by radiolabels stands out against the background, whereas the signal from a fluorescent probe is a visible spectrum photon, which may arise by non-specific interferants. However, routine use of these radiolabeled analogues is costly and requires a specialized institution where isotopes can be handled.

The rate of radioisotopic 3MG transport is determined according to Whitesel and Glienmann [277], Karnieli and coworkers [278], and Basi and coworkers [279] by a modification of the L-arabinose uptake method described by Foley and coworkers [280]. 3MG is a non-phosphorylatable glucose analog which can be used for the accurate measurement of true initial glucose transport rate without interference with the subsequent glucose-metabolizing steps (e.g. phosphorylation to glucose-6-phosphate). However, 3MG necessitates a very short incubation time due to fast equilibration of the analog across plasma membranes and requires either rapid separation of cells from the aqueous incubation medium, usually by centrifugation through a suitable oil cushion with a buoyant density of less than 1, or the prevention of 3MG efflux by washing with a mercuric chloride solution. Sokoloff and coworkers described a radioautographic method to measure regional rates of brain glucose consumption with 2-[^{14}C]deoxyglucose [133] and the method has been widely used in not only the brain but also the muscle, fat tissue and so on. The method is based on the fact that glucose and 2DG are similarly transported into cells and phosphorylated by hexokinase, but the DG6P formed accumulates because it cannot be converted to an analog of fructose 6-phosphate or otherwise rapidly metabolized. This assay can measure the total glucose uptake encompassing the transport of the non-metabolizable glucose analog, 2DG, via the specific glucose transporters (i.e. GLUT1 and GLUT4), and the molecular mechanism of their movement from intracellular vesicles to the plasma membrane (GLUT translocation) including the underling signaling cascade through which insulin stimulates glucose transport in adipose and muscle cells. 2DG is phosphorylated to a stable and impermeable derivative, DG6P, by hexokinase or glucokinase, which may accumulate at a specific intracellular compartment, ensuring less rapid equilibration, slower kinetics and more convenient of 2DG transport compared to 3MG. For routine purpose 2DG rather than 3MG is commonly preferred.

3MG is non-phosphorylatable glucose analog which can be used for the accurate measurement of true initial glucose transport rate without interference with the subsequent glucose-metabolizing

steps. However, assaying the uptake of 3MG necessitates sophisticated experimental procedures enabling start and termination of transport reaction within a few seconds or for fewer than 1 minute. Assaying the uptake of 2DG than 3MG is more convenient because 2DG is converted to a stable and impermeable derivative DG6P through phosphorylation by hexokinase or glucokinase. Therefore, 2DG is often considered to be the gold standard in reference tracers of glucose transport and phosphorylation. For routine purpose 2DG rather than 3MG is commonly preferred. However, the rate-limiting step of glucose uptake at low glucose concentration is the transport via GLUT1/4 rather than the phosphorylation. This results in apparently longer linear periods of glucose uptake in comparison to use of non-phosphorylatable glucose analogs, such as 3MG and thereby considerably facilitates the experimental procedure and kinetic analysis. So on that point, investigator should use both 3MG and 2DG as the situation demands, or select a suitable assay for investigator's goal.

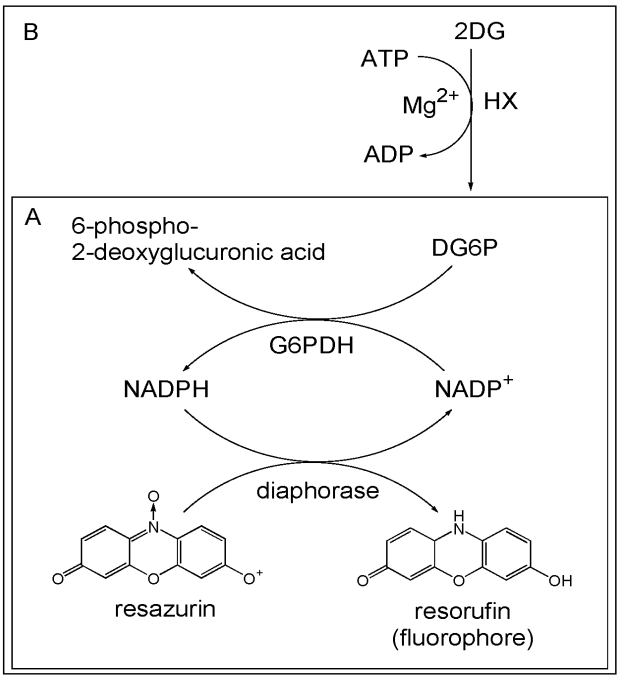

Fig. 7-1. Principle of the assay for measuring DG6P. (A) Scheme of the reaction by the assay solution in our basic protocols. In the first reaction, G6PDH catalyzes the conversion of DG6P to 2-deoxy-6-phosphogluconate, coupled with the conversion of $NADP^+$ to NADPH. In the second reaction, diaphorase catalyzes the conversion of resazurin to resorufin, coupled with the conversion of NADPH to $NADP^+$. In this chain reaction, $NADP^+$ and NADPH are recycled between the first and second reaction. Theoretically, this chain reaction should continue until DG6P are consumed, and the resorufin fluorophore generated should be equivalent to the amount of DG6P. (B) Scheme of the reaction by the assay solution in alternate protocol. Standard curve can be generated by placing 2DG standard solution. In the reaction step, DG6P is generated by hexokinase catalyzing the phosphorylation of 2DG, coupled with the conversion of ATP to ADP. To achieve this reaction, the addition of Mg^{2+} is required because ATP binds to the enzyme as a complex with Mg^{2+}. 2DG, 2-deoxy-D-glucose; DG6P, 2-deoxyglucose 6-phosphate; G6PDH, glucose 6-phosphate dehydrogenase; HX, hexokinase.

Manchester and coworkers [139] and Sasson and coworkers [131] developed a nonradioisotopic, enzymatic assay for measuring of DG6P in tissues and cultured cells. These methods enable the detection of DG6P accumulating in cells by measuring of fluorescence of NADPH produced from $NADP^+$, which is coupled to oxidation of DG6P to 6-phospho-2-deoxyglucuronic acid by G6PDH. This approach, however, requires the cultivation of many cells on large plates and preparation of cell extracts because the fluorescence of NADPH is rather weak. The NADPH produced could be detected by direct fluorescent measurement of the stoichiometric amount of NADPH generated or by amplification of NADPH by enzymatic cycling.

Consequently and recently, we have linked a diaphorase–resazurin-amplifying system that produces a potent fluorescent substance in the presence of NADPH [159,160,162] (***see Chapter 2 and 3***). Resazurin, which is also known under the name of AlamarBlue™, is useful for detecting reductive activities in cells and has been widely used for measuring cell proliferation and mitochondrial metabolic activity. Resazurin itself is non-fluorescent until it is reduced to the highly red fluorescent compound resorufin. Usually, NADPH or NADH is the reductant that converts resazurin to resorufin in the presence of the enzyme diaphorase. Thus, resazurin can be used to detect NAD(P)H or diaphorase levels. Furthermore, the resazurin–diaphorase system can be used to detect any biological or enzyme activity that is involved in a biochemical reaction generating NAD(P)H [168-173]. In addition, the fluorescence of resorufin is beyond the autofluorescence of most biological samples. Based on the above information, we adapted the resazurin–diaphorase system to facilitate the measurement of NADPH in the 2DG uptake assay in cultured cells [159] (***see Chapter 2***). This assay is based on direct fluorometric measurement of stoichiometric amounts of resorufin generated and can be performed in 96-well or 384-well format. The assay solution can be prepared easily by mixing stock solution and the actual reaction step is very simple, involving only a single incubation with the assay solution followed by the reading of fluorescence. This protocol is provided along with rapid, microplate-based protocols for measuring 2DG uptake in cultured cells, and is useful for in vitro high-through-put screening and for evaluating glucose-uptake regulators. However, this method is limited the validation of the assay to the measurement of 2DG uptake in cell culture. To evaluate nonlaveled-2DG uptake in an in vivo study, we proposed an advanced, simpler and easier method to measure glucose, 2DG, G6P and DG6P separately using four independent single-reaction mixtures, which are modified from this method [160,162] (***see Chapter 3***).

To evaluate 2DG uptake in an *in vivo* study using the enzymatic method, separate detection of glucose, 2DG, G6P, and DG6P was needed because the tissue levels of glucose are much higher than those of 2DG and DG6P. To determine 2DG and DG6P, Chi and coworkers [174,175] and Akabayashi and coworkers [176] developed enzymatic assays. Their methods are based on HK–G6PDH assay in the same way as our method and directly detect NADPH derived from the reactions or detect NADPH by amplification with a NADP cycling reagent. They also used elimination reaction steps in their methods. Using these elimination reagents involved many steps and operations are complicated. In our method we do not use such elimination reagents and we proposed using four independent

single-reaction mixtures containing G6PDH from *Leuconostoc mesenteroides* and *Candida utilis* [160] (***see Chapter 3***). The components of each assay solution are similar to each other and each assay solution can be prepared easily by mixing stock solutions. The actual reaction step is very simple, involving only a single assay solution followed by reading of fluorescence. However, later Sigma–Aldrich stopped selling *C. utilis* G6PDH and a substitute distributor did not exist. So, we improved our assay method by incorporating minor modifications for the use of *L. mesenteroides* G6PDH [162] (***see Chapter 3***). Using this improved assay system, concentration of glucose, 2DG, G6P, and DG6P were easily measured as well as our previous assay system.

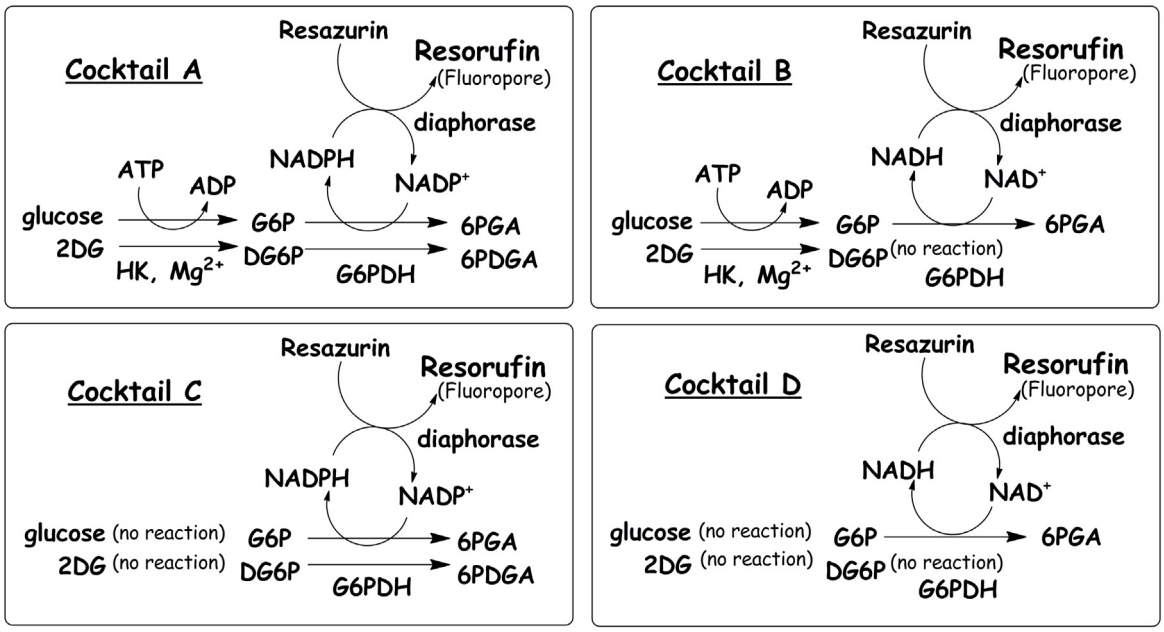

Fig. 7-2. Principle of the assay system for measuring glucose, 2DG, G6P and DG6P, and schematic representation of the chain reaction and the detection of target molecules by each assay solution. (i) HK catalyzes the conversion of 'glucose to G6P' and '2DG to DG6P' (ii) G6PDH catalyzes the conversion of 'G6P to 6PGA' and 'DG6P to 6PDGA', coupled with the conversion of 'NAD(P)$^+$ to NAD(P)H'. (iii) Diaphorase catalyzes the conversion of 'resazurin to resorufin', coupled with the conversion of 'NAD(P)H to NAD(P)$^+$'. Theoretically, the amount of resorufin derived should be equal to the total amount of glucose, 2DG, G6P and DG6P when assay cocktail A is used. HK in cocktail A and B catalyzes conversion of both 'glucose to G6P' and '2DG to DG6P'. Use of high units of G6PDH and NADP$^+$ in cocktail A and C catalyzes conversion of both 'G6P to 6PGA' and 'DG6P to 6PDGA', and use of low units of G6PDH and NAD$^+$ in cocktail B and D catalyzes the conversion of only G6P to 6PGA. Assay cocktail A detects total glucose, 2DG, G6P and DG6P. Assay cocktail B detects total glucose and G6P. Assay cocktail C detects total G6P and DG6P and assay cocktail D detects only G6P. The compositions of each assay cocktail are described in Table 4-1. 2DG, 2-deoxyglucose; G6P, glucose-6-phosphate; DG6P, 2-deoxyglucose-6-phosphate; 6PGA, 6-phosphoglucuronic acid; 6PDGA, 6-phospho-2-deoxyglucuronic acid; HK, hexokinase; G6PDH, glucose-6-phosphate dehydrogenase.

Methods for evaluation of glucose uptake are applied in a wide range of fields because facilitative glucose transport systems are ubiquitous in animal cells and are responsible for transporting glucose across the cell membrane. Our protocols have been devised a simple and reliable method for evaluation of glucose uptake in cells and that it can be applied in a wide range of fields.

Approach to promising functional food substance for the maintenance of the blood glucose

Diabetes is a metabolic disease, which is characterized by insufficient or inefficient insulin secretary response and elevated blood glucose level. Clinically, T2DM is more common and accounts for 90–95% of all diabetic incidence. Many patients with diabetes will eventually result in multiple diabetic complications like nephropathy, retinopathy, diabetic foot, ketoacidosis, and even increased risk of CVD and hypertension. Currently, there are estimated 170 million people worldwide suffering from diabetes and number may probably double by the year 2030 [281]. Diabetes causes about 5% of all deaths globally each year, and diabetic deaths are likely to increase by more than 50% in the next 10 years without urgent action (http://www.who.int/diabetes/en). Therefore, developing novel drugs or new therapies to combat diabetes has become urgent need.

Increasing studies have confirmed that the pathogenesis of diabetes is related to various signaling pathways, such as insulin signaling pathway [282], carbohydrate metaboling pathway [283,284], endoplasmic reticulum stress related pathway [285], the pathways involving insulin secretion [154] and PPAR regulation [286], and chromatin modification pathways [287,288]. Recent studies suggest that insulin signaling pathway promotes the transport of glucose into its target cells, adipocytes and myotubes. Furthermore, insulin-mediated glucose transport is essential for glucose uptake and metabolism by enhancing the translocation and activation of GLUT4. Adipocyte and muscle cells are highly insulin-sensitive cells and play a major role in regulating insulin signaling pathways associated with GLUT4. A novel pathway of insulin signaling what involves the glucose transport system is initiated by insulin binding to the cell surface of the IR to activate tyrosine kinase activity. In addition, the subsequent activation of two kinds of pathways (PI3K and p38-MAPK) is required for the transport of GLUT4 to the cell surface. This results in the tyrosine phosphorylation of a family of IRS proteins and activation of a complex network of downstream molecules, including PI3K and the serine/threonine kinase Akt. Recent studies show that AMPK is one of the most important factors for cellular energy balance and recognized as a potential therapeutic target in the prevention and treatment T2DM. Some drugs for the treatment of T2DM (metformin and thiazolidinediones) activate AMPK and this activation may potentially have ant-diabetic effects. The activation of AMPK via exercise is one of the most effective therapies in T2DM.

These signaling pathways have thus become the major source of the promising novel drug

target to treat metabolic diseases and diabetes. For example, insulin sensitizing drug biguanides (metformin) and thiazolidinediones (rosiglitazone and pioglitazone) have been used for years in the treatment of diabetes, although several clinical side effects have been later determined with these anti-diabetic drugs [289]. Compared with synthetic compounds, natural products contain larger-scale structural diversity inherently. They have become the major resources for bioactive agents and played a key role in the discovery of lead compounds for new drug research [290]. To date, a great number of active components derived from natural resources have been determined to function in the regulation of diabetic pathophysiological signaling pathways and exhibit anti-diabetic activity [290-292].

Using our 2DG-uptake method, we surveyed herbal extracts that promote uptake of glucose in cultured L6 cells, and discovered that an ethanol extract of *A. princeps* (APE) was a promising stimulator of glucose uptake. APE facilitated glucose uptake *via* GLUT4 translocation (***see Chapter 4***). The results of our study indicate that *A. princeps* stimulated the PI3K-dependent aPKC pathway and the AMPK pathway and had insulin-mimetic activity, suggesting that an insulin-independent pathway is the major mechanism by which APE exerts anti-diabetic potential. Next, we investigated the effects of APE on obesity and hyperglycemia in C57BL/6 mice fed a high-fat diet (***see Chapter 5***). Dietary APE prevented body weight gain, fat accumulation, and hyperglycemia in mice fed an HF diet. APE supplementation suppressed hyperleptinemia, which may prevent hepatic lipid accumulation through inhibition of FAS activity in the liver. This inhibition of hepatic lipid accumulation will thus contribute to the prevention of hyperglycemia. The results also suggested that *A. princeps* might be an excellent natural food additive because of its antiobesity and antidiabetic properties, and that it could be useful for the development of a more potent and selective agent.

We also surveyed natural compound that promote uptake of glucose in cultured L6 cells using our non-RI assay and we found some active compounds influencing the uptake of glucose in L6 myotubes. Our findings suggest chalcones, flavonols and flavones to be important targets for glucose-uptake-promoting polyphenols. Flavanones, flavonols, chalcones, retrochalcones and dehydrochalcones are biochemically related compounds of restricted occurrence. For this reason, they are described as minor flavonoids despite sometimes being present in foods at a dietary significant concentration. Flavanones and flavonols have a saturated C-ring. Chalcones and retrochalcones are unsaturated and, along with dehydrochalcones have an open structure and carbon skeleton numbered in a way different from other flavonoids. Contribution of flavonoids to glucose uptake enhancing activity is also apparent from several reports. Several homoisoflavonoids without glucose in the structure are reported to exhibit glucose uptake enhancing activity [293]. Two flavonoids, kaempferol and quercetin, are also known to improve glucose uptake [294]. Recently, we reported 15 active compounds influencing the uptake of glucose in L6 myotubes [4]. In this study, among the active compounds, 4-hydroxyderricine, xanthohumol and xanthoangelol, all of which are C-prenylated chalcones, showed much higher levels of activity. Chalcones were originally isolated from natural

plant sources and have been reported to variety of biological properties. This suggests that chalcones are promising compounds for maintenance of blood glucose levels thorough their stimulation of skeletal-muscle-associated glucose uptake. Next, we showed that cardamonin and its 4'-*O*-methylated analog, flavokawain B, enhanced glucose uptake into L6 myotubes through GLUT4 translocation (***see Chapter 6***). A wider range of polyphenols needs to be investigated using our screening method to be determine the structure-activity relationship, through the current and previous results suggest that the α,β-unsaturated carbonyl group and the 2'-hydroxy group in the chalcone structure are both important. These results suggest that chalcones may provide the basis for the development of novel hypoglycemic substances, though more studies are needed to evaluate their *in vivo* effects in humans.

Conclusions

The pathogenesis of diabetes and metabolic syndrome is complicated, and development of the safe and effective drugs or health foods against diabetes and metabolic syndrome is full of challenge. Currently, researchers have been engaged in anti-diabetic lead compound discovery by targeting the key targets or pathways involved in the disease. In comparison with synthetic compounds, natural molecules exert multiple advantages for their large-scale structure and target diversity both in single target and signaling pathway based drug discovery strategies. To date, emerging strategies are developed to speed up the drug discovery process. To explore more effective lead compounds against diabetes and metabolic syndrome, efficient disease models should be established, according to the type and pathogenesis of diseases. In addition, to increase the activity of natural molecules, compound synthesis and optimization methods, high throughput screening or high content screening technologies should be developed.

The HTS field continues to dynamic and extremely competitive one, where a newer technique or method is being reported at a very frequent basis. The need to increase the throughput of drug-discovery screening operations while reducing development and operating costs is continuing to drive the development of homogeneous, fluorescence-based assays in miniaturized formats. The use of 384-well and higher density plates and commercially available plate-handling robotics has made HTS a reality, and has allowed some screening groups to achieve ultra-high throughput rates in excess of 100,000 samples per day. As the density of plate increases the volume of sample required for the assay is decreased drastically, as a result the assay of expensive drugs can be carried out at lower cost, which compensates the initial setup cost. The combination of nanoliter-scale liquid-handling, integrated devices for compound dilution and assay functionality, and state-of-the-art fluorescence detection techniques has the potential to revolutionize the drug discovery screening process.

In this thesis, we have developed method for evaluating glucose uptake in cultured cells and tissues without using radioisotope. Our assay for DG, DG6P and glucose are based on direct

fluorometric measurement of stoichiometric amounts of resorufin and can be performed in 96-well or 384-well formats. This direct assay is simpler than previous assays. Furthermore, the processing of the sample is also simplified. In addition, our method does not require radiolabeled 2DG or a specialized institution registered for using radioactive isotopes. Using this assay system, the effects of insulin, cytochalasin B (hexose uptake inhibitor), LY294002 (inhibitor of glucose transporter translocation), and pioglitazone hydrochloride (insulin-sensitizing agent) on 2DG uptake into the cells could be assessed clearly. Therefore, our simple method may be useful for *in vitro* HTS and for evaluating regulators glucose uptake. Using this methodology, we explore the possibility that naturally occurring chemicals (phytochemicals) found in vegetables and spices have the power to restore insulin sensitivity, and thus normal glucose metabolism, in individuals with T2DM. From the surveying natural plants and compounds, we found the possibility of the drug development and the health food substance among *A. princeps* and chalcone compound, etc. Methods for evaluation of glucose uptake are applied in a wide range of fields because facilitative glucose transport systems are ubiquitous in animal cells and are responsible for transporting glucose across the cell membrane. We believe that we have devised a simple and reliable method for *in vitro* and *in vivo* evaluation of glucose uptake in cells and that it can be applied in a wide range of fields.

References

1. Himsworth H. Diabetes mellitus: a differentiation into insulin-sensitive and insulin-insensitive types. *Lancet* 1936, **1**:127-130
2. DeFronzo RA. Lilly lecture 1987. The triumvirate: beta-cell, muscle, liver. A collusion responsible for NIDDM. *Diabetes* 1988, **37**:667-687
3. Simpson IA and Cushman SW. Hormonal regulation of mammalian glucose transport. *Annu Rev Biochem* 1986, **55**:1059-1089
4. Kawabata K, Sawada K, Ikeda K, Fukuda I, Kawasaki K, Yamamoto N and Ashida H. Prenylated chalcones 4-hydroxyderricin and xanthoangelol stimulate glucose uptake in skeletal muscle cells by inducing GLUT4 translocation. *Mol Nutr Food Res* 2011, **55**:467-475
5. Gould GW and Holman GD. The glucose transporter family: structure, function and tissue-specific expression. *Biochem J* 1993, **295 (Pt 2)**:329-341
6. Shen SW, Reaven GM and Farquhar JW. Comparison of impedance to insulin-mediated glucose uptake in normal subjects and in subjects with latent diabetes. *J Clin Invest* 1970, **49**:2151-2160
7. Ginsberg H, Kimmerling G, Olefsky JM and Reaven GM. Demonstration of insulin resistance in untreated adult onset diabetic subjects with fasting hyperglycemia. *J Clin Invest* 1975, **55**:454-461
8. Rea S and James DE. Moving GLUT4: the biogenesis and trafficking of GLUT4 storage vesicles. *Diabetes* 1997, **46**:1667-1677
9. Reaven GM, Lerner RL, Stern MP and Farquhar JW. Role of insulin in endogenous hypertriglyceridemia. *J Clin Invest* 1967, **46**:1756-1767
10. Olefsky JM, Farquhar JW and Reaven GM. Reappraisal of the role of insulin in hypertriglyceridemia. *Am J Med* 1974, **57**:551-560
11. Orchard TJ, Becker DJ, Bates M, Kuller LH and Drash AL. Plasma insulin and lipoprotein concentrations: an atherogenic association? *Am J Epidemiol* 1983, **118**:326-337
12. Olefsky JM, Kolterman OG and Scarlett JA. Insulin action and resistance in obesity and noninsulin-dependent type II diabetes mellitus. *Am J Physiol* 1982, **243**:E15-30
13. Stern MP and Haffner SM. Body fat distribution and hyperinsulinemia as risk factors for diabetes and cardiovascular disease. *Arteriosclerosis* 1986, **6**:123-130
14. Modan M, Halkin H, Almog S, Lusky A, Eshkol A, Shefi M, Shitrit A and Fuchs Z. Hyperinsulinemia. A link between hypertension obesity and glucose intolerance. *J Clin Invest* 1985, **75**:809-817
15. Haffner SM, Fong D, Hazuda HP, Pugh JA and Patterson JK. Hyperinsulinemia, upper body adiposity, and cardiovascular risk factors in non-diabetics. *Metabolism* 1988, **37**:338-345
16. Ferrannini E, Buzzigoli G, Bonadonna R, Giorico MA, Oleggini M, Graziadei L, Pedrinelli R, Brandi L and Bevilacqua S. Insulin resistance in essential hypertension. *N Engl J Med* 1987, **317**:350-357
17. Hu G, Qiao Q, Tuomilehto J, Eliasson M, Feskens EJ and Pyorala K. Plasma insulin and cardiovascular

mortality in non-diabetic European men and women: a meta-analysis of data from eleven prospective studies. *Diabetologia* 2004, **47**:1245-1256

18. Carr DB, Utzschneider KM, Hull RL, Kodama K, Retzlaff BM, Brunzell JD, Shofer JB, Fish BE, Knopp RH and Kahn SE. Intra-abdominal fat is a major determinant of the National Cholesterol Education Program Adult Treatment Panel III criteria for the metabolic syndrome. *Diabetes* 2004, **53**:2087-2094
19. Saad MF, Lillioja S, Nyomba BL, Castillo C, Ferraro R, De Gregorio M, Ravussin E, Knowler WC, Bennett PH, Howard BV and et al. Racial differences in the relation between blood pressure and insulin resistance. *N Engl J Med* 1991, **324**:733-739
20. Anderson PJ, Critchley JA, Chan JC, Cockram CS, Lee ZS, Thomas GN and Tomlinson B. Factor analysis of the metabolic syndrome: obesity vs insulin resistance as the central abnormality. *Int J Obes Relat Metab Disord* 2001, **25**:1782-1788
21. Despres JP, Lemieux I, Bergeron J, Pibarot P, Mathieu P, Larose E, Rodes-Cabau J, Bertrand OF and Poirier P. Abdominal obesity and the metabolic syndrome: contribution to global cardiometabolic risk. *Arterioscler Thromb Vasc Biol* 2008, **28**:1039-1049
22. Avramoglu RK, Basciano H and Adeli K. Lipid and lipoprotein dysregulation in insulin resistant states. *Clin Chim Acta* 2006, **368**:1-19
23. Scott CL. Diagnosis, prevention, and intervention for the metabolic syndrome. *Am J Cardiol* 2003, **92**:35i-42i
24. Zimmet P, Alberti KG and Shaw J. Global and societal implications of the diabetes epidemic. *Nature* 2001, **414**:782-787
25. Carey VJ, Walters EE, Colditz GA, Solomon CG, Willett WC, Rosner BA, Speizer FE and Manson JE. Body fat distribution and risk of non-insulin-dependent diabetes mellitus in women. The Nurses' Health Study. *Am J Epidemiol* 1997, **145**:614-619
26. Lee IM, Manson JE, Hennekens CH and Paffenbarger RS, Jr. Body weight and mortality. A 27-year follow-up of middle-aged men. *Jama* 1993, **270**:2823-2828
27. Pouliot MC, Despres JP, Lemieux S, Moorjani S, Bouchard C, Tremblay A, Nadeau A and Lupien PJ. Waist circumference and abdominal sagittal diameter: best simple anthropometric indexes of abdominal visceral adipose tissue accumulation and related cardiovascular risk in men and women. *Am J Cardiol* 1994, **73**:460-468
28. Ohlson LO, Larsson B, Svardsudd K, Welin L, Eriksson H, Wilhelmsen L, Bjorntorp P and Tibblin G. The influence of body fat distribution on the incidence of diabetes mellitus. 13.5 years of follow-up of the participants in the study of men born in 1913. *Diabetes* 1985, **34**:1055-1058
29. Rexrode KM, Carey VJ, Hennekens CH, Walters EE, Colditz GA, Stampfer MJ, Willett WC and Manson JE. Abdominal adiposity and coronary heart disease in women. *Jama* 1998, **280**:1843-1848
30. Pan DA, Lillioja S, Kriketos AD, Milner MR, Baur LA, Bogardus C, Jenkins AB and Storlien LH. Skeletal muscle triglyceride levels are inversely related to insulin action. *Diabetes* 1997, **46**:983-988
31. Phillips DI, Caddy S, Ilic V, Fielding BA, Frayn KN, Borthwick AC and Taylor R. Intramuscular triglyceride and muscle insulin sensitivity: evidence for a relationship in nondiabetic subjects. *Metabolism*

1996, **45**:947-950

32. Groop LC, Bonadonna RC, DelPrato S, Ratheiser K, Zyck K, Ferrannini E and DeFronzo RA. Glucose and free fatty acid metabolism in non-insulin-dependent diabetes mellitus. Evidence for multiple sites of insulin resistance. *J Clin Invest* 1989, **84**:205-213
33. Blaak EE. Metabolic fluxes in skeletal muscle in relation to obesity and insulin resistance. *Best Pract Res Clin Endocrinol Metab* 2005, **19**:391-403
34. Kiens B. Skeletal muscle lipid metabolism in exercise and insulin resistance. *Physiol Rev* 2006, **86**:205-243
35. Thiebaud D, Jacot E, DeFronzo RA, Maeder E, Jequier E and Felber JP. The effect of graded doses of insulin on total glucose uptake, glucose oxidation, and glucose storage in man. *Diabetes* 1982, **31**:957-963
36. Thorens B and Mueckler M. Glucose transporters in the 21st Century. *Am J Physiol Endocrinol Metab* 2010, **298**:E141-145
37. Marty N, Dallaporta M and Thorens B. Brain glucose sensing, counterregulation, and energy homeostasis. *Physiology (Bethesda)* 2007, **22**:241-251
38. Schelbert HR and Buxton D. Insights into coronary artery disease gained from metabolic imaging. *Circulation* 1988, **78**:496-505
39. DeFronzo RA, Gunnarsson R, Bjorkman O, Olsson M and Wahren J. Effects of insulin on peripheral and splanchnic glucose metabolism in noninsulin-dependent (type II) diabetes mellitus. *J Clin Invest* 1985, **76**:149-155
40. Rigo P, Paulus P, Kaschten BJ, Hustinx R, Bury T, Jerusalem G, Benoit T and Foidart-Willems J. Oncological applications of positron emission tomography with fluorine-18 fluorodeoxyglucose. *Eur J Nucl Med* 1996, **23**:1641-1674
41. Medina RA and Owen GI. Glucose transporters: expression, regulation and cancer. *Biol Res* 2002, **35**:9-26
42. Pao SS, Paulsen IT and Saier MH, Jr. Major facilitator superfamily. *Microbiol Mol Biol Rev* 1998, **62**:1-34
43. Joost HG, Bell GI, Best JD, Birnbaum MJ, Charron MJ, Chen YT, Doege H, James DE, Lodish HF, Moley KH, Moley JF, Mueckler M, Rogers S, Schurmann A, Seino S and Thorens B. Nomenclature of the GLUT/SLC2A family of sugar/polyol transport facilitators. *Am J Physiol Endocrinol Metab* 2002, **282**:E974-976
44. Young DA, Uhl JJ, Cartee GD and Holloszy JO. Activation of glucose transport in muscle by prolonged exposure to insulin. Effects of glucose and insulin concentrations. *J Biol Chem* 1986, **261**:16049-16053
45. Burant CF, Sivitz WI, Fukumoto H, Kayano T, Nagamatsu S, Seino S, Pessin JE and Bell GI. Mammalian glucose transporters: structure and molecular regulation. *Recent Prog Horm Res* 1991, **47**:349-387; discussion 387-348
46. Klip A and Paquet MR. Glucose transport and glucose transporters in muscle and their metabolic regulation. *Diabetes Care* 1990, **13**:228-243

47. Mueckler M. Facilitative glucose transporters. *Eur J Biochem* 1994, **219**:713-725

48. Marette A, Richardson JM, Ramlal T, Balon TW, Vranic M, Pessin JE and Klip A. Abundance, localization, and insulin-induced translocation of glucose transporters in red and white muscle. *Am J Physiol* 1992, **263**:C443-452

49. Douen AG, Ramlal T, Rastogi S, Bilan PJ, Cartee GD, Vranic M, Holloszy JO and Klip A. Exercise induces recruitment of the "insulin-responsive glucose transporter". Evidence for distinct intracellular insulin- and exercise-recruitable transporter pools in skeletal muscle. *J Biol Chem* 1990, **265**:13427-13430

50. Rodnick KJ, Slot JW, Studelska DR, Hanpeter DE, Robinson LJ, Geuze HJ and James DE. Immunocytochemical and biochemical studies of GLUT4 in rat skeletal muscle. *J Biol Chem* 1992, **267**:6278-6285

51. Goodyear LJ, Hirshman MF and Horton ES. Exercise-induced translocation of skeletal muscle glucose transporters. *Am J Physiol* 1991, **261**:E795-799

52. Hirshman MF, Goodyear LJ, Wardzala LJ, Horton ED and Horton ES. Identification of an intracellular pool of glucose transporters from basal and insulin-stimulated rat skeletal muscle. *J Biol Chem* 1990, **265**:987-991

53. Lund S, Holman GD, Schmitz O and Pedersen O. Glut 4 content in the plasma membrane of rat skeletal muscle: comparative studies of the subcellular fractionation method and the exofacial photolabelling technique using ATB-BMPA. *FEBS Lett* 1993, **330**:312-318

54. Mueckler M, Caruso C, Baldwin SA, Panico M, Blench I, Morris HR, Allard WJ, Lienhard GE and Lodish HF. Sequence and structure of a human glucose transporter. *Science* 1985, **229**:941-945

55. Fukumoto H, Seino S, Imura H, Seino Y and Bell GI. Characterization and expression of human HepG2/erythrocyte glucose-transporter gene. *Diabetes* 1988, **37**:657-661

56. Fukumoto H, Kayano T, Buse JB, Edwards Y, Pilch PF, Bell GI and Seino S. Cloning and characterization of the major insulin-responsive glucose transporter expressed in human skeletal muscle and other insulin-responsive tissues. *J Biol Chem* 1989, **264**:7776-7779

57. Kayano T, Fukumoto H, Eddy RL, Fan YS, Byers MG, Shows TB and Bell GI. Evidence for a family of human glucose transporter-like proteins. Sequence and gene localization of a protein expressed in fetal skeletal muscle and other tissues. *J Biol Chem* 1988, **263**:15245-15248

58. Buse JB, Yasuda K, Lay TP, Seo TS, Olson AL, Pessin JE, Karam JH, Seino S and Bell GI. Human GLUT4/muscle-fat glucose-transporter gene. Characterization and genetic variation. *Diabetes* 1992, **41**:1436-1445

59. Chiaramonte R, Martini R, Taramelli R and Comi P. Identification of the 5' end of the gene encoding a human insulin-responsive glucose transporter. *Gene* 1993, **130**:307-308

60. Choi WH, O'Rahilly S, Buse JB, Rees A, Morgan R, Flier JS and Moller DE. Molecular scanning of insulin-responsive glucose transporter (GLUT4) gene in NIDDM subjects. *Diabetes* 1991, **40**:1712-1718

61. Kayano T, Burant CF, Fukumoto H, Gould GW, Fan YS, Eddy RL, Byers MG, Shows TB, Seino S and Bell GI. Human facilitative glucose transporters. Isolation, functional characterization, and gene

localization of cDNAs encoding an isoform (GLUT5) expressed in small intestine, kidney, muscle, and adipose tissue and an unusual glucose transporter pseudogene-like sequence (GLUT6). *J Biol Chem* 1990, **265**:13276-13282

62. Concha, II, Velasquez FV, Martinez JM, Angulo C, Droppelmann A, Reyes AM, Slebe JC, Vera JC and Golde DW. Human erythrocytes express GLUT5 and transport fructose. *Blood* 1997, **89**:4190-4195
63. Doege H, Bocianski A, Joost HG and Schurmann A. Activity and genomic organization of human glucose transporter 9 (GLUT9), a novel member of the family of sugar-transport facilitators predominantly expressed in brain and leucocytes. *Biochem J* 2000, **350 Pt 3**:771-776
64. Waddell ID, Zomerschoe AG, Voice MW and Burchell A. Cloning and expression of a hepatic microsomal glucose transport protein. Comparison with liver plasma-membrane glucose-transport protein GLUT 2. *Biochem J* 1992, **286 (Pt 1)**:173-177
65. Carayannopoulos MO, Chi MM, Cui Y, Pingsterhaus JM, McKnight RA, Mueckler M, Devaskar SU and Moley KH. GLUT8 is a glucose transporter responsible for insulin-stimulated glucose uptake in the blastocyst. *Proc Natl Acad Sci U S A* 2000, **97**:7313-7318
66. Doege H, Schurmann A, Bahrenberg G, Brauers A and Joost HG. GLUT8, a novel member of the sugar transport facilitator family with glucose transport activity. *J Biol Chem* 2000, **275**:16275-16280
67. Ibberson M, Uldry M and Thorens B. GLUTX1, a novel mammalian glucose transporter expressed in the central nervous system and insulin-sensitive tissues. *J Biol Chem* 2000, **275**:4607-4612
68. Phay JE, Hussain HB and Moley JF. Cloning and expression analysis of a novel member of the facilitative glucose transporter family, SLC2A9 (GLUT9). *Genomics* 2000, **66**:217-220
69. McVie-Wylie AJ, Lamson DR and Chen YT. Molecular cloning of a novel member of the GLUT family of transporters, SLC2a10 (GLUT10), localized on chromosome 20q13.1: a candidate gene for NIDDM susceptibility. *Genomics* 2001, **72**:113-117
70. Doege H, Bocianski A, Scheepers A, Axer H, Eckel J, Joost HG and Schurmann A. Characterization of human glucose transporter (GLUT) 11 (encoded by SLC2A11), a novel sugar-transport facilitator specifically expressed in heart and skeletal muscle. *Biochem J* 2001, **359**:443-449
71. Rogers S, Macheda ML, Docherty SE, Carty MD, Henderson MA, Soeller WC, Gibbs EM, James DE and Best JD. Identification of a novel glucose transporter-like protein-GLUT-12. *Am J Physiol Endocrinol Metab* 2002, **282**:E733-738
72. Uldry M, Ibberson M, Horisberger JD, Chatton JY, Riederer BM and Thorens B. Identification of a mammalian H(+)-myo-inositol symporter expressed predominantly in the brain. *Embo J* 2001, **20**:4467-4477
73. Wu X and Freeze HH. GLUT14, a duplicon of GLUT3, is specifically expressed in testis as alternative splice forms. *Genomics* 2002, **80**:553-557
74. White MF. The IRS-signalling system: a network of docking proteins that mediate insulin action. *Mol Cell Biochem* 1998, **182**:3-11
75. Lietzke SE, Bose S, Cronin T, Klarlund J, Chawla A, Czech MP and Lambright DG. Structural basis of 3-phosphoinositide recognition by pleckstrin homology domains. *Mol Cell* 2000, **6**:385-394

76. Okada T, Kawano Y, Sakakibara T, Hazeki O and Ui M. Essential role of phosphatidylinositol 3-kinase in insulin-induced glucose transport and antilipolysis in rat adipocytes. Studies with a selective inhibitor wortmannin. *J Biol Chem* 1994, **269**:3568-3573

77. Cheatham B, Vlahos CJ, Cheatham L, Wang L, Blenis J and Kahn CR. Phosphatidylinositol 3-kinase activation is required for insulin stimulation of pp70 S6 kinase, DNA synthesis, and glucose transporter translocation. *Mol Cell Biol* 1994, **14**:4902-4911

78. Vanhaesebroeck B and Alessi DR. The PI3K-PDK1 connection: more than just a road to PKB. *Biochem J* 2000, **346 Pt 3**:561-576

79. Le Good JA, Ziegler WH, Parekh DB, Alessi DR, Cohen P and Parker PJ. Protein kinase C isotypes controlled by phosphoinositide 3-kinase through the protein kinase PDK1. *Science* 1998, **281**:2042-2045

80. Bandyopadhyay G, Standaert ML, Galloway L, Moscat J and Farese RV. Evidence for involvement of protein kinase C (PKC)-zeta and noninvolvement of diacylglycerol-sensitive PKCs in insulin-stimulated glucose transport in L6 myotubes. *Endocrinology* 1997, **138**:4721-4731

81. Bandyopadhyay G, Standaert ML, Zhao L, Yu B, Avignon A, Galloway L, Karnam P, Moscat J and Farese RV. Activation of protein kinase C (alpha, beta, and zeta) by insulin in 3T3/L1 cells. Transfection studies suggest a role for PKC-zeta in glucose transport. *J Biol Chem* 1997, **272**:2551-2558

82. Karylowski O, Zeigerer A, Cohen A and McGraw TE. GLUT4 is retained by an intracellular cycle of vesicle formation and fusion with endosomes. *Mol Biol Cell* 2004, **15**:870-882

83. Wertheim N, Cai Z and McGraw TE. The transcription factor CCAAT/enhancer-binding protein alpha is required for the intracellular retention of GLUT4. *J Biol Chem* 2004, **279**:41468-41476

84. Martin S, Tellam J, Livingstone C, Slot JW, Gould GW and James DE. The glucose transporter (GLUT-4) and vesicle-associated membrane protein-2 (VAMP-2) are segregated from recycling endosomes in insulin-sensitive cells. *J Cell Biol* 1996, **134**:625-635

85. Li D, Randhawa VK, Patel N, Hayashi M and Klip A. Hyperosmolarity reduces GLUT4 endocytosis and increases its exocytosis from a VAMP2-independent pool in l6 muscle cells. *J Biol Chem* 2001, **276**:22883-22891

86. Becker C, Sevilla L, Tomas E, Palacin M, Zorzano A and Fischer Y. The endosomal compartment is an insulin-sensitive recruitment site for GLUT4 and GLUT1 glucose transporters in cardiac myocytes. *Endocrinology* 2001, **142**:5267-5276

87. Egert S, Nguyen N and Schwaiger M. Myocardial glucose transporter GLUT1: translocation induced by insulin and ischemia. *J Mol Cell Cardiol* 1999, **31**:1337-1344

88. Shimizu Y, Nikami H, Tsukazaki K, Machado UF, Yano H, Seino Y and Saito M. Increased expression of glucose transporter GLUT-4 in brown adipose tissue of fasted rats after cold exposure. *Am J Physiol* 1993, **264**:E890-895

89. Nagase I, Sasaki N, Tsukazaki K, Yoshida T, Morimatsu M and Saito M. Hyperplasia of brown adipose tissue after chronic stimulation of beta 3-adrenergic receptor in rats. *Jpn J Vet Res* 1994, **42**:137-145

90. Gasparetti AL, de Souza CT, Pereira-da-Silva M, Oliveira RL, Saad MJ, Carneiro EM and Velloso LA. Cold exposure induces tissue-specific modulation of the insulin-signalling pathway in Rattus norvegicus.

J Physiol 2003, **552**:149-162

91. Shimizu Y, Satoh S, Yano H, Minokoshi Y, Cushman SW and Shimazu T. Effects of noradrenaline on the cell-surface glucose transporters in cultured brown adipocytes: novel mechanism for selective activation of GLUT1 glucose transporters. *Biochem J* 1998, **330 (Pt 1)**:397-403
92. Hardie DG, Scott JW, Pan DA and Hudson ER. Management of cellular energy by the AMP-activated protein kinase system. *FEBS Lett* 2003, **546**:113-120
93. Musi N and Goodyear LJ. AMP-activated protein kinase and muscle glucose uptake. *Acta Physiol Scand* 2003, **178**:337-345
94. Kahn BB, Alquier T, Carling D and Hardie DG. AMP-activated protein kinase: ancient energy gauge provides clues to modern understanding of metabolism. *Cell Metab* 2005, **1**:15-25
95. Winder WW and Hardie DG. AMP-activated protein kinase, a metabolic master switch: possible roles in type 2 diabetes. *Am J Physiol* 1999, **277**:E1-10
96. Carling D. The AMP-activated protein kinase cascade--a unifying system for energy control. *Trends Biochem Sci* 2004, **29**:18-24
97. Corton JM, Gillespie JG and Hardie DG. Role of the AMP-activated protein kinase in the cellular stress response. *Curr Biol* 1994, **4**:315-324
98. Hardie DG, Carling D and Carlson M. The AMP-activated/SNF1 protein kinase subfamily: metabolic sensors of the eukaryotic cell? *Annu Rev Biochem* 1998, **67**:821-855
99. Kudo N, Barr AJ, Barr RL, Desai S and Lopaschuk GD. High rates of fatty acid oxidation during reperfusion of ischemic hearts are associated with a decrease in malonyl-CoA levels due to an increase in 5'-AMP-activated protein kinase inhibition of acetyl-CoA carboxylase. *J Biol Chem* 1995, **270**:17513-17520
100. Mu J, Brozinick JT, Jr., Valladares O, Bucan M and Birnbaum MJ. A role for AMP-activated protein kinase in contraction- and hypoxia-regulated glucose transport in skeletal muscle. *Mol Cell* 2001, **7**:1085-1094
101. Fujii N, Hayashi T, Hirshman MF, Smith JT, Habinowski SA, Kaijser L, Mu J, Ljungqvist O, Birnbaum MJ, Witters LA, Thorell A and Goodyear LJ. Exercise induces isoform-specific increase in 5'AMP-activated protein kinase activity in human skeletal muscle. *Biochem Biophys Res Commun* 2000, **273**:1150-1155
102. Kelly M, Keller C, Avilucea PR, Keller P, Luo Z, Xiang X, Giralt M, Hidalgo J, Saha AK, Pedersen BK and Ruderman NB. AMPK activity is diminished in tissues of IL-6 knockout mice: the effect of exercise. *Biochem Biophys Res Commun* 2004, **320**:449-454
103. Arner P. The adipocyte in insulin resistance: key molecules and the impact of the thiazolidinediones. *Trends Endocrinol Metab* 2003, **14**:137-145
104. Fruebis J, Tsao TS, Javorschi S, Ebbets-Reed D, Erickson MR, Yen FT, Bihain BE and Lodish HF. Proteolytic cleavage product of 30-kDa adipocyte complement-related protein increases fatty acid oxidation in muscle and causes weight loss in mice. *Proc Natl Acad Sci U S A* 2001, **98**:2005-2010
105. Iglesias MA, Ye JM, Frangioudakis G, Saha AK, Tomas E, Ruderman NB, Cooney GJ and Kraegen EW.

AICAR administration causes an apparent enhancement of muscle and liver insulin action in insulin-resistant high-fat-fed rats. *Diabetes* 2002, **51**:2886-2894

106. Tomas E, Tsao TS, Saha AK, Murrey HE, Zhang Cc C, Itani SI, Lodish HF and Ruderman NB. Enhanced muscle fat oxidation and glucose transport by ACRP30 globular domain: acetyl-CoA carboxylase inhibition and AMP-activated protein kinase activation. *Proc Natl Acad Sci U S A* 2002, **99**:16309-16313
107. Fryer LG and Carling D. AMP-activated protein kinase and the metabolic syndrome. *Biochem Soc Trans* 2005, **33**:362-366
108. Yamauchi T, Kamon J, Minokoshi Y, Ito Y, Waki H, Uchida S, Yamashita S, Noda M, Kita S, Ueki K, Eto K, Akanuma Y, Froguel P, Foufelle F, Ferre P, Carling D, Kimura S, Nagai R, Kahn BB and Kadowaki T. Adiponectin stimulates glucose utilization and fatty-acid oxidation by activating AMP-activated protein kinase. *Nat Med* 2002, **8**:1288-1295
109. Minokoshi Y, Kim YB, Peroni OD, Fryer LG, Muller C, Carling D and Kahn BB. Leptin stimulates fatty-acid oxidation by activating AMP-activated protein kinase. *Nature* 2002, **415**:339-343
110. Heilbronn LK, Smith SR and Ravussin E. The insulin-sensitizing role of the fat derived hormone adiponectin. *Curr Pharm Des* 2003, **9**:1411-1418
111. Ruderman NB, Saha AK and Kraegen EW. Minireview: malonyl CoA, AMP-activated protein kinase, and adiposity. *Endocrinology* 2003, **144**:5166-5171
112. El-Mir MY, Nogueira V, Fontaine E, Averet N, Rigoulet M and Leverve X. Dimethylbiguanide inhibits cell respiration via an indirect effect targeted on the respiratory chain complex I. *J Biol Chem* 2000, **275**:223-228
113. Brunmair B, Staniek K, Gras F, Scharf N, Althaym A, Clara R, Roden M, Gnaiger E, Nohl H, Waldhausl W and Furnsinn C. Thiazolidinediones, like metformin, inhibit respiratory complex I: a common mechanism contributing to their antidiabetic actions? *Diabetes* 2004, **53**:1052-1059
114. Fryer LG, Parbu-Patel A and Carling D. The Anti-diabetic drugs rosiglitazone and metformin stimulate AMP-activated protein kinase through distinct signaling pathways. *J Biol Chem* 2002, **277**:25226-25232
115. Merrill GF, Kurth EJ, Hardie DG and Winder WW. AICA riboside increases AMP-activated protein kinase, fatty acid oxidation, and glucose uptake in rat muscle. *Am J Physiol* 1997, **273**:E1107-1112
116. Leclerc I and Rutter GA. AMP-activated protein kinase: a new beta-cell glucose sensor?: Regulation by amino acids and calcium ions. *Diabetes* 2004, **53 Suppl 3**:S67-74
117. Yin W, Mu J and Birnbaum MJ. Role of AMP-activated protein kinase in cyclic AMP-dependent lipolysis In 3T3-L1 adipocytes. *J Biol Chem* 2003, **278**:43074-43080
118. Sullivan JE, Brocklehurst KJ, Marley AE, Carey F, Carling D and Beri RK. Inhibition of lipolysis and lipogenesis in isolated rat adipocytes with AICAR, a cell-permeable activator of AMP-activated protein kinase. *FEBS Lett* 1994, **353**:33-36
119. Rossmeisl M, Flachs P, Brauner P, Sponarova J, Matejkova O, Prazak T, Ruzickova J, Bardova K, Kuda O and Kopecky J. Role of energy charge and AMP-activated protein kinase in adipocytes in the control of body fat stores. *Int J Obes Relat Metab Disord* 2004, **28 Suppl 4**:S38-44
120. Salt IP, Connell JM and Gould GW. 5-aminoimidazole-4-carboxamide ribonucleoside (AICAR) inhibits

insulin-stimulated glucose transport in 3T3-L1 adipocytes. *Diabetes* 2000, **49**:1649-1656

121. Sakoda H, Ogihara T, Anai M, Fujishiro M, Ono H, Onishi Y, Katagiri H, Abe M, Fukushima Y, Shojima N, Inukai K, Kikuchi M, Oka Y and Asano T. Activation of AMPK is essential for AICAR-induced glucose uptake by skeletal muscle but not adipocytes. *Am J Physiol Endocrinol Metab* 2002, **282**:E1239-1244
122. Ferrannini E, Bjorkman O, Reichard GA, Jr., Pilo A, Olsson M, Wahren J and DeFronzo RA. The disposal of an oral glucose load in healthy subjects. A quantitative study. *Diabetes* 1985, **34**:580-588
123. Katz LD, Glickman MG, Rapoport S, Ferrannini E and DeFronzo RA. Splanchnic and peripheral disposal of oral glucose in man. *Diabetes* 1983, **32**:675-679
124. Holloszy JO and Narahara HT. Studies of tissue permeability. X. Changes in permeability to 3-methylglucose associated with contraction of isolated frog muscle. *J Biol Chem* 1965, **240**:3493-3500
125. Wallberg-Henriksson H and Holloszy JO. Activation of glucose transport in diabetic muscle: responses to contraction and insulin. *Am J Physiol* 1985, **249**:C233-237
126. Cartee GD, Young DA, Sleeper MD, Zierath J, Wallberg-Henriksson H and Holloszy JO. Prolonged increase in insulin-stimulated glucose transport in muscle after exercise. *Am J Physiol* 1989, **256**:E494-499
127. Richter EA, Garetto LP, Goodman MN and Ruderman NB. Muscle glucose metabolism following exercise in the rat: increased sensitivity to insulin. *J Clin Invest* 1982, **69**:785-793
128. DeFronzo RA and Ferrannini E. Insulin resistance. A multifaceted syndrome responsible for NIDDM, obesity, hypertension, dyslipidemia, and atherosclerotic cardiovascular disease. *Diabetes Care* 1991, **14**:173-194
129. Narahara HT and Ozand P. Studies of tissue permeability. IX. The effect of insulin on the penetration of 3-methylglucose-H3 in frog muscle. *J Biol Chem* 1963, **238**:40-49
130. Jenkins AB, Furler SM and Kraegen EW. 2-deoxy-D-glucose metabolism in individual tissues of the rat in vivo. *Int J Biochem* 1986, **18**:311-318
131. Sasson S, Oron R and Cerasi E. Enzymatic assay of 2-deoxyglucose 6-phosphate for assessing hexose uptake rates in cultured cells. *Anal Biochem* 1993, **215**:309-311
132. Walker PS, Ramlal T, Donovan JA, Doering TP, Sandra A, Klip A and Pessin JE. Insulin and glucose-dependent regulation of the glucose transport system in the rat L6 skeletal muscle cell line. *J Biol Chem* 1989, **264**:6587-6595
133. Sokoloff L, Reivich M, Kennedy C, Des Rosiers MH, Patlak CS, Pettigrew KD, Sakurada O and Shinohara M. The [14C]deoxyglucose method for the measurement of local cerebral glucose utilization: theory, procedure, and normal values in the conscious and anesthetized albino rat. *J Neurochem* 1977, **28**:897-916
134. Kahn BB. Type 2 diabetes: when insulin secretion fails to compensate for insulin resistance. *Cell* 1998, **92**:593-596
135. Pessin JE and Bell GI. Mammalian facilitative glucose transporter family: structure and molecular regulation. *Annu Rev Physiol* 1992, **54**:911-930

136. Klip A and Marette A. Acute and chronic signals controlling glucose transport in skeletal muscle. *J Cell Biochem* 1992, **48**:51-60

137. Mitsumoto Y, Burdett E, Grant A and Klip A. Differential expression of the GLUT1 and GLUT4 glucose transporters during differentiation of L6 muscle cells. *Biochem Biophys Res Commun* 1991, **175**:652-659

138. Mitsumoto Y and Klip A. Development regulation of the subcellular distribution and glycosylation of GLUT1 and GLUT4 glucose transporters during myogenesis of L6 muscle cells. *J Biol Chem* 1992, **267**:4957-4962

139. Manchester JK, Chi MM, Carter JG, Pusateri ME, McDougal DB and Lowry OH. Measurement of 2-deoxyglucose and 2-deoxyglucose 6-phosphate in tissues. *Anal Biochem* 1990, **185**:118-124

140. Brewer GJ, Torricelli JR, Evege EK and Price PJ. Optimized survival of hippocampal neurons in B27-supplemented Neurobasal, a new serum-free medium combination. *J Neurosci Res* 1993, **35**:567-576

141. Shanahan MF. Modulation of hexose transport in cultured skeletal muscle. *Mol Cell Endocrinol* 1984, **38**:171-178

142. Kaliman P, Vinals F, Testar X, Palacin M and Zorzano A. Phosphatidylinositol 3-kinase inhibitors block differentiation of skeletal muscle cells. *J Biol Chem* 1996, **271**:19146-19151

143. Ikeda H, Taketomi S, Sugiyama Y, Shimura Y, Sohda T, Meguro K and Fujita T. Effects of pioglitazone on glucose and lipid metabolism in normal and insulin resistant animals. *Arzneimittelforschung* 1990, **40**:156-162

144. Sugiyama Y, Taketomi S, Shimura Y, Ikeda H and Fujita T. Effects of pioglitazone on glucose and lipid metabolism in Wistar fatty rats. *Arzneimittelforschung* 1990, **40**:263-267

145. Perret P, Ghezzi C, Ogier L, Abbadi M, Morin C, Mathieu JP and Fagret D. Biological studies of radiolabeled glucose analogues iodinated in positions 3, 4 or 6. *Nucl Med Biol* 2004, **31**:241-250

146. Johannsson A, Ellis DH, Bates DL, Plumb AM and Stanley CJ. Enzyme amplification for immunoassays. Detection limit of one hundredth of an attomole. *J Immunol Methods* 1986, **87**:7-11

147. Nakamura S, Arimura K, Ogawa K and Yagi T. Use of 1-methoxy-5-methylphenazinium methyl sulfate (1-methoxyPMS) in the assay of some enzymes of diagnostic importance. *Clin Chim Acta* 1980, **101**:321-326

148. Cook DB and Self CH. Determination of one thousandth of an attomole (1 zeptomole) of alkaline phosphatase: application in an immunoassay of proinsulin. *Clin Chem* 1993, **39**:965-971

149. Olive C, Geroch ME and Levy HR. Glucose 6-phosphate dehydrogenase from Leuconostoc mesenteroides. Kinetic studies. *J Biol Chem* 1971, **246**:2047-2057

150. Summers SA, Yin VP, Whiteman EL, Garza LA, Cho H, Tuttle RL and Birnbaum MJ. Signaling pathways mediating insulin-stimulated glucose transport. *Ann N Y Acad Sci* 1999, **892**:169-186

151. Yonemitsu S, Nishimura H, Shintani M, Inoue R, Yamamoto Y, Masuzaki H, Ogawa Y, Hosoda K, Inoue G, Hayashi T and Nakao K. Troglitazone induces GLUT4 translocation in L6 myotubes. *Diabetes* 2001, **50**:1093-1101

152. Lohrke B, Shahi SK, Kruger B, Schmidt P, Renne U and Dietl G. Thiazolidinedione-induced activation of the transcription factor peroxisome proliferator-activated receptor gamma in cells adjacent to the murine

skeletal muscle: implications for fibroblast functions. *Pflugers Arch* 2000, **439**:288-296

153. Smith AG and Muscat GE. Skeletal muscle and nuclear hormone receptors: Implications for cardiovascular and metabolic disease. *Int J Biochem Cell Biol* 2005, **37**:2047-2063
154. Frayn KN. Obesity and metabolic disease: is adipose tissue the culprit? *Proc Nutr Soc* 2005, **64**:7-13
155. Maher F, Davies-Hill TM, Lysko PG, Henneberry RC and Simpson IA. Expression of two glucose transporters, GLUT1 and GLUT3, in cultured cerebellar neurons: Evidence for neuron-specific expression of GLUT3. *Mol Cell Neurosci* 1991, **2**:351-360
156. Miichi Y, Sakurai T, Akisaki T and Yokono K. Effects of insulin and amyloid beta(1-42) oligomers on glucose incorporation and mitochondrial function in cultured rat hippocampal neurons. *Geriatr Gerontol Int* (in press),
157. Zierath JR, Krook A and Wallberg-Henriksson H. Insulin action and insulin resistance in human skeletal muscle. *Diabetologia* 2000, **43**:821-835
158. Bjornholm M and Zierath JR. Insulin signal transduction in human skeletal muscle: identifying the defects in Type II diabetes. *Biochem Soc Trans* 2005, **33**:354-357
159. Yamamoto N, Sato T, Kawasaki K, Murosaki S and Yamamoto Y. A nonradioisotope, enzymatic assay for 2-deoxyglucose uptake in L6 skeletal muscle cells cultured in a 96-well microplate. *Anal Biochem* 2006, **351**:139-145
160. Yamamoto N, Kawasaki K, Sato T, Hirose Y and Muroyama K. A nonradioisotope, enzymatic microplate assay for in vivo evaluation of 2-deoxyglucose uptake in muscle tissue. *Anal Biochem* 2008, **375**:397-399
161. Miwa I, Okudo J, Maeda K and Okuda G. Mutarotase effect on colorimetric determination of blood glucose with -D-glucose oxidase. *Clin Chim Acta* 1972, **37**:538-540
162. Yamamoto N, Kawasaki K, Kawabata K and Ashida H. An enzymatic fluorimetric assay to quantitate 2-deoxyglucose and 2-deoxyglucose-6-phosphate for in vitro and in vivo use. *Anal Biochem* 2010, **404**:238-240
163. Chi MM, Lowry CV and Lowry OH. An improved enzymatic cycle for nicotinamide-adenine dinucleotide phosphate. *Anal Biochem* 1978, **89**:119-129
164. de Fries R and Mitsuhashi M. Quantification of mitogen induced human lymphocyte proliferation: comparison of alamarBlue assay to 3H-thymidine incorporation assay. *J Clin Lab Anal* 1995, **9**:89-95
165. Shahan TA, Siegel PD, Sorenson WG, Kuschner WG and Lewis DM. A sensitive new bioassay for tumor necrosis factor. *J Immunol Methods* 1994, **175**:181-187
166. Springer JE, Azbill RD and Carlson SL. A rapid and sensitive assay for measuring mitochondrial metabolic activity in isolated neural tissue. *Brain Res Brain Res Protoc* 1998, **2**:259-263
167. Dart MG, Mesta J, Crenshaw C and Ericsson SA. Modified resazurin reduction test for determining the fertility potential of bovine spermatozoa. *Arch Androl* 1994, **33**:71-75
168. Hanson NQ and Freier EF. Effect of protein on the determination of total bile acids in serum. *Clin Chem* 1983, **29**:171-175
169. Shahangian S, Ash KO and Rollins DE. An enzymatic method for the analysis of formate in human plasma. *J Anal Toxicol* 1984, **8**:273-276

170. De Jong DW and Woodlief WG. Fluorimetric assay of tobacco leaf dehydrogenases with resazurin. *Biochim Biophys Acta* 1977, **484**:249-259

171. Barnes S and Spenney JG. Stoichiometry of the NADH-oxidoreductase reaction for dehydrogenase determinations. *Clin Chim Acta* 1980, **107**:149-154

172. Winartasaputra H, Mallet VN, Kuan SS and Guilbault GG. Fluorometric and colorimetric enzymic determination of triglycerides (triacylglycerols) in serum. *Clin Chem* 1980, **26**:613-617

173. Miura T, Kashiwamura M and Kimura M. An enzymatic method for the assay of serum argininosuccinate lyase. *Anal Biochem* 1987, **164**:482-487

174. Chi MM, Pusateri ME, Carter JG, Norris BJ, McDougal DB, Jr. and Lowry OH. Enzymatic assays for 2-deoxyglucose and 2-deoxyglucose 6-phosphate. *Anal Biochem* 1987, **161**:508-513

175. Chi MM, Manchester JK, Carter JG, Pusateri ME, McDougal DB and Lowry OH. A refinement of the Akabayashi-Saito-Kato modification of the enzymatic methods for 2-deoxyglucose and 2-deoxyglucose 6-phosphate. *Anal Biochem* 1993, **209**:335-338

176. Akabayashi A, Saito T and Kato T. An enzymatic microassay method for deoxyglucose and deoxyglucose 6-phosphate. *Biomed Res* 1989, **10**:173-177

177. Sakakibara H, Honda Y, Nakagawa S, Ashida H and Kanazawa K. Simultaneous determination of all polyphenols in vegetables, fruits, and teas. *J Agric Food Chem* 2003, **51**:571-581

178. Furuyashiki T, Nagayasu H, Aoki Y, Bessho H, Hashimoto T, Kanazawa K and Ashida H. Tea catechin suppresses adipocyte differentiation accompanied by down-regulation of PPARgamma2 and C/EBPalpha in 3T3-L1 cells. *Biosci Biotechnol Biochem* 2004, **68**:2353-2359

179. Nishiumi S and Ashida H. Rapid preparation of a plasma membrane fraction from adipocytes and muscle cells: application to detection of translocated glucose transporter 4 on the plasma membrane. *Biosci Biotechnol Biochem* 2007, **71**:2343-2346

180. Jung UJ, Baek NI, Chung HG, Bang MH, Yoo JS, Jeong TS, Lee KT, Kang YJ, Lee MK, Kim HJ, Yeo JY and Choi MS. The anti-diabetic effects of ethanol extract from two variants of Artemisia princeps Pampanini in C57BL/KsJ-db/db mice. *Food Chem Toxicol* 2007, **45**:2022-2029

181. Kang YJ, Jung UJ, Lee MK, Kim HJ, Jeon SM, Park YB, Chung HG, Baek NI, Lee KT, Jeong TS and Choi MS. Eupatilin, isolated from Artemisia princeps Pampanini, enhances hepatic glucose metabolism and pancreatic beta-cell function in type 2 diabetic mice. *Diabetes Res Clin Pract* 2008, **82**:25-32

182. Ryder JW, Yang J, Galuska D, Rincon J, Bjornholm M, Krook A, Lund S, Pedersen O, Wallberg-Henriksson H, Zierath JR and Holman GD. Use of a novel impermeable biotinylated photolabeling reagent to assess insulin- and hypoxia-stimulated cell surface GLUT4 content in skeletal muscle from type 2 diabetic patients. *Diabetes* 2000, **49**:647-654

183. Koistinen HA, Galuska D, Chibalin AV, Yang J, Zierath JR, Holman GD and Wallberg-Henriksson H. 5-amino-imidazole carboxamide riboside increases glucose transport and cell-surface GLUT4 content in skeletal muscle from subjects with type 2 diabetes. *Diabetes* 2003, **52**:1066-1072

184. Chang SH, Jung EJ, Park YH, Lim DG, Ko NY, Choi WS, Her E, Kim SH, Choi KD, Bae JH, Kim SH, Kang CD, Han DJ and Kim SC. Anti-inflammatory effects of Artemisia princeps in antigen-stimulated T

cells and regulatory T cells. *J Pharm Pharmacol* 2009, **61**:1043-1050

185. Geissman TA. Sesquiterpenoid lactones of Artemisia species. I. Artemisia princeps pamp. *J Org Chem* 1966, **31**:2523-2526

186. Ryu SY, Oak MH and Kim KM. Yomogin inhibits the degranulation of mast cells and the production of the nitric oxide in activated RAW 264.7 cells. *Planta Med* 2000, **66**:171-173

187. Umano K, Hagi Y, Nakahara K, Shoji A and Shibamoto T. Volatile chemicals identified in extracts from leaves of Japanese mugwort (Artemisia princeps pamp.). *J Agric Food Chem* 2000, **48**:3463-3469

188. Alessi DR, James SR, Downes CP, Holmes AB, Gaffney PR, Reese CB and Cohen P. Characterization of a 3-phosphoinositide-dependent protein kinase which phosphorylates and activates protein kinase Balpha. *Curr Biol* 1997, **7**:261-269

189. Hill MM, Clark SF, Tucker DF, Birnbaum MJ, James DE and Macaulay SL. A role for protein kinase Bbeta/Akt2 in insulin-stimulated GLUT4 translocation in adipocytes. *Mol Cell Biol* 1999, **19**:7771-7781

190. Kohn AD, Summers SA, Birnbaum MJ and Roth RA. Expression of a constitutively active Akt Ser/Thr kinase in 3T3-L1 adipocytes stimulates glucose uptake and glucose transporter 4 translocation. *J Biol Chem* 1996, **271**:31372-31378

191. Tanti JF, Grillo S, Gremeaux T, Coffer PJ, Van Obberghen E and Le Marchand-Brustel Y. Potential role of protein kinase B in glucose transporter 4 translocation in adipocytes. *Endocrinology* 1997, **138**:2005-2010

192. Wang Q, Somwar R, Bilan PJ, Liu Z, Jin J, Woodgett JR and Klip A. Protein kinase B/Akt participates in GLUT4 translocation by insulin in L6 myoblasts. *Mol Cell Biol* 1999, **19**:4008-4018

193. Kotani K, Ogawa W, Matsumoto M, Kitamura T, Sakaue H, Hino Y, Miyake K, Sano W, Akimoto K, Ohno S and Kasuga M. Requirement of atypical protein kinase clambda for insulin stimulation of glucose uptake but not for Akt activation in 3T3-L1 adipocytes. *Mol Cell Biol* 1998, **18**:6971-6982

194. Standaert ML, Galloway L, Karnam P, Bandyopadhyay G, Moscat J and Farese RV. Protein kinase C-zeta as a downstream effector of phosphatidylinositol 3-kinase during insulin stimulation in rat adipocytes. Potential role in glucose transport. *J Biol Chem* 1997, **272**:30075-30082

195. Lawlor MA and Alessi DR. PKB/Akt: a key mediator of cell proliferation, survival and insulin responses? *J Cell Sci* 2001, **114**:2903-2910

196. Alessi DR, Deak M, Casamayor A, Caudwell FB, Morrice N, Norman DG, Gaffney P, Reese CB, MacDougall CN, Harbison D, Ashworth A and Bownes M. 3-Phosphoinositide-dependent protein kinase-1 (PDK1): structural and functional homology with the Drosophila DSTPK61 kinase. *Curr Biol* 1997, **7**:776-789

197. Williams MR, Arthur JS, Balendran A, van der Kaay J, Poli V, Cohen P and Alessi DR. The role of 3-phosphoinositide-dependent protein kinase 1 in activating AGC kinases defined in embryonic stem cells. *Curr Biol* 2000, **10**:439-448

198. Tsurutani J, Fukuoka J, Tsurutani H, Shih JH, Hewitt SM, Travis WD, Jen J and Dennis PA. Evaluation of two phosphorylation sites improves the prognostic significance of Akt activation in non-small-cell lung cancer tumors. *J Clin Oncol* 2006, **24**:306-314

199. Sarbassov DD, Guertin DA, Ali SM and Sabatini DM. Phosphorylation and regulation of Akt/PKB by the

rictor-mTOR complex. *Science* 2005, **307**:1098-1101

200. Dong LQ and Liu F. PDK2: the missing piece in the receptor tyrosine kinase signaling pathway puzzle. *Am J Physiol Endocrinol Metab* 2005, **289**:E187-196
201. Liu XJ, Yang C, Gupta N, Zuo J, Chang YS and Fang FD. Protein kinase C-zeta regulation of GLUT4 translocation through actin remodeling in CHO cells. *J Mol Med* 2007, **85**:851-861
202. Holloszy JO and Hansen PA. Regulation of glucose transport into skeletal muscle. *Rev Physiol Biochem Pharmacol* 1996, **128**:99-193
203. Hayashi T, Hirshman MF, Kurth EJ, Winder WW and Goodyear LJ. Evidence for 5' AMP-activated protein kinase mediation of the effect of muscle contraction on glucose transport. *Diabetes* 1998, **47**:1369-1373
204. Hawley SA, Boudeau J, Reid JL, Mustard KJ, Udd L, Makela TP, Alessi DR and Hardie DG. Complexes between the LKB1 tumor suppressor, STRAD alpha/beta and MO25 alpha/beta are upstream kinases in the AMP-activated protein kinase cascade. *J Biol* 2003, **2**:28
205. Woods A, Johnstone SR, Dickerson K, Leiper FC, Fryer LG, Neumann D, Schlattner U, Wallimann T, Carlson M and Carling D. LKB1 is the upstream kinase in the AMP-activated protein kinase cascade. *Curr Biol* 2003, **13**:2004-2008
206. Hawley SA, Pan DA, Mustard KJ, Ross L, Bain J, Edelman AM, Frenguelli BG and Hardie DG. Calmodulin-dependent protein kinase kinase-beta is an alternative upstream kinase for AMP-activated protein kinase. *Cell Metab* 2005, **2**:9-19
207. Woods A, Dickerson K, Heath R, Hong SP, Momcilovic M, Johnstone SR, Carlson M and Carling D. Ca2+/calmodulin-dependent protein kinase kinase-beta acts upstream of AMP-activated protein kinase in mammalian cells. *Cell Metab* 2005, **2**:21-33
208. Hurley RL, Anderson KA, Franzone JM, Kemp BE, Means AR and Witters LA. The Ca2+/calmodulin-dependent protein kinase kinases are AMP-activated protein kinase kinases. *J Biol Chem* 2005, **280**:29060-29066
209. Takahashi M, Ikemoto S and Ezaki O. Effect of the fat/carbohydrate ratio in the diet on obesity and oral glucose tolerance in C57BL/6J mice. *J Nutr Sci Vitaminol (Tokyo)* 1999, **45**:583-593
210. Surwit RS, Feinglos MN, Rodin J, Sutherland A, Petro AE, Opara EC, Kuhn CM and Rebuffe-Scrive M. Differential effects of fat and sucrose on the development of obesity and diabetes in C57BL/6J and A/J mice. *Metabolism* 1995, **44**:645-651
211. Nishikawa S, Yasoshima A, Doi K, Nakayama H and Uetsuka K. Involvement of sex, strain and age factors in high fat diet-induced obesity in C57BL/6J and BALB/cA mice. *Exp Anim* 2007, **56**:263-272
212. Lewis GF, Carpentier A, Adeli K and Giacca A. Disordered fat storage and mobilization in the pathogenesis of insulin resistance and type 2 diabetes. *Endocr Rev* 2002, **23**:201-229
213. Korenblat KM, Fabbrini E, Mohammed BS and Klein S. Liver, muscle, and adipose tissue insulin action is directly related to intrahepatic triglyceride content in obese subjects. *Gastroenterology* 2008, **134**:1369-1375
214. Hwang JH, Stein DT, Barzilai N, Cui MH, Tonelli J, Kishore P and Hawkins M. Increased intrahepatic

triglyceride is associated with peripheral insulin resistance: in vivo MR imaging and spectroscopy studies. *Am J Physiol Endocrinol Metab* 2007, **293**:E1663-1669

215. Ginsberg HN, Zhang YL and Hernandez-Ono A. Regulation of plasma triglycerides in insulin resistance and diabetes. *Arch Med Res* 2005, **36**:232-240
216. Ribnicky DM, Poulev A, Watford M, Cefalu WT and Raskin I. Antihyperglycemic activity of Tarralin, an ethanolic extract of Artemisia dracunculus L. *Phytomedicine* 2006, **13**:550-557
217. Xing XH, Zhang ZM, Hu XZ, Wu RQ and Xu C. Antidiabetic effects of Artemisia sphaerocephala Krasch. gum, a novel food additive in China, on streptozotocin-induced type 2 diabetic rats. *J Ethnopharmacol* 2009, **125**:410-416
218. Sun Y, Li YH, Wu XX, Zheng W, Guo ZH, Li Y, Chen T, Hua ZC and Xu Q. Ethanol extract from Artemisia vestita, a traditional Tibetan medicine, exerts anti-sepsis action through down-regulating the MAPK and NF-kappaB pathways. *Int J Mol Med* 2006, **17**:957-962
219. Han JM, Kim MJ, Baek SH, An S, Jin YY, Chung HG, Baek NI, Choi MS, Lee KT and Jeong TS. Antiatherosclerotic effects of Artemisia princeps Pampanini cv. Sajabal in LDL receptor deficient mice. *J Agric Food Chem* 2009, **57**:1267-1274
220. Kim MJ, Han JM, Jin YY, Baek NI, Bang MH, Chung HG, Choi MS, Lee KT, Sok DE and Jeong TS. In vitro antioxidant and anti-inflammatory activities of Jaceosidin from Artemisia princeps Pampanini cv. Sajabal. *Arch Pharm Res* 2008, **31**:429-437
221. Yamamoto N, Ueda M, Kawabata K, Sato T, Kawasaki K, Hashimoto T and Ashida H. Artemisia princeps extract promoted glucose uptake in cultured L6 muscle cells via glucose transporter 4 translocation. *Biosci Biotechnol Biochem* 2010, **74**:2036-2042
222. Trout KK, Homko C and Tkacs NC. Methods of measuring insulin sensitivity. *Biol Res Nurs* 2007, **8**:305-318
223. Nepokroeff CM, Lakshmanan MR and Porter JW. Fatty-acid synthase from rat liver. *Methods Enzymol* 1975, **35**:37-44
224. Kelley DS, Nelson GJ and Hunt JE. Effect of prior nutritional status on the activity of lipogenic enzymes in primary monolayer cultures of rat hepatocytes. *Biochem J* 1986, **235**:87-90
225. Osumi T and Hashimoto T. Acyl-CoA oxidase of rat liver: a new enzyme for fatty acid oxidation. *Biochem Biophys Res Commun* 1978, **83**:479-485
226. Markwell MA, McGroarty EJ, Bieber LL and Tolbert NE. The subcellular distribution of carnitine acyltransferases in mammalian liver and kidney. A new peroxisomal enzyme. *J Biol Chem* 1973, **248**:3426-3432
227. Bonnefont JP, Djouadi F, Prip-Buus C, Gobin S, Munnich A and Bastin J. Carnitine palmitoyltransferases 1 and 2: biochemical, molecular and medical aspects. *Mol Aspects Med* 2004, **25**:495-520
228. Menendez JA, Vazquez-Martin A, Ortega FJ and Fernandez-Real JM. Fatty acid synthase: association with insulin resistance, type 2 diabetes, and cancer. *Clin Chem* 2009, **55**:425-438
229. Smith S. The animal fatty acid synthase: one gene, one polypeptide, seven enzymes. *Faseb J* 1994, **8**:1248-1259

230. Tilg H and Moschen AR. Insulin resistance, inflammation, and non-alcoholic fatty liver disease. *Trends Endocrinol Metab* 2008, **19**:371-379

231. van de Laar FA, Lucassen PL, Akkermans RP, van de Lisdonk EH, Rutten GE and van Weel C. Alpha-glucosidase inhibitors for patients with type 2 diabetes: results from a Cochrane systematic review and meta-analysis. *Diabetes Care* 2005, **28**:154-163

232. Yoshino K, Miyauchi Y, Kanetaka T, Takagi Y and Koga K. Anti-diabetic activity of a leaf extract prepared from Salacia reticulata in mice. *Biosci Biotechnol Biochem* 2009, **73**:1096-1104

233. Mai TT and Chuyen NV. Anti-hyperglycemic activity of an aqueous extract from flower buds of Cleistocalyx operculatus (Roxb.) Merr and Perry. *Biosci Biotechnol Biochem* 2007, **71**:69-76

234. Matsui T, Ebuchi S, Fujise T, Abesundara KJ, Doi S, Yamada H and Matsumoto K. Strong antihyperglycemic effects of water-soluble fraction of Brazilian propolis and its bioactive constituent, 3,4,5-tri-O-caffeoylquinic acid. *Biol Pharm Bull* 2004, **27**:1797-1803

235. Gastaldelli A, Miyazaki Y, Pettiti M, Matsuda M, Mahankali S, Santini E, DeFronzo RA and Ferrannini E. Metabolic effects of visceral fat accumulation in type 2 diabetes. *J Clin Endocrinol Metab* 2002, **87**:5098-5103

236. Hotamisligil GS. Inflammation and metabolic disorders. *Nature* 2006, **444**:860-867

237. Bertin E, Nguyen P, Guenounou M, Durlach V, Potron G and Leutenegger M. Plasma levels of tumor necrosis factor-alpha (TNF-alpha) are essentially dependent on visceral fat amount in type 2 diabetic patients. *Diabetes Metab* 2000, **26**:178-182

238. You T, Yang R, Lyles MF, Gong D and Nicklas BJ. Abdominal adipose tissue cytokine gene expression: relationship to obesity and metabolic risk factors. *Am J Physiol Endocrinol Metab* 2005, **288**:E741-747

239. Fabbrini E, Magkos F, Mohammed BS, Pietka T, Abumrad NA, Patterson BW, Okunade A and Klein S. Intrahepatic fat, not visceral fat, is linked with metabolic complications of obesity. *Proc Natl Acad Sci U S A* 2009, **106**:15430-15435

240. Herzberg GR and Rogerson M. Interaction of dietary carbohydrate and fat in the regulation of hepatic and extrahepatic lipogenesis in the rat. *Br J Nutr* 1988, **59**:233-241

241. Kim TS and Freake HC. High carbohydrate diet and starvation regulate lipogenic mRNA in rats in a tissue-specific manner. *J Nutr* 1996, **126**:611-617

242. Jung UJ, Baek NI, Chung HG, Jeong TS, Lee KT, Lee MK and Choi MS. Antilipogenic and hypolipidemic effects of ethanol extracts from two variants of Artemisia princeps Pampanini in obese diabetic mice. *J Med Food* 2009, **12**:1238-1244

243. Buettner C, Muse ED, Cheng A, Chen L, Scherer T, Pocai A, Su K, Cheng B, Li X, Harvey-White J, Schwartz GJ, Kunos G, Rossetti L and Buettner C. Leptin controls adipose tissue lipogenesis via central, STAT3-independent mechanisms. *Nat Med* 2008, **14**:667-675

244. Jiang L, Wang Q, Yu Y, Zhao F, Huang P, Zeng R, Qi RZ, Li W and Liu Y. Leptin contributes to the adaptive responses of mice to high-fat diet intake through suppressing the lipogenic pathway. *PLoS One* 2009, **4**:e6884

245. Miyazawa S, Hayashi H, Hijikata M, Ishii N, Furuta S, Kagamiyama H, Osumi T and Hashimoto T.

Complete nucleotide sequence of cDNA and predicted amino acid sequence of rat acyl-CoA oxidase. *J Biol Chem* 1987, **262**:8131-8137

246. Wanders RJ, Vreken P, Ferdinandusse S, Jansen GA, Waterham HR, van Roermund CW and Van Grunsven EG. Peroxisomal fatty acid alpha- and beta-oxidation in humans: enzymology, peroxisomal metabolite transporters and peroxisomal diseases. *Biochem Soc Trans* 2001, **29**:250-267
247. Dimmock JR, Elias DW, Beazely MA and Kandepu NM. Bioactivities of chalcones. *Curr Med Chem* 1999, **6**:1125-1149
248. Lim SS, Jung SH, Ji J, Shin KH and Keum SR. Inhibitory effects of 2'-hydroxychalcones on rat lens aldose reductase and rat platelet aggregation. *Chem Pharm Bull (Tokyo)* 2000, **48**:1786-1789
249. Lim SS, Jung SH, Ji J, Shin KH and Keum SR. Synthesis of flavonoids and their effects on aldose reductase and sorbitol accumulation in streptozotocin-induced diabetic rat tissues. *J Pharm Pharmacol* 2001, **53**:653-668
250. Lin YM, Zhou Y, Flavin MT, Zhou LM, Nie W and Chen FC. Chalcones and flavonoids as anti-tuberculosis agents. *Bioorg Med Chem* 2002, **10**:2795-2802
251. Yang EB, Guo YJ, Zhang K, Chen YZ and Mack P. Inhibition of epidermal growth factor receptor tyrosine kinase by chalcone derivatives. *Biochim Biophys Acta* 2001, **1550**:144-152
252. Tomeckova V, Perjesi P, Guzy J, Kusnir J, Chovanova Z, Chavkova Z and Marekova M. Comparison of effect of selected synthetic chalcone analogues on mitochondrial outer membrane determined by fluorescence spectroscopy. *J Biochem Biophys Methods* 2004, **61**:135-141
253. Kuroyanagi M, Noro T, Fukushima S, Aiyama R, Ikuta A, Itokawa H and Morita M. Studies on the constituents of the seeds of Alpinia katsumadai Hayata. *Chem Pharm Bull (Tokyo)* 1983, **31**:1544-1550
254. Sirat HM, Rahman AA, Itokawa H and Morita H. Constituents of the rhizomes of two Alpinia species of Malaysia. *Planta Med* 1996, **62**:188-189
255. Yamamoto T, Yoshimura M, Yamaguchi F, Kouchi T, Tsuji R, Saito M, Obata A and Kikuchi M. Anti-allergic activity of naringenin chalcone from a tomato skin extract. *Biosci Biotechnol Biochem* 2004, **68**:1706-1711
256. Cong LN, Chen H, Li Y, Zhou L, McGibbon MA, Taylor SI and Quon MJ. Physiological role of Akt in insulin-stimulated translocation of GLUT4 in transfected rat adipose cells. *Mol Endocrinol* 1997, **11**:1881-1890
257. Hayashi T, Hirshman MF, Fujii N, Habinowski SA, Witters LA and Goodyear LJ. Metabolic stress and altered glucose transport: activation of AMP-activated protein kinase as a unifying coupling mechanism. *Diabetes* 2000, **49**:527-531
258. Kim EH and Surh YJ. 15-deoxy-Delta12,14-prostaglandin J2 as a potential endogenous regulator of redox-sensitive transcription factors. *Biochem Pharmacol* 2006, **72**:1516-1528
259. Ishiki M and Klip A. Minireview: recent developments in the regulation of glucose transporter-4 traffic: new signals, locations, and partners. *Endocrinology* 2005, **146**:5071-5078
260. Zaid H, Antonescu CN, Randhawa VK and Klip A. Insulin action on glucose transporters through molecular switches, tracks and tethers. *Biochem J* 2008, **413**:201-215

261. Wijesekara N, Tung A, Thong F and Klip A. Muscle cell depolarization induces a gain in surface GLUT4 via reduced endocytosis independently of AMPK. *Am J Physiol Endocrinol Metab* 2006, **290**:E1276-1286
262. Breen DM, Sanli T, Giacca A and Tsiani E. Stimulation of muscle cell glucose uptake by resveratrol through sirtuins and AMPK. *Biochem Biophys Res Commun* 2008, **374**:117-122
263. Deng JY, Hsieh PS, Huang JP, Lu LS and Hung LM. Activation of estrogen receptor is crucial for resveratrol-stimulating muscular glucose uptake via both insulin-dependent and -independent pathways. *Diabetes* 2008, **57**:1814-1823
264. Russell RR, 3rd, Bergeron R, Shulman GI and Young LH. Translocation of myocardial GLUT-4 and increased glucose uptake through activation of AMPK by AICAR. *Am J Physiol* 1999, **277**:H643-649
265. Hawley SA, Gadalla AE, Olsen GS and Hardie DG. The antidiabetic drug metformin activates the AMP-activated protein kinase cascade via an adenine nucleotide-independent mechanism. *Diabetes* 2002, **51**:2420-2425
266. Huang S and Czech MP. The GLUT4 glucose transporter. *Cell Metab* 2007, **5**:237-252
267. Tominaga H, Ishiyama M, Ohseto F, Sasamoto K, Hamamoto T, Suzuki K and Watanabe M. A water-soluble tetrazolium salt useful for colorimetric cell viability assay. *Anal Commun* 1999, **36**:47-50
268. Berridge MV, Herst PM and Tan AS. Tetrazolium dyes as tools in cell biology: new insights into their cellular reduction. *Biotechnol Annu Rev* 2005, **11**:127-152
269. Ishiyama M, Shiga M, Sasamoto K, Mizoguchi M and He P. A new sulfonated tetrazolium salt that produces a highly water-soluble formazan dye. *Chem Pharm Bull (Tokyo)* 1993, **41**:1118-1122
270. Talorete TP, Bouaziz M, Sayadi S and Isoda H. Influence of medium type and serum on MTT reduction by flavonoids in the absence of cells. *Cytotechnology* 2006, **52**:189-198
271. He W, Li Y, Liu J, Hu Z and Chen X. Specific interaction of chalcone-protein: cardamonin binding site II on the human serum albumin molecule. *Biopolymers* 2005, **79**:48-57
272. Murakami A, Kondo A, Nakamura Y, Ohigashi H and Koshimizu K. Possible anti-tumor promoting properies of edible plants from Thiland, and identification of an active constituent, cardamonin, of Boesenbergia pandurata. *Biosci Biotechnol Biochem* 1993, **57**:1971-1973
273. Ahmad S, Israf DA, Lajis NH, Shaari K, Mohamed H, Wahab AA, Ariffin KT, Hoo WY, Aziz NA, Kadir AA, Sulaiman MR and Somchit MN. Cardamonin, inhibits pro-inflammatory mediators in activated RAW 264.7 cells and whole blood. *Eur J Pharmacol* 2006, **538**:188-194
274. Jantan I, Raweh SM, Sirat HM, Jamil S, Mohd Yasin YH, Jalil J and Jamal JA. Inhibitory effect of compounds from Zingiberaceae species on human platelet aggregation. *Phytomedicine* 2008, **15**:306-309
275. Huang Y, Yao XQ, Tsang SY, Lau CW and Chen ZY. Role of endothelium/nitric oxide in vascular response to flavonoids and epicatechin. *Acta Pharmacol Sin* 2000, **21**:1119-1124
276. Liao Q, Shi DH, Zheng W, Xu XJ and Yu YH. Antiproliferation of cardamonin is involved in mTOR on aortic smooth muscle cells in high fructose-induced insulin resistance rats. *Eur J Pharmacol* 2010, **641**:179-186
277. Whitesell RR and Gliemann J. Kinetic parameters of transport of 3-O-methylglucose and glucose in adipocytes. *J Biol Chem* 1979, **254**:5276-5283

278. Karnieli E, Zarnowski MJ, Hissin PJ, Simpson IA, Salans LB and Cushman SW. Insulin-stimulated translocation of glucose transport systems in the isolated rat adipose cell. Time course, reversal, insulin concentration dependency, and relationship to glucose transport activity. *J Biol Chem* 1981, **256**:4772-4777

279. Basi NS, Thomaskutty KG and Pointer RH. Regulation of glucose transport in isolated adipocytes by levamisole. *Can J Physiol Pharmacol* 1992, **70**:1190-1194

280. Foley JE, Cushman SW and Salans LB. Glucose transport in isolated rat adipocytes with measurements of L-arabinose uptake. *Am J Physiol* 1978, **234**:E112-119

281. Mohler ML, He Y, Wu Z, Hwang DJ and Miller DD. Recent and emerging anti-diabetes targets. *Med Res Rev* 2009, **29**:125-195

282. Huang XF and Chen JZ. Obesity, the PI3K/Akt signal pathway and colon cancer. *Obes Rev* 2009, **10**:610-616

283. Henke BR and Sparks SM. Glycogen phosphorylase inhibitors. *Mini Rev Med Chem* 2006, **6**:845-857

284. Hardie DG. AMP-activated protein kinase as a drug target. *Annu Rev Pharmacol Toxicol* 2007, **47**:185-210

285. Ozcan U, Cao Q, Yilmaz E, Lee AH, Iwakoshi NN, Ozdelen E, Tuncman G, Gorgun C, Glimcher LH and Hotamisligil GS. Endoplasmic reticulum stress links obesity, insulin action, and type 2 diabetes. *Science* 2004, **306**:457-461

286. Balint BL and Nagy L. Selective modulators of PPAR activity as new therapeutic tools in metabolic diseases. *Endocr Metab Immune Disord Drug Targets* 2006, **6**:33-43

287. Gray SG and De Meyts P. Role of histone and transcription factor acetylation in diabetes pathogenesis. *Diabetes Metab Res Rev* 2005, **21**:416-433

288. Hales CN and Barker DJ. Type 2 (non-insulin-dependent) diabetes mellitus: the thrifty phenotype hypothesis. *Diabetologia* 1992, **35**:595-601

289. Moller DE. New drug targets for type 2 diabetes and the metabolic syndrome. *Nature* 2001, **414**:821-827

290. Prabhakar PK and Doble M. A target based therapeutic approach towards diabetes mellitus using medicinal plants. *Curr Diabetes Rev* 2008, **4**:291-308

291. Ivorra MD, Paya M and Villar A. A review of natural products and plants as potential antidiabetic drugs. *J Ethnopharmacol* 1989, **27**:243-275

292. Vuksan V and Sievenpiper JL. Herbal remedies in the management of diabetes: lessons learned from the study of ginseng. *Nutr Metab Cardiovasc Dis* 2005, **15**:149-160

293. Zhang H, Yang F, Qi J, Song XC, Hu ZF, Zhu DN and Yu BY. Homoisoflavonoids from the fibrous roots of Polygonatum odoratum with glucose uptake-stimulatory activity in 3T3-L1 adipocytes. *J Nat Prod*, **73**:548-552

294. Fang XK, Gao J and Zhu DN. Kaempferol and quercetin isolated from Euonymus alatus improve glucose uptake of 3T3-L1 cells without adipogenesis activity. *Life Sci* 2008, **82**:615-622

Acknowledgements

First of all, I would like to appreciate Professor Hitoshi Ashida, my main supervisor, for giving me the chance to work with him and for all the support he gave me. I am especially grateful for his scientific help and fruitful discussions, and above all his friendship.

I would like to thank Professor Masashi Miyake, Professor Ken-ichi Yoshida, and Professor Yasuhito Shirai, who found time in their busy schedules to coach me along the way, as the members of my Ph.D. committee.

Thanks also to Dr. Takashi Hashimoto, Dr. Kyuichi Kawabata and Dr. Itsuko Fukuda for helpful suggestions. For research assistance, thanks to: Mr. Takuya Sato, Mr. Kengo Kawasaki, Mr. Manabu Ueda, Miss Yuki Kanamoto, and Mr. Keisuke Sawada.

I am also indebt to Dr. Yoshihiro Yamamoto, Dr. Shinji Murosaki, Dr. Akira Murakami, Dr. Koutarou Muroyama, and Dr. Yoshitaka Hirose, who gave me invaluable comments and warm encouragements.

I would like to thank the anonymous reviewers for their useful comments and to express my gratitude to all those who gave me the possibility to complete this thesis.

It is my pleasure to acknowledge the supports, dedication, and encouragement of members of Laboratory of Biochemistry Frontiers, Faculty of Agriculture, Kobe University and members of Food Science Research Center, House Wellness Foods Corporation.

I would also like to express my gratitude to my family for their moral support and warm encouragements.

Part of the work in this thesis was supported by the program Special Coordination Funds for Promoting Science and Technology, Creation of Innovation Center for Advanced Interdisciplinary Research Areas (Innovative Bioproduction Kobe), MEXT, Japan.

I wish to thank House Wellness Foods Corporation for permission to publish this thesis.

List of Publications

Original Papers

1. Ryo Yamauchi, **Norio Yamamoto** and Koji Kato; Iron-catalyzed reaction products of α-tocopherol with methyl 13(*S*)-hyroperoxy-9(*Z*),11(*E*)-octadecadienoate. *Lipids* 1995, **30**(5):395–404.

2. Edson L. da Silva, Marius K. Piskla, **Norio Yamamoto**, Jae-Hak Moon and Junji Terao; Quercetin metabolites inhibit copper ion-induced lipid peroxidation in rat plasma. *FEBS Letters* 1998, **430**(3):405–408.

3. Junji Terao, Edson L. da Silva, Marius K. Piskla, **Norio Yamamoto** and Jae-Hak Moon; Absorption and Metabolism of dietary flavonoids and their mechanism antioxidant activity. *Free Radicals in Clinical Medicine* 1998, **13**:85–89. [in Japanese]

4. **Norio Yamamoto**, Jae-Hak Moon, Tojiro Tsushida, Akihiko Nagao and Junji Terao; Inhibitory effect of quercetin metabolites and their related derivatives on copper ion-induced lipid peroxidation in human low-density lipoprotein. *Archives Biochemistry Biophysics* 1999, **372**(2):347–354.

5. **Norio Yamamoto**, Takuya Sato, Kengo Kawasaki, Shinji Murosaki and Yoshihiro Yamamoto; A nonradioisotope, enzymatic assay for 2-deoxyglucose uptake in L6 skeletal muscle cells cultured in a 96-well microplate. *Analytical Biochemistry* 2006, **351**(1):139–145.

6. Koutarou Muroyama, **Norio Yamamoto**, Shinji Murosaki, Akitoshi Ishijima, Yoshihiro Yamamoto and Yasuhiko Watanabe; Evaluation of the effectiveness of tea containing thiamin, arginine, caffeine and citric acid on moderately obese subjects with visceral obesity and its safety. *Japanese Pharmacology & Therapeutics* 2006, **34**(10):1097–1105. [in Japanese]

7. Shin Nishiumi, **Norio Yamamoto**, Rie Kodoi, Itsuko Fukuda, Ken-ichi Yoshida and Hitoshi Ashida; Antagonistic and agonistic effects of indigoids on the transformation of an aryl hydrocarbon receptor. *Archives of Biochemistry and Biophysics* 2008, **470**:187–199.

8. **Norio Yamamoto**, Kengo Kawasaki, Takuya Sato, Yoshitaka Hirose, Koutarou Muroyama; A nonradioisotopic, enzymatic microplate assay for in vivo evaluation of 2-deoxyglucose uptake in muscle tissue. *Analytical Biochemistry* 2008, **375**(2):397–399.

9. **Norio Yamamoto**, Kengo Kawasaki, Kyuichi Kawabata, Hitoshi Ashida; An enzymatic fluorimetric assay to quantitate 2-deoxyglucose and 2-deoxyglucose-6-phosphate for in vitro and in vivo use. *Analytical Biochemistry* 2010, **404**(2):238–240.

10. **Norio Yamamoto**, Manabu Ueda, Kyuichi Kawabata, Takuya Sato, Kengo Kawasaki, Takashi Hashimoto and Hitoshi Ashida; Artemisia princeps Extract Promotes Glucose Uptake in Cultured L6 Muscle Cells via Glucose Transporter 4 Translocation., *Bioscience, Biotechnology, and Biochemistry* 2010, **74**(10):2036–2042.

11. Kyuichi Kawabata, Keisuke Sawada, Kazunori Ikeda, Itsuko Fukuda, Kengo Kawasaki, **Norio Yamamoto** and Hitoshi Ashida. Prenylated chalcones 4-hydroxyderricin and xanthoangelol stimulate glucose uptake in skeletal muscle cells by inducing GLUT4 translocation. *Molecular Nutrition and Food Research* 2011, **55**(3):467–475.

12. **Norio Yamamoto**, Yuki Kanamoto, Manabu Ueda, Kengo Kawasaki, Itsuko Fukuda and Hitoshi Ashida, Anti-obesity and anti-diabetic effects of ethanol extract of Artemisia princeps in C57BL/6 mice fed a high-fat diet. *Food & Function* 2011, **2**(1):45–52.

13. **Norio Yamamoto**, Kyuichi Kawabata, Keisuke Sawada, Manabu Ueda, Kengo Kawasaki, Itsuko Fukuda, Akira Murakami and Hitoshi Ashida; Cardamonin stimulated glucose uptake in L6 myotubes through translocation of glucose transporter-4. *Phytotherapy Research* (in press), DOI: 10.1002/ptr.3416

14. Amane Takahashi, **Norio Yamamoto** and Akira Murakami; Cardamonin suppresses nitric oxide production via blocking the IFN-γ/STAT pathway in endotoxin-challenged peritoneal macrophages of ICR mice. *Life Science* (in press).